Institute of Crop Science

University of Hohenheim

Nutritional Crop Physiology

Prof. Dr. Uwe Ludewig

Plant ammonium transporter (AMT) integration in regulatory networks.

Dissertation

submitted in fulfillment of the regulations to acquire the degree

"Doktor der Agrarwissenschaften"

(Dr.sc.agr. in Agricultural Sciences)

to the

Faculty of Agricultural Sciences

presented by

Tatsiana Straub

Mogilev, Belarus

2016

This thesis was accepted as a doctoral thesis (Dissertation) in fulfilment of the regulations to acquire the doctoral degree "Doktor der Agrarwissenschaften" by the Faculty of Agricultural Sciences at University of Hohenheim on 13.06.2016.

Date of the oral examination: 12.07.2016

Examination Committee

Head of the oral examination	Prof. Dr. Wünsche
Supervisor and Reviewer	Prof. Dr. Ludewig
Co-Reviewer	Prof. Dr. Harter
Additional examiner	Prof. Dr. Vögele

Table of contents

List of abbreviations

aa	Amino acid
AKT1	K$^+$ transporter 1
amiRNA	artificial microRNA
AMT	Ammonium transporter
BiFC	Bimolecular fluorescence complementation
CBL	Calcineurin B-like protein
CIPK	Calcineurin B like (CBL)-interacting protein kinase
DNA	Deoxyribonucleic acid
DTT	Dithiothreitol
DW	Dry weight
ECL	Enhanced chemi-luminescence
EDTA	Ethylenediaminetetraacetic acid
FW	Fresh weight
GFP	Green fluorescent protein
HAK5	High affinity K$^+$ transporter 5
HATS	High-affinity transport system
HL	Hoagland medium
HRP	Horseradish peroxidase
KAT1	Potassium channel 1
kDa	Kilodalton
KO	Knock-out
KUP	K$^+$ uptake permease
LATS	Low-affinity transport system
LB medium	Lysogeny broth medium
LysC	protease from *Lysobacter enzymogenes*
MeA	Methylammonium
MEP	Methylammonium/ammonium permease

MES	2-(N-morpholino)ethanesulfonic acid
MS	Murashige and Skoog medium
MSX	Methionine sulfoximine
NC	Nitrocellulose membrane
nm	Nanometer
NRT1	Nitrate transporter 1
NTC	No template control
ON	Over night
PCR	Polymerase chain reaction
qko	Quadruple Arabidopsis mutant (*amt1;1 amt1;2 amt1;3 amt2;1*)
Rh	Mammalian rhesus factor
RNA	Ribonucleic acid
RT	Room temperature
RT-PCR	Real-time polymerase chain reaction
SD	Standard deviation
SDS	Sodium dodecyl sulfate
SDS-PAGE	Sodium dodecyl sulfate – Polyacrylamide gel electrophoresis
TFA	Trifluoroacetic acid
WB	Western blot
WT	Wild type (*Atabidopsis thaliana*, Col-0)
YFP	Yellow fluorescent protein

List of tables

List of figures

1 Summary

Ammonium is a ubiquitous key nutrient in agricultural soils and the preferred nitrogen source for plants. However, excessive ammonium accumulation represses plant growth and development. Ammonium is taken up by plant cells via high-affinity ammonium transporters (AMTs). Six *AMT* genes were identified in Arabidopsis, which are separated in two distinct clades, five *AMT1s* and one *AMT2*. In the plasma membrane, AMT proteins form homo- and heterotrimers with extra-cytoplasmic N-termini and cytoplasmic C-termini. In addition to transcriptional and post-transcriptional control of *AMTs* by ammonium, phosphorylation in the C-terminus serves as a rapid allosteric switch of the AMT activity and prevents further internal ammonium accumulation.

In a physiological screen, a kinase (CIPK23) was identified, which directly regulates ammonium transport activity under high-NH_4^+ conditions. Interestingly, CIPK23 is already known to regulate nitrate and potassium uptake in roots. Lesion of the *CIPK23* gene significantly increased ammonium uptake, but caused growth inhibition. As expected, *cipk23* plants were also limited in potassium accumulation, but high potassium availability failed to rescue the *cipk23* phenotype. Furthermore, *cipk23* plants were more susceptible to methylammonium (MeA), a non-metabolizable analogue of ammonium. The sensitivity to MeA was lost upon genetic suppression of *AMT1* genes in the *cipk23* background.

The data suggest that CIPK23 directly phosphorylates AMT1s in a complex with CBL1 (calcineurin B-like protein) and thereby regulates transport activity. The expression of the *CIPK23* and the *CBL1* genes were ammonium-dependent and increased when N-starved plants were resupplied with ammonium. Furthermore, *cbl1* mutants had enhanced NH_4^+ accumulation; this phenocopies the larger ammonium uptake in the *cipk23 loss-of-function* mutant. *In vivo* experiments demonstrated bimolecular interaction between CIPK23, AMT1;1, and AMT1;2, but not with AMT2;1, suggesting direct phosphorylation of AMT1-type ammonium transporters by CIPK23.

However, Western blot analysis with the *cipk23* mutant suggested that the loss of the kinase was not sufficient to completely abolish AMT1;1 and AMT1;2 phosphorylation, indicating several independent pathways to regulate ammonium transport activity in AMT trimers.

The data identify complex post-translational regulation of ammonium transporters via the CBL1–CIPK23 pathway, which ensures reduction of AMT1 activity and suppression of ammonium uptake under high external NH_4^+ concentrations.

2   Introduction

Nitrogen is an essential element in all known organisms on earth. While animals secrete excessive nitrogen, plant growth is often limited by available nitrogen sources. Initial visual nitrogen deficiency symptoms in plants are pale and yellowish-green leaves due to reduced chlorophyll content. Older plant leaves are affected first, since nitrogen is a mobile nutrient. In addition, nitrogen deficiency causes reduction in protein and starch contents which results in smaller leaves, decreased branching and tillering (Walburg, Bauer, and Daughtry 1982; Harper 1994).

To uptake nitrogen containing compounds from the soil plants compete with other plants, but also with soil born microorganisms. Some plants harbor nitrogen fixing bacteria to make gaseous nitrogen available (Gage 2004), others collaborate with certain fungi to improve their nitrogen nutrition (Smith and Smith 1997; Hodge and Storer 2014). But all plants face the challenge to import sufficient nitrogen into their system, either from the soil or their interaction partner, and to distribute it within themselves. Different systems and strategies have evolved during evolution to transport this valuable nutrient (von Wirén and Merrick 2004; Kaldenhoff et al. 2007).

2.1   Ammonium use in agriculture

Plants have a fundamental dependence on inorganic nitrogen. Lack of nitrogen in the soil reduces plant growth, thus decreases the yield. Each year around 85–90 million tonnes of nitrogenous fertilizers are added to the soil world-wide (Good et al. 2007). Ammonium and urea, which is rapidly degraded to ammonium by soil urease, comprise a principal component of the majority of chemical nitrogen fertilizers used in modern agriculture. While soil-born microorganisms rapidly convert ammonium to nitrate (nitrification), the major nitrogen source in temperate agroecosystems, urea- or ammonium-based fertilizers are frequently stabilized with urease inhibitors or nitrification inhibitors to increase ammonium availability to crops.

Although gaseous nitrogen is the most abundant element in the Earth's atmosphere, nitrogen is usually inaccessible to plants. In order to make gaseous di-nitrogen usable for plants, it has to be fixed to ammonia, however this process needs to break one of the strongest bonds in organic chemistry (Blanksby and Ellison 2003). Direct biological fixation of the nitrogen in plants is restricted to legumes aided by their symbiotic interaction with bacteria. Mankind utilizes the

Haber-Bosch process, which uses high pressure and high temperatures to overcome the bond-dissociation energy of nitrogen, under vast energy consumption. Approximately 1-2% of the world's energy is consumed in nitrogen fixation ("Market Outlooks Reports" 2015). The Haber-Bosch process was called the most important innovation of the 20th century (Smil 1999).

Once the nitrogen is brought to the field by fertilizers, it is easily lost due to bacterial activity or leaching. While ammonium (dependent on the cation exchange capacity of the soil) is not easily leached, ammonium conversion to nitrate via nitrification yields an easier leached inorganic nitrogen form, due to its negative charge. Nitrate leaching is recognized as a serious pollution hazard in the world and proper management practices should be in place to control for nitrogen loss from soil. To achieve the maximum benefits from nitrogen fertilizers and reduce their environmental impact, it is crucial to understand how plants assimilate nitrogen and what molecular mechanisms underlay this process.

2.2 Ammonium transport (LATS, HATS)

Most plant species are able to uptake and assimilate nitrate, ammonium, urea and amino acids as nitrogen sources, but the preference for one form of nitrogen varies depending on the plant species. For instance, white spruce accumulates 140 times more ammonium in the cytoplasm than nitrate after nitrogen starvation (Kronzucker, Siddiqi, and Glass 1997). Indeed, the roots of most plants prefer to take up ammonium compared to nitrate when supplied at the same concentrations. Furthermore, ammonium rapidly inhibits nitrate uptake (Lee and Drew 1989; Mehrer and Mohr 1989; Clarkson, Jones, and Purves 1992; Gazzarrini et al. 1999; Kronzucker, Glass, and Siddiqi 1999).

In soils, soluble ammonium ion (NH_4^+) is the predominant form, however, it deprotonates in alkaline solutions to volatile ammonia (NH_3) with a pK_a = 9.25. The ratio of ammonium to ammonia in solutions depends on the pH value (Fig. 1). The uncharged ammonia is very well soluble in water, but may evaporate and then forms a colourless gas. Due to the neutral pH of the cytosol, the ammonium cation dominates in plant cells (MacDonald et al. 1994; Sumner 1999; Schjoerring et al. 2002).
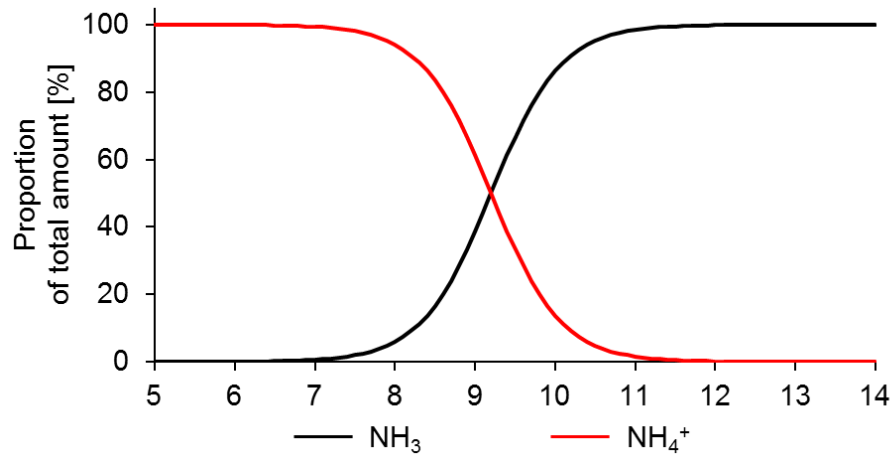
Figure 1: Schematic model of ammonium (NH_4^+) and ammonia (NH_3) proportions dependent on pH.
In acidic solution and also the neutral cell cytosol, the ammonium ion is the most abundant species.
However, neutral ammonia is dominant in highly alkaline solutions.

Ammonium acquisition is mediated by at least two transport systems with distinct thermodynamic characteristics, high-affinity and low-affinity system (Wang et al. 1993; Kronzucker, Siddiqi, and Glass 1996). Generally, the activity of each system depends on the external ammonium concentration. The low-affinity transport system (LATS) is a non-saturable system that exhibits a linear increase in activity when ammonium concentration increases (Wang et al. 1993; Mäck and Tischner 1994; Kronzucker, Siddiqi, and Glass 1996).

In roots, the low-affinity transport system is primarily responsible for ammonium acquisition from the soil at high ammonium concentration. Several distinct mechanisms are probably involved in this process. Members of the aquaporin super-family are highly expressed in roots and facilitate transport of ammonia in addition to water (Niemietz and Tyerman 2000; Jahn et al. 2004; Saparov et al. 2007). The charged ammonium ion might be transported either by unspecific transport of non-selective cation channels (Demidchik, Davenport, and Tester 2002) or by potassium channels, such as AKT1 in roots and KAT1 in leaves (Schachtman et al. 1992; Bertl et al. 1997).

In contrast, the high-affinity transport system (HATS) is a saturable system, that catalyses the thermodynamically secondary active uptake of ammonium against a chemical gradient when the external concentration is low (Wang et al. 1993; Kronzucker, Siddiqi, and Glass 1996).

2.3 High affinity ammonium transporters

In 1994, the first genes encoding ammonium transporting proteins were identified in *Saccharomyces cerevisiae*, methylammonium/ammonium permeases (MEP), and *Arabidopsis thaliana*, ammonium transporters (AMT), by functional complementation of a mutant yeast defective in ammonium uptake (Marini et al. 1994; Ninnemann, Jauniaux, and Frommer 1994). Later on, proteins from the ammonium transporter family have been identified in a wide range of organisms, including bacteria, plants and yeasts (Siewe et al. 1996; Montesinos et al. 1998; Meletzus et al. 1998; Blakey et al. 2002). The ammonium transporter family includes three subfamilies: mammalian rhesus factors (Rh), yeast MEP and plant (AMT) ammonium transporters (Fig. 2) (Ludewig et al. 2001; McDonald, Dietrich, and Lutzoni 2012). Land plant ammonium transporters AMT1 belong to the AMT subfamily, while plant AMT2 transporters are more closely related to bacterial AmtB (Sohlenkamp et al. 2002) and belong to the MEP subfamily. Fungal ammonium transporters are also part of the MEP subfamily (Monahan, Fraser, et al. 2002). The third subfamily (Rh) includes Rhesus blood-group associated glycoproteins in animals (Marini et al. 1997).
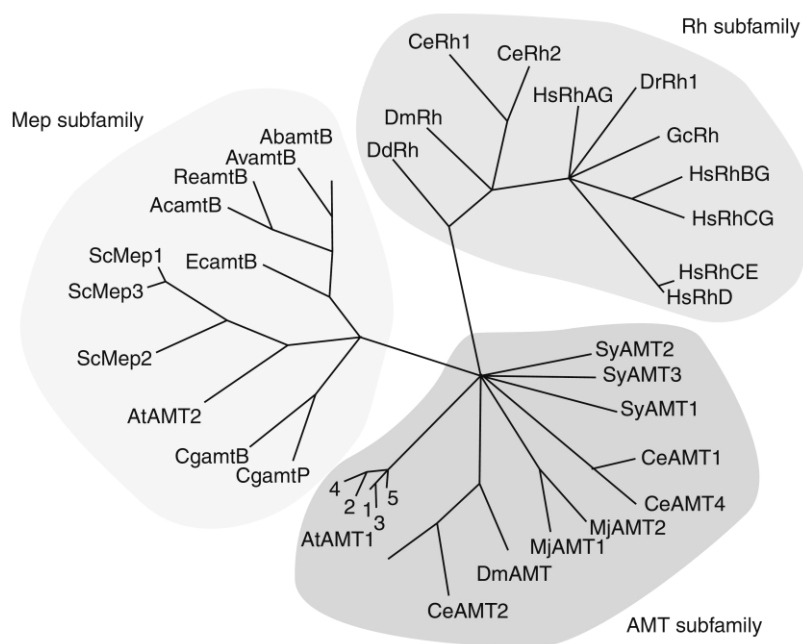
Figure 2: Phylogenetic tree of high affinity ammonium transporters.
The transporter family is divided into three subfamilies, mammalian rhesus factors (Rh), yeast MEP and plant (AMT) ammonium transporters (Ludewig et al. 2001).

2.3.1 Structure

AMTs are generally proteins of 45–50 kDa (around 400 – 450 amino acids), however the size of the protein can be increased up to 600 amino acids due to an extended C-terminus (Ninnemann, Jauniaux, and Frommer 1994; Blakey et al. 2002). Generally, AMTs are located in cell membranes and have 11 hydrophobic regions that span the membrane in kinked helices.

AmtB from *Escherichia coli* was the first ammonium transporter with its exact structure revealed by protein crystallography (Zheng et al. 2004; Nygaard et al. 2006). The folding of ammonium transporters is unique among membrane protein families. Each AmtB has 11 transmembrane α-helices (M1-M11) which form two contiguous α-helical bundles and have an antiparallel architecture (Fig. 3) (Thomas, Mullins, and Merrick 2000; Khademi et al. 2004; Zheng et al. 2004; Nygaard et al. 2006).

Each *E. coli* AmtB monomer is able to transport ammonium/ammonia (Javelle et al. 2008) through a central hydrophobic pore, right between the pseudosymmetry-related helical domains. AmtB forms a trimer in the plasma membrane (Blakey et al. 2002; Conroy et al. 2004; Zheng et al. 2004). The interaction between AmtB monomers is based on interaction of specific helices. Amino acid residues of M1, M6, M7, M8, and M9 of one monomer interact with helices M1, M2, and M3 of the neighbouring monomer (Fig. 3) (Khademi et al. 2004). The chemical properties of the trimer facilitate its directed insertion into the membrane with negative charged structures facing outward and the positive charged surface in the cytoplasm (Khademi et al. 2004). Consequently, the N-terminus of *E. coli* AmtB is facing the extracellular space and the C-terminal domain is oriented into the cytoplasm. The C-terminal tail of 32 residues is present in all MEP/AMT proteins and includes three highly conserved residues. In eukaryotes, this region is extended even more (Thomas, Mullins, and Merrick 2000). The high conservation of the C-terminus suggests its structural or functional significance. AmtB lacking its C-terminal tail has significantly reduced, but not abolished, transport activity (Thomas, Mullins, and Merrick 2000).
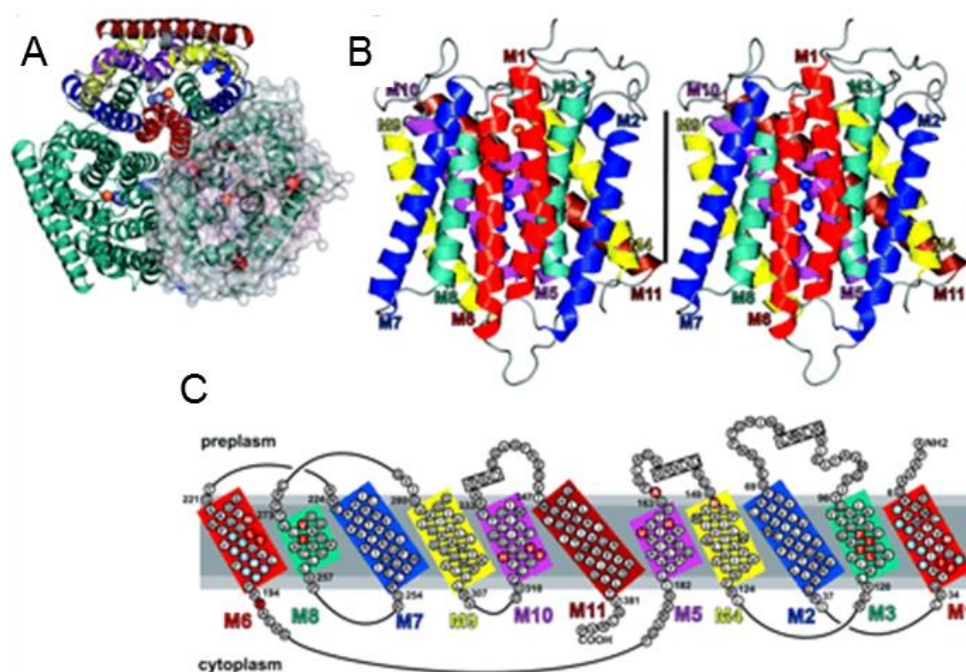
Figure 3: Structure of *Escherichia coli* AmtB.
(A) Top-view on the AMT trimer. (B) Side view on one AmtB monomer. (C) Schematic model of the eleven transmembrane helices (M1-M11), the conserved C-terminal tail after helix M11 reaches into the cytoplasm (Khademi et al. 2004).

2.4 Regulation of ammonium transport

As nitrogen is often the limiting element in plant nutrition, competition with soil living microorganisms is high. However, high ammonium levels are toxic and the plant ion status can make transport adjustments necessary. Therefore, the ammonium transport system is under strict control at several levels.

2.5 Transcriptional regulation

The transcription of ammonium transporter genes is regulated diurnally. In nitrogen uptake studies, ammonium influx increased from the start until the end of the light period, but declined rapidly when the light was turned off (Ourry et al. 1996; Gazzarrini et al. 1999). These changes in transport capacity were correlated with mRNA levels of several ammonium transporters and depended on sucrose supply as signal for the plant energy status (Lejay et al. 2003). Like ammonium, many inorganic nutrients need to be assimilated with the help of photosynthesis products and therefore their active import is often light dependent.

Ammonium transporters transcript levels are also influenced by the plant nitrogen status. Already a few days of nitrogen deficiency strongly induce *AMT1;1* transcription in *A. thaliana* (Rawat et al. 1999) and rice (LI, LI, and SHI 2012) while e.g. *AMT2;1* response to nitrogen starvation is significantly slower (Loqué and von Wirén 2004). By contrast, sufficient nitrogen feeding triggers reduction of *AMT1;1* transcripts in *A. thaliana* (Rawat et al. 1999) and *Medicago truncatula* (Straub, Ludewig, and Neuhäuser 2014). Furthermore, ammonium resupply to plants grown under limited nitrogen condition or under nitrogen starvation alters ammonium transporters transcript levels in various ways. For instance, when ammonium was resupplied to nitrogen-starved rice plants, *OsAMT1;2* and *OsAMT3;3* genes were down-regulated, while *OsAMT1;3* was up-regulated (LI, LI, and SHI 2012).

AMT homologs in different species are often not similar regulated and might reflect the different nutritional needs of the particular species (Loqué and von Wirén 2004).

2.5.1 Posttranslational regulation of ammonium transport

2.5.1.1 Regulation of ammonium transport by GlnK in E. coli

Regulation of ammonium transport by posttranscriptional mechanisms has been shown in a number of organisms. The activity of ammonium transporters is regulated in *E. coli* by the PII like signal-transduction protein GlnK. GlnK is able to sterically block AmtB ammonium transport through each of the three pores (Conroy et al. 2007). However, under nitrogen-limiting conditions GlnK is uridylylated by GlnD and cannot interact with its targets. Conversely, under conditions of nitrogen sufficiency, GlnK is de-uridylylated and inhibits AmtB, while it also activates the key regulator NtrB/NtrC of nitrogen-regulated genes. Thereby GlnK integrates nitrogen (glutamine), energy (ATP) and carbon (2-oxoglutarate) status to regulate nitrogen uptake and processing (Dixon and Kahn 2004).
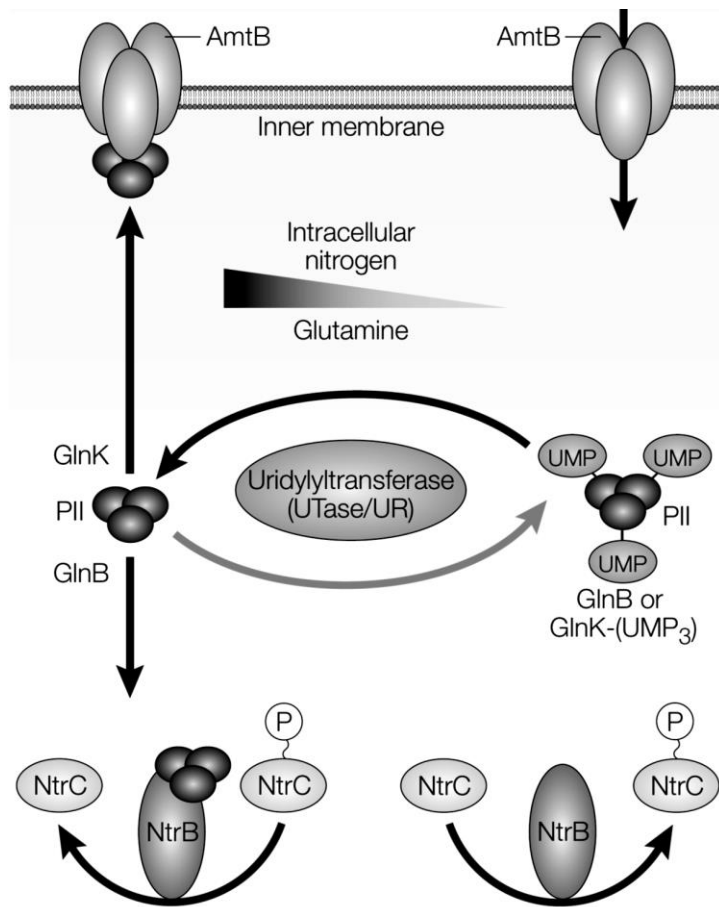
Figure 4: PII regulates ammonium transporter AmtB in *E. coli*.
Left: GlnK inhibits AmtB ammonium transport by direct interaction under high intracellular nitrogen concentrations. Right: Under nitrogen-limiting conditions GlnK is uridylylated by GlnD and does not inhibit AmtB transport activity (Dixon and Kahn 2004).

PII proteins are found in bacteria, archaea and plants. However, in plants PII proteins are comparted in the chloroplasts and therefore unlikely to perform the regulation of ammonium transporters (Hsieh et al. 1998; Sugiyama et al. 2004).

2.5.1.2 *Regulation of ammonium transport by phosphorylation*

Ammonium transport in yeasts is mediated by the MEP subfamily of ammonium transporters. In *Saccharomyces cerevisiae* and *Candida albicans* ammonium transport activity depends on an active NPR1 kinase (Boeckstaens, André, and Marini 2007; Neuhäuser et al. 2011). Growth of *S. cerevisiae* without active NPR1 under standard growth conditions is inhibited, like in yeast defective in MEPs. In *S. cerevisiae*, NPR1 regulates MEP2 activity by phosphorylation of C-terminal serine residue 457 (Boeckstaens et al. 2014).

Also in *A. thaliana*, rapid closure of AMT trimers is achieved by phosphorylation. One phosphorylated AMT1;2 subunit is able to influence other subunits and renders the whole trimer inactive (Fig. 5) (Neuhäuser et al. 2007).
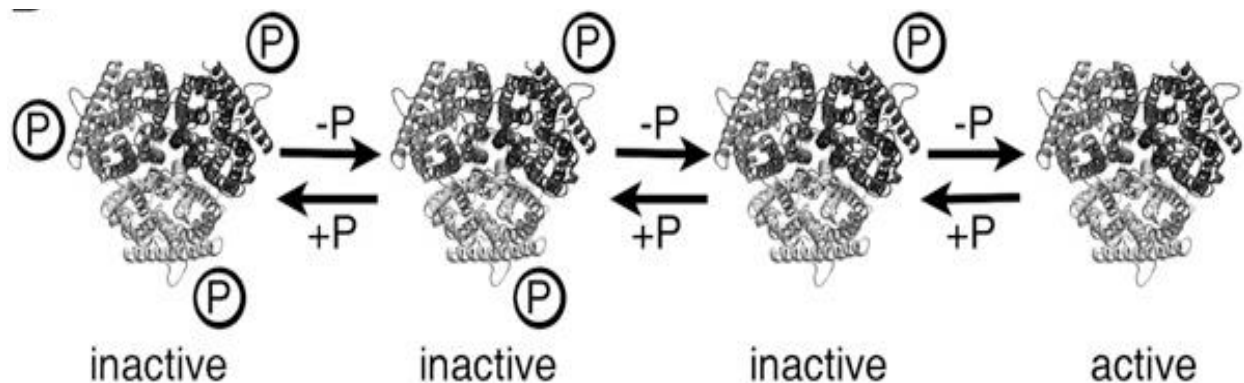
Figure 5: Phosphorylation of one AMT1;2 subunit renders the whole trimer inactive.
The phosphorylated trimer (left) is dephosphorylated by an unknown mechanism, but remains inactive until all three AMT subunits are free of phosphate modifications. Phosphorylation by an unknown kinase can diminish ammonium transport activity (Neuhäuser et al. 2007).

The phosphorylation of *At*AMT1;1 takes place at the C-terminal threonine 460 (Loqué and von Wirén 2004; Nühse et al. 2004), while *At*AMT1;2 is phosphorylated at position 472 (Neuhäuser et al. 2007).

Until now, it is unknown which kinase regulates ammonium transport in plants. Plant kinases related to *S. cerevisiae* NPR1 are members of the Calcineurin-B like (CBL)-interacting protein kinases (CIPK) and some CIPKs are upregulated in response to ammonium (Patterson et al. 2010; Canales et al. 2014; Engelsberger and Schulze 2012). However, an involvement of CIPKs in plant ammonium transport has not been shown yet.

2.5.1.3   Regulation by hetero-oligomerization

The inhibition of one AMT subunit by phosphorylation can inhibit other non-phosphorylated AMTs in the trimer. In yeasts and plants, AMTs are forming not only functional homo-oligomers, but also hetero-oligomers with their respective homologs. In *S. cerevisiae* and *Aspergillus*, one ammonium transporter with inhibitory mutation in the C-terminus also strongly reduced the functionality of other unmodified ammonium transporters (Marini et al. 2000; Monahan, Unkles, et al. 2002).

AMT oligomerization was also shown in tomato, where an amino acid exchange in the C-terminus of *Le*AMT1;1 rendered the protein unfunctional and also affected the transport activity of the wild type protein. Furthermore, unfunctional *Le*AMT1;1 inhibited *Le*AMT1;2 in electrophysiological measurements with *Xenopus laevis* oocytes. Further investigations by Western blot analysis and SDS-PAGE confirmed oligomerization of *Le*AMT1;1 and *Le*AMT1;2 also *in planta* (Ludewig et al. 2003; Graff et al. 2011).

In *A. thaliana*, AMT1;1 and AMT1;3 form functional homo- and heterotrimers. Mutated AMT1;3 with a phosphomimic residue in the C-terminus regulates both homo- and heterotrimers in a dominant-negative fashion *in vivo* (Yuan et al. 2013).

2.5.1.4 Ammonium sensing and signaling

In *Arabidopsis*, external ammonium rather than the internal nitrogen status serves as a signal for AMT phosphorylation (Lanquar et al. 2009). In the fungi *S. cerevisiae* and *C. albicans*, the MEP2 transporter has been identified as a transceptor, a protein that possesses both transporter and receptor functions at the same time (Thevelein et al. 2005). Lanquar and colleagues proposed two models for plant ammonium sensing and signalling: a transceptor model and a receptor kinase model (Fig. 6). In the transceptor model, membrane located AMT1 function as transceptor, much like MEP2. Thus, high external ammonium levels trigger the phosphorylation of AMT1s C-terminus and shut down ammonium import. In the receptor kinase model, AMT1s function only as transporters and a receptor kinase senses high external ammonium levels and phosphorylates AMT1s.

Furthermore, *Arabidopsis* nitrate transporter NRT1.1 has been characterized as nitrate transporter with receptor activity (Ho et al. 2009).

A Transceptor model

low NH$_4^+$ · · · high NH$_4^+$

apoplasm

cytosol

AMT1;1 T$_{460}$ · T$_{460}$ · P

soluble kinase

B Receptor kinase model

low NH$_4^+$ · high NH$_4^+$

T$_{460}$ · RLK · T$_{460}$ · P
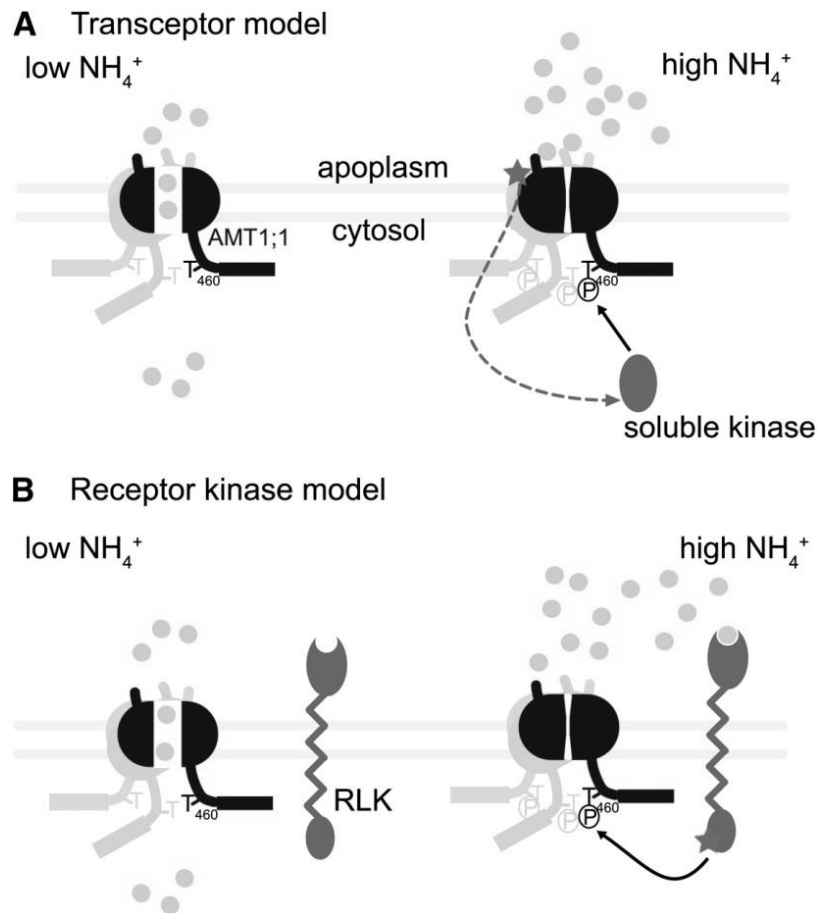
Figure 6: Transceptor and Receptor kinase models in ammonium sensing and signalling.
(A) AMTs as transceptors possess both transporter and receptor functions at the same time. Upon high external ammonium levels, the AMT1 C-terminus is phosphorylated by a kinase and ammonium import is shut down. (B) AMT is only functioning as a transporter and an additional receptor kinase phosphorylates AMTs when external ammonium concentrations are high (Lanquar et al. 2009).

2.6   CBL-CIPK23

In plants, potential candidates for AMT phosphorylation and thus inhibition are Calcineurin-B like (CBL)-interacting protein kinases (CIPK). These kinases rely on calcium binding CBL proteins.

2.6.1   Calcineurin B-like proteins (CBLs) are sensing calcium signatures and interact with kinases.

Plants react to a wide range of abiotic, biotic and developmental stimuli with a temporal change in cytosolic calcium concentration. Such stimulus induced fluctuation of free calcium in

the cytoplasm is referred to as "calcium signature". Plants are equipped with a diverse array of proteins for sensing the calcium signature and for further signal transduction. These proteins can be classified in two groups, sensor relays and sensor responders (Weinl and Kudla 2009; Hashimoto and Kudla 2011; Sanyal, Pandey, and Pandey 2015). The latter combine a calcium sensing function with a response activity in one protein (Kolukisaoglu et al. 2004; Weinl and Kudla 2009; Kudla, Batistič, and Hashimoto 2010; Hashimoto and Kudla 2011; Sanyal, Pandey, and Pandey 2015). Sensor relays, however, are able to regulate target proteins via calcium dependent protein-protein interaction. Among other protein families, Ca^{2+}-binding calcineurin B-like proteins (CBL) are sensor relays (Luan et al. 2002; Hashimoto and Kudla 2011). CBLs sense the calcium signature, the first component of the calcium signalling pathway, and regulate CBL-interacting protein kinases (CIPKs) proteins (Kim et al. 2000; Albrecht et al. 2001).

The genome of *Arabidopsis thaliana* encodes 10 CBL proteins and all are rather small with around 23-26 kDa (Weinl and Kudla 2009). CBLs share 29 – 92% of sequence homology (Kolukisaoglu et al. 2004; Weinl and Kudla 2009) and have different cell localisation (Sanyal, Pandey, and Pandey 2015) (Table 1).

Table 1: Localisation of CBLs in the cell.

CBL1	PM
CBL2	tonoplast
CBL3	tonoplast
CBL4	whole cell
CBL5	whole cell
CBL6	tonoplast
CBL7	cytoplasm, nucleus
CBL8	PM, cytoplasm, nucleus
CBL9	PM
CBL10	PM, tonoplast

CBLs consist of four EF-hand domains, and each EF-hand consists of a helix-loop-helix structure (Kolukisaoglu et al. 2004; Luan 2009; Weinl and Kudla 2009; Hashimoto and Kudla 2011). The loop of each EF-hand is able to bind cytosolic calcium ions (Luan et al. 2002; Sanyal, Pandey, and Pandey 2015). Upon calcium binding, CBLs undergo conformational changes, that allow them to interact with CIPK kinases (Sanyal, Pandey, and Pandey 2015).

2.6.2 CBL-interacting protein kinases (CIPKs)

The *Arabidopsis thaliana* genome encodes 26 CBL-interacting protein kinases (CIPKs) (Hrabak et al. 2003; Weinl and Kudla 2009). CIPKs are serine/threonine protein kinases with two general structural components, the N-terminal catalytic domain and the C-terminal regulatory domain. These domains are unique to the CIPK protein family and are separated by a variable junction domain (Fig. 7) (Weinl and Kudla 2009; Sanyal, Pandey, and Pandey 2015).
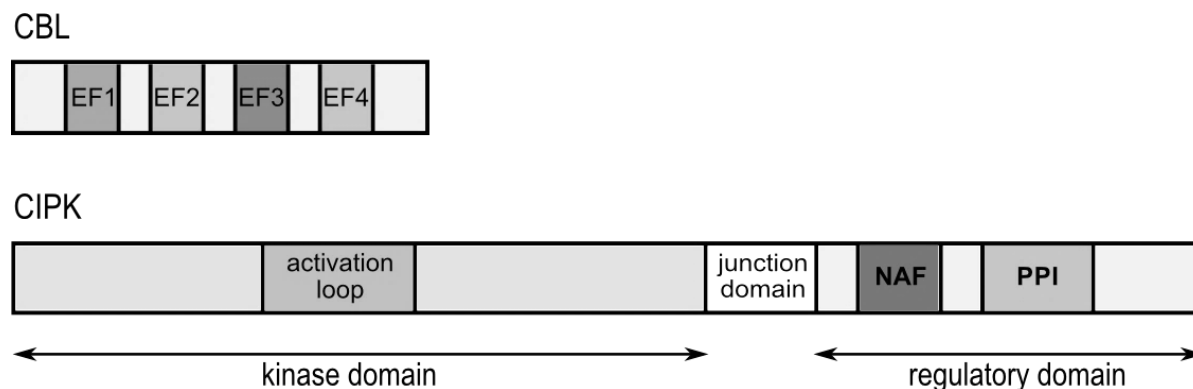
Figure 7: Structural components of CBLs and CIPKs.
EF, elongation factor hand domain; NAF, Asn-Ala-Phe domain; PPI, protein-protein interaction domain. Modified from (Weinl and Kudla 2009; Sanyal, Pandey, and Pandey 2015).

The C-terminal regulatory domain harbours the NAF domain and the protein-phosphatase interacting domain. The NAF-domain is a highly conserved hydrophobic region that is required for the interaction with CBL proteins (Kim et al. 2000; Albrecht et al. 2001). The NAF domain consists of 21 amino acids, where N (Asn), A (Ala) and F (Phe) are the most conserved amino acids. Mutation of certain conserved amino acids in the NAF-domain either completely abolishes or significantly diminishes interaction with CBLs (Albrecht et al. 2001). Binding of

calcium activated CBLs to the NAF-domain liberates the kinase domain from the C-terminal auto-inhibitory domain and allows phosphorylation activity (Guo et al. 2001).

Next to the NAF domain in the C-terminal regulatory region is the protein-phosphatase interacting (PPI) domain, that is responsible for the interaction with type-2C protein phosphatases (PP2Cs) (Ohta et al. 2003; Lee et al. 2007). The PPI domain consists of 37 variable amino acids, that results in specific combinations of CIPKs to a particular PP2C phosphatase (Gong et al. 2004). Studies with CBL4 revealed that either a CBL protein or a PP2C phosphatase exclusively may bind to the regulatory domain of CIPKs, and that formation of a trimeric complex is unlikely (Sánchez-Barrena et al. 2007).

2.6.3   CBL-CIPK signalling

In the CBL-CIPK signalling network, increased cytosolic calcium binds to EF-hands of CBLs, transferring CBL into an active state. Activated CBL binds to the C-terminal NAF-domain of CIPK and thereby removes auto-inhibition from the kinase domain and the kinase moves to the active form (Fig. 8). Interestingly, higher kinase activity can be achieved by further auto- and trans-phosphorylation in the activation loop of the kinase domain, the latter by an unknown kinase (Gong et al. 2002; Batistic and Kudla 2009). Furthermore, the CBL protein is also phosphorylated by an interacting CIPK, that either stabilizes the CBL-CIPK complex or is required for increasing the affinity to downstream protein targets (Lin et al. 2009; Du et al. 2011). Additionally, the cellular localization of the CBL-CIPK complex is determined by interacting CBL proteins. For instance, CIPK23-GFP was observed in cytoplasm and nucleus (Batistic et al. 2010), but the interaction between CIPK23 and CBL1 or CBL9 targeted the CBL-CIPK complex to the plasma membrane (Xu et al. 2006; Cheong et al. 2007).
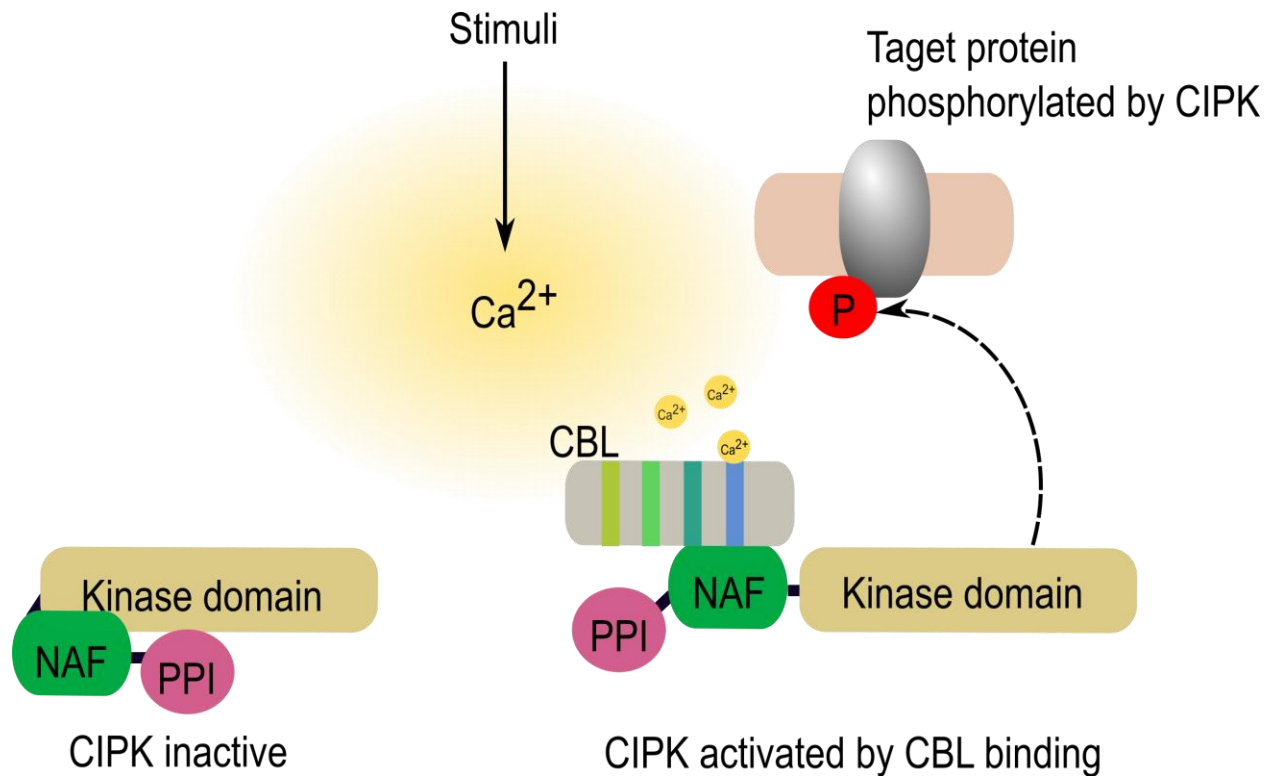
Figure 8: CIPK-CBL model of calcium signatures sensing.
Cytosolic calcium ions interact with EF-domains of CBLs. Activated CBL affiliates to CIPK's NAF-domain, releases the auto-inhibitory domain and finally activates CIPK's kinase domain. Consequently, CIPK's target proteins are phosphorylated. Modified from (Hashimoto and Kudla 2011).

2.6.4 CBL1/9-CIPK23 complex regulates potassium uptake

K^+ TRANSPORTER 1 (AKT1) is one of the most important potassium transporters in *Arabidopsis* (Lagarde et al. 1996; Hirsch et al. 1998; Spalding et al. 1999) and mediates potassium uptake into roots over a wide range of external potassium concentrations. AKT1 is a high-affinity K^+ importer and therefore exhibits its importance in potassium starved plants (Hirsch et al. 1998; Spalding et al. 1999; Xu et al. 2006).

AKT1 is activated by CIPK23 under low external K^+ concentration (Fig. 9). Initially, a low potassium status triggers the increase of cytosolic calcium, that is sensed and bound by CBLs. Calcium activated CBL1 and CBL9 proteins are able to interact physically with CIPK23 and thereby stimulate the phosphorylation activity of CIPK23. Additionally, the CBL-CIPK complex is relocated to the plasma membrane. And finally AKT1 is phosphorylated and low affinity potassium acquisition is initiated (Xu et al. 2006; Cheong et al. 2007).
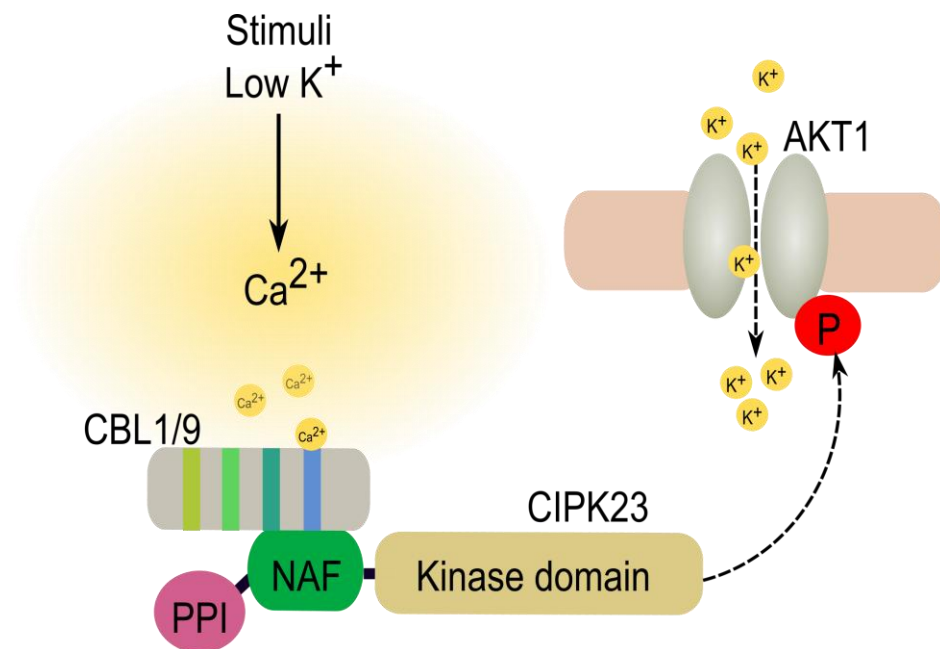
Figure 9: The CBL1/9–CIPK23 pathway regulates AKT1 at low potassium stress.
Low potassium changes the cells calcium signature and calcium activates by direct interaction CBLs, which activate CIPK23. The kinase phosphorylates AKT1 and stimulates potassium transport activity.

2.6.5   CBL1/9-CIPK23 complex regulates nitrate uptake

The CBL-CIPK23 complex regulates not only potassium uptake, but also nitrate (NO_3^-) uptake in plants (Ho et al. 2009). NITRATE TRANSPORTER 1.1 (NRT1.1) is a dual affinity plant nitrate transporter (Liu and Tsay 2003; Ho et al. 2009; Sun et al. 2014) and phosphorylation by CIPK23 switches affinity (Ho et al. 2009). At high nitrate concentrations, homodimeric NRT1.1 acts as low-affinity nitrate transporter in the plasma membrane in a non-phosphorylated state. However, a low external nitrate concentration stimulates NRT1.1 phosphorylation and thereby prevents dimerization, thus each monomer functions as an autonomic high-affinity nitrate transporter (Fig. 10) (Liu, Huang, and Tsay 1999; Liu and Tsay 2003; Ho et al. 2009; Sun et al. 2014).
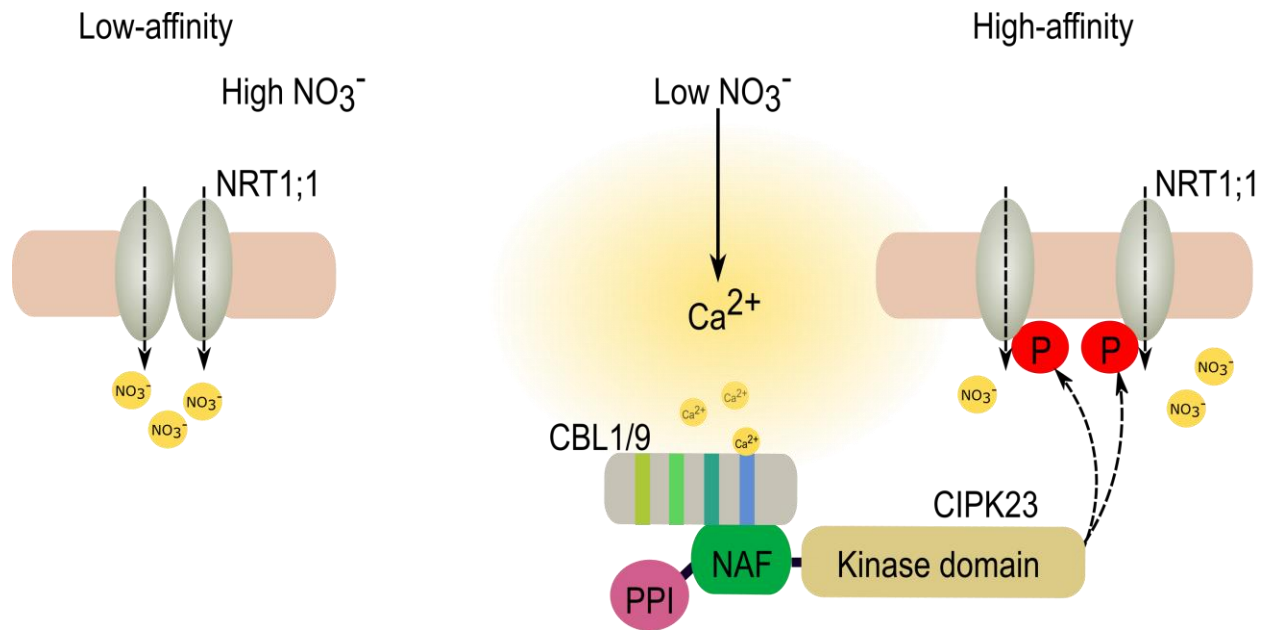
Figure 10: CIPK23 switches NRT1.1 affinity.
NRT1.1 imports nitrate with low affinity at high external nitrate concentrations in a non-phosphorylated stage. When low external nitrate stimulates changes in cell calcium concentration CBL are activated and stimulate CIPK23 kinase activity. CIPK23 phosphorylates NRT1.1 and induces high affinity nitrate transport.

2.7 Research questions and hypotheses

It is hypothesized that *At*AMT function is integrated into a larger regulatory network. This network regulates their expression, degradation and activity by sensing the metabolic state of the cell and integrate this information with other cellular functions. However, crucial components of this regulation had not yet been identified. This work now answers the following questions:

- Which kinase regulates ammonium transport by direct interaction and phosphorylation of AMTs *in planta*?
- Does this kinase specifically interact with individual AMTs, such as AtAMT1;1, AtAMT1;2 and AtAMT2;1?

Starting with candidates from a genetic screen and the simple hypothesis above, straightforward genetic, physiologic and growth experiments were initiated to answer the above research question, summarized schematically in Fig. 11.
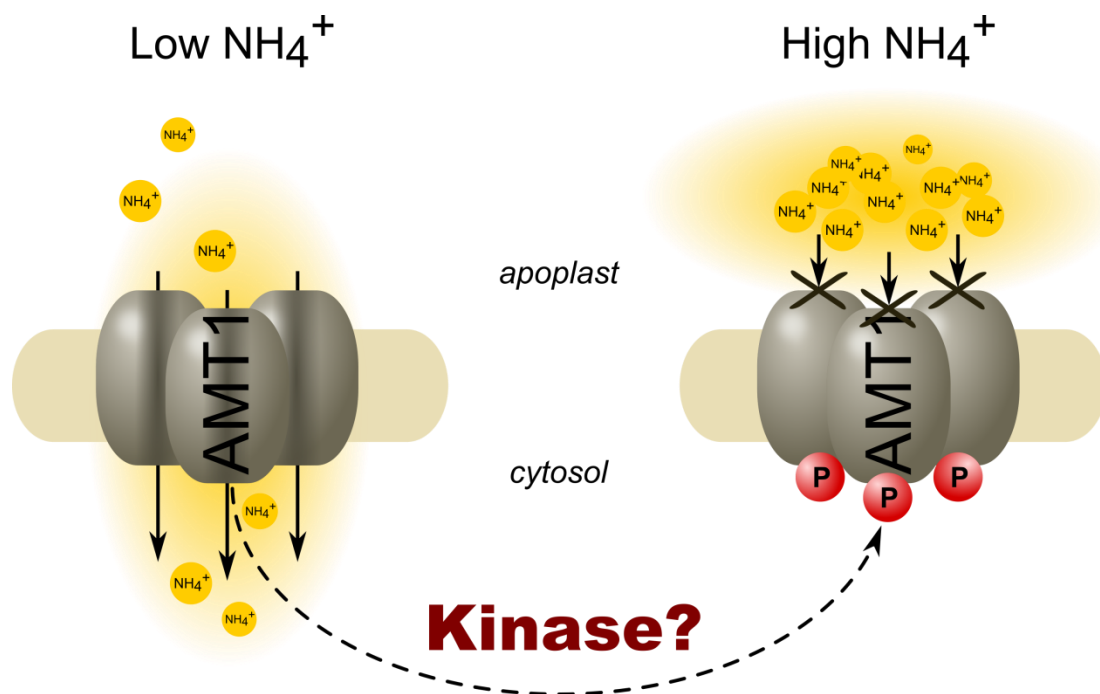
Figure 11: Ammonium transporters (AMT) are regulated by phosphorylation.
Ammonium import is facilitated by the AMT trimer at low ammonium concentrations (left). At high ammonium concentrations in the apoplast AMT transport is shut down by phosphorylation (right). The regulatory kinase is unknown. AMT, ammonium transporter; P (red), phosphorylation.

3 Material

3.1 Chemicals and enzymes

3.1.1 Enzymes

Restriction Endonucleases, 10 U/µl (FastDigest)	Thermo Scientific
Shrimp Alkaline Phosphatase (SAP), 1 U/µl	Thermo Scientific
Ribonuclease A (RNase A) DNase free, 10 µg/µl	AppliChem
T4 DNA Ligase, 400 U/µl	BioLabs
Phusion Polymerase	Thermo Scientific

3.1.2 Enzyme inhibitors

Aprotinin, 10 µg/µl in ddH$_2$O	Sigma-Aldrich
Leupeptin, 10 µg/µl in ddH$_2$O	Sigma-Aldrich
Pepstatin A, 1 µM in MeOH	Sigma-Aldrich
PMSF, 1 mM in MeOH	Sigma-Aldrich
EGTA, 5 mM in ddH2O	Sigma-Aldrich
PhosStop Phosphatase Inhibitor Cocktail	Roche
Phosphatase inhibitor cocktail 2	Sigma-Aldrich
Phosphatase inhibitor cocktail 3	Sigma-Aldrich
Protease inhibitor cocktail	Sigma-Aldrich

3.1.3 Agarose gel electrophoresis

Ethidium bromide 1%, 10 mg/ml	AppliChem
GeneRuler DNA Ladder Mix	Thermo Scientific
Agarose Basic	AppliChem

3.1.4 Mass Spectrometry

Trypsin	Promega
TiO$_2$	GL-Science
Lactic acid	WAKO
Piperidine	WAKO

3.1.5 Western blot

Miracloth	Calbiochem
Watman paper	Haeberle
Nitrocellulose membrane	Peqlab
Super RX-film	Fujifilm
PageRuler Prestained Protein Ladder	Thermo Scientific

3.1.6 Kits

Table 2: Kits with corresponding application and supplier.

Kit	Application	Supplier
NucleoSpin Plasmid Mini	Plasmid-DNA isolation from prokaryotic cells	Macherey Nagel
NucleoBond Xtra Midi	Plasmid-DNA isolation from prokaryotic cells	Macherey Nagel
NucleoSpin Gel and PCR Clean up	DNA purification from agarose gel	Macherey Nagel
InnuPREP Plant NA	RNA isolation from plants	Analytik Jena
KAPA3G direct PCR Plant	Plant direct PCR	Peqlab
Reverse Transcription	Reverse transcription	Qiagen
KAPA YBR FAST qPCR	RT-qPCR analysis	Peqlab

3.2 Buffers and standard solutions

All buffers and standard solutions were made in conformity with standard protocols.

Additional buffers and standard solutions are given in the particular subsections of the chapter 4, Methods.

TAE	40 mM TRIS - pH 8
	1 mM EDTA
	40 mM Glacial acetic acid
TBS	50 mM TRIS - pH 7.6 (HCl)
	150 mM NaCl

| TBST (1%) | TBS - pH 7.9 |
| | 1% (v/v) Tween 20 |

3.3 Bacteria strain, culture medium

DH5α	*Escherichia coli*	**plasmid amplification**
LB medium	1% (w/v) bacto-tryptone	
	0.5% (w/v) bacto-yeast extract	
	1% (w/v) NaCl	
Agar plates	1.5% (w/v) agar in LB medium	
Kanamycin	50 µg/ml (final concentration)	
Spectinomycin	50 µg/ml (final concentration)	
GV3101	*Agrobacterium tumefaciens*	**plant transformation**
Spectinomycin	100 µg/ml (final concentration)	
Rifampicin	100 µg/ml (final concentration)	
Gentamycin	40 µg/ml (final concentration)	

3.4 Expression plasmids

Table 3: Plasmid backbones used in this study.

| Plasmid | Resistance | | Comments |
	E. coli/ A. tumefaciens	*Plant*	
TOPO-blunt	Kanamycin	-	Amplification and sequencing of PCR product, Life Technologies
pTkan+	Spectinomycin	Kanamycin	Generation split YFP plasmids, obtained from Karin Schumacher
pTbar	Spectinomycin	MSX	Generation split YFP plasmids
pUTbar	Spectinomycin	MSX	Generation *amiRNA* construct under ubiquitin-10 promoter
pRS300	-	-	As template for microRNA precursor

Table 4: Available plasmid with a sequence of fluorescent protein used in this study.

Plasmid	Resistance		Comments
	E. coli/ A. tumefaciens	*Plant*	
pTbar-GFP	Spectinomycin	MSX	AMTs localisation in *cipk23* plant line

Table 5: Newly generated plasmids with a sequence of fluorescent protein used in this study.

Plasmid	Resistance		Comments
	E. coli/ A. tumefaciens	*Plant*	
pTkan+-YN	Spectinomycin	Kanamycin	Plant transformation, split YFP assay
pTbar-YC	Spectinomycin	MSX	Plant transformation, split YFP assay

3.5 Oligonucleotides

Oligonucleotides used in this study were ordered in Thermo Fisher Scientific Company. All oligonucleotides were dissolved in ddH$_2$O to a final concentration of 10 µM and stored in aliquots at -20°C.

3.5.1 Sequencing primers and sequence analysis

The DNA sequence analysis was done by the GATC Biotech Company, Germany.

Sequences of inserts in *pTbar* vector were confirmed by the primer:

RB: 5'-ATGTGAGTTAGCTCACTC-3'

Sequences of PCR products in *TOPO-blunt* vector were confirmed by standard primers available at GATC Biotech Company:

M13 FW: 5'- GTAAAACGACGGCCAG-3'

M13 RV: 5'- CAGGAAACAGCTATGAC-3'

3.5.2 Real-time quantitative PCR (RT-qPCR) primers

RT-qPCR primers were designed by the instrumentality of Primer3Plus program (Untergasser et al. 2007).

Table 6: Primers for RT-qPCR gene expression analysis.

Gene	Locus	Forward Primer (5'→3')	Reverse Primer (5'→3')
AMT 1;1	AT4G13510	CGCGGCGCTGACAACCCTAT	GAGGACTAGGGCCGCCACGA
AMT 1;2	AT1G64780	GGCCGGTCCGTGGCTTTACG	GACCGCGGTGCGACCTACAG
AMT 1;3	AT3G24300	CGGCCACTCTGCCTCGCTAG	CCGCACACAATCGCTGCCCA
AMT 1;5	AT3G24290	TTCAACCCTGGTTCCTTCAC	ACGTTTTCCGAAGAGTGTGG
AMT 2;1	AT2G38290	GGTGCTCCTTACGCGGCCAA	CGGGAGTGACGCCGGCTAAG
CIPK23	AT1G30270	CGTTTTGGAATTCGTCACTG	TGTTGGAAATACTTCCTCGC
CBL1	AT4G17615	CATTGAACGACAAGAGGTCA	CTTGATTCACGTCTGCATCT
CBL9	AT5G47100	ATTGAGCGCCAAGAGGTGAA	CCATCCCGATCCACATCTGC
AKT1	AT2G26650	CGGTGATGACGAATGTTCTG	TGCCATTGTTATCCGATTCA
KUP4	AT4G23640	ACGGAGGCTATCTTTGCTGA	TGCTTGACTAGCGACCATTG
KUP8	AT5G14880	CGCACTCTCCTTCATCTTCC	CGAGACAAGTTCGGTGTTGA
PDF	AT1G13320	TAACGTGGCCAAAATGATGC	GTTCTCCACAACCGCTTGGT
SAND	AT2G28390	CAGACAAGGCGATGGCGATA	GCTTTCTCTCAAGGGTTTCTGGGT

3.5.3 SALK T-DNA verification primers

To verify knock-out lines homozygous, primers designed by the program of Salk Institute Genomic Analysis Laboratory were used ("T-DNA Primer Design" 2015).

Table 7: SALK primers.

Gene	SALK number	RP Primer/ **LP Primer** (5'→3')	LBb1.3 Primer (5'→3')
AT1G30270	036154C	AATCATCCCGGACAAAGTACC/ **TTGTGATCCTCTTGCATAGGG**	ATTTTGCCGATTTCGGAAC
AT2G41890	058928C	ATTCTCAGATTACCATCCCGG/ **ATCTTGGGTCCCATTTTTCAG**	ATTTTGCCGATTTCGGAAC

3.5.4 Primers to create artificial microRNA

Primers for microRNA (5'-TAGCATAGCGAAGTCGGGCTG-3') were obtained with the help of the WMD3 designer (Ossowski, Schwab, and Weigel 2008).

Table 8: *AmiRNA* primers.

Primer name	Primer sequence (5'→3')
I (miR-s)	GATAGCATAGCGAAGTCGGGCTGTCTCTCTTTTGTATTCC
II (miR-a)	GACAGCCCGACTTCGCTATGCTATCAAAGAGAATCAATGA
III (miR*s)	GACAACCCGACTTCGGTATGCTTTCACAGGTCGTGATATG
IV (miR*a)	GAAAGCATACCGAAGTCGGGTTGTCTACATATATATTCCT
A	CTGCAAGGCGATTAAGTTGGGTAAC
B	GCGGATAACAATTTCACACAGGAAACAG

3.5.5 Primers for split eYFP plasmid construction

Primers for split YFP assay are listed in the corresponding subsections, where the split YFP subcloning strategy is described (subsections *4.4.3.2 – 4.4.3.5*, Tables 15–17).

3.6 Antibodies used in Western blot

Table 9: Antibodies used in Western blot (WB).

Primary antibody	Type of antibody	Dilution	Source
Anti-GFP	Rabbit, polyclonal IgG	1:20000	Rockland
Anti-phospho-pep40227 (anti-P)	Rabbit, monoclonal IgG	1:1000	BioGenes
Secondary antibody	Type of antibody	Dilution	Source
Anti-rabbit	Goat, polyclonal IgG, conjugated to horseradish peroxidase (HRP)	1:5000	Roth

3.7 Plant material

3.7.1 Plant lines

Several transgenic plant lines were used in this study, some were newly generated, others were already available. All plant lines are in *Arabidopsis thaliana*, ecotype Columbia-0 (Col-0).

Table 10: Obtained plant lines.

Plant line	Source/ Reference
k1-1 (cipk23-1), SALK_036154C	SALK
k1-2 (cipk23-2), SALK_112091C	SALK
k2, SALK_058928C	SALK
qko	von Wiren (Yuan et al. 2007)
cbl1, SALK_110426C	SALK
cbl9, SALK_142774C	SALK

Table 11: Newly generated transgenic *A. thaliana* plants.

Plant line name	Plasmids used for plants' transformation	Plants' resistance
cipk23-AMT1;1-GFP	*pTbar pAMT1;1::AMT1;1-GFP*	MSX
cipk23-AMT1;2-GFP	*pTbar pAMT1;2::AMT1;2-GFP*	MSX
cipk23-AMT2;1-GFP	*pTbar pAMT2;1::AMT2;1-GFP*	MSX
*AMT1;1-NY/**AMT1;1-CY***	*pTkan⁺ pAMT1;1::AMT1;1-NY/* ***pTbar pAtAMT1;1:AMT1;1-CY***	Kanamycin MSX
*AMT1;2-NY/**AMT1;2-CY***	*pTkan⁺ pAMT1;2::AMT1;2-NY/* ***pTbar pAMT1;2::AMT1;2-CY***	Kanamycin MSX
*AMT1;1-NY/**CIPK23-CY***	*pTkan⁺ pAMT1;1::AMT1;1-NY/* ***pTbar pCIPK23::CIPK23-CY***	Kanamycin MSX
*CIPK23-NY/**AMT1;1-CY***	*pTkan⁺ pCIPK23::CIPK23-NY/* ***pTbar pAMT1;1::AMT1;1-CY***	Kanamycin MSX
*AMT1;2-NY/**CIPK23-CY***	*pTkan⁺ pAMT1;2::AMT1;2-NY/* ***pTbar pCIPK23::CIPK23-CY***	Kanamycin MSX
*CIPK23-NY/**AMT1;2-CY***	*pTkan⁺ pCIPK23::CIPK23-NY/* ***pTbar pAMT1;2::AMT1;2-CY***	Kanamycin MSX
*AMT2;1-NY/**CIPK23-CY***	*pTkan⁺ pAMT2;1::AMT2;1-NY/* ***pTbar pCIPK23::CIPK23-CY***	Kanamycin MSX
AMT1;1-NY/ ***pCIPK23::CY***	*pTkan⁺ pAMT1;1::AMT1;1-NY/* ***pTbar pCIPK23::CY***	Kanamycin MSX
AMT1;2:NY/ ***pCIPK23::CY***	*pTkan⁺ pAMT1;2::AMT1;2-NY/* ***pTbar pCIPK23::CY***	Kanamycin MSX
AMT2;1-NY/ ***pCIPK23::CY***	*pTkan⁺ pAMT2;1::AMT2;1-NY/* ***pTbar pCIPK23::CY***	Kanamycin MSX
cipk23-amiRNA	*pUTbar amiRNA*	MSX
pCIPK23::CIPK23-1	*pTbar pCIPK23::CIPK23*	MSX
pCIPK23::CIPK23-3	*pTbar pCIPK23::CIPK23*	MSX

3.7.2 Plant mediums

Hydroponic plant culture and root growth analysis on agar plates were done on Modified Hoagland medium (HL).

Table 12: Modified Hoagland medium.

Salt	Concentration, µM
KH_2PO_4	1000
$MgSO_4$	500
$CaCl_2$	1000
$MnCl_2$	9
$ZnSO_4$	0.765
$CuSO_4$	0.32
H_3BO_3	46
Na_2MoO_4	0.016
FeNaEDTA	50

Nitrogen supply in HL medium was dependent on experiment requirement and described in the corresponding chapters.

Selection of transgenic plants was done on ½ strength of Murashige and Skoog (MS) medium basal salt mixture (Duchefa Biochemie) with required selection agent.

Agar plates contained 0.8% (w/v) Phyto agar (Duchefa Biochemie) in HL or MS medium.

4 Methods

4.1 Molecular biological methods

4.1.1 Plasmid DNA extraction: Alkaline lysis of *E. coli*

Required solutions:	TEG:	25 m Tris pH 8
		10 mM EDTA
		50 mM glucose
	SDS-NaOH:	200mM NaOH
		1 % SDS
	KAc:	3M pH 4.8

1.5 ml of fresh bacteria overnight culture containing the plasmid of interest was first centrifuged at full speed for 2 min. The supernatant was discarded, and the pellet was then suspended in 100 µl TEG buffer with RNAse. 200 µl of SDS-NaOH solution was added and samples were mixed by inversion. Finally 150 µl potassium acetate was added and again mixed by inversion. The precipitate was pelleted by full speed centrifugation (20000g) for 10 min. 200 µl of the plasmid-containing supernatant was carefully transferred to 800 µl cold 70% ethanol to recover and clean up the plasmid DNA. A final centrifugation step (10°C, full speed) collected the plasmid DNA in a pellet. The DNA was dissolved in 30 µl distilled water and stored at -20°C.

4.1.2 Plasmid DNA double digestion with restriction enzymes

Double restriction of DNA has been done with Thermo Scientific universal 10x FastDigest Green Buffer (Thermo Scientific).

Reaction conditions:

10X FastDigest Green Buffer	2 µl
DNA	1 µg
FastDigest restriction enzyme I	0.5 µl
FastDigest restriction enzyme II	0.5 µl
H_2O	up to 20 µl

Restriction ingredients were mixed gently and incubated at 37°C in a heating block. One hour later the mix was subjected to agarose gel electrophoresis.

4.1.3 Agarose gel electrophoresis

For visualization and purification, DNA fragments were separated according to their size range by agarose gel electrophoresis. The concentration of the agarose gel in TAE buffer dependent on the expected size of DNA fragment and was between 0.8 - 2% (w/v). Additionally to the DNA sample, 10 µl of "GeneRuler DNA Ladder Mix" (Thermo Scientific) was loaded on the agarose gel to estimate the molecular weight of DNA fragments. The gel was run at 80 – 120 V for 1 - 2 hours. When necessary DNA was extracted from the agarose gel and purified by NucleoSpin Gel and PCR Clean-up Kit (Macherey-Nagel) according to the manufacturer's instructions.

4.1.4 Vector dephosphorylation

In order to prevent vector self-ligation, 5' phosphates of linearized vectors were released by Shrimp Alkaline Phosphatase (SAP).

Reaction conditions:

10X SAP buffer	2 µl
DNA	15 µl
Shrimp Alkaline Phosphatase	0.5 µl
H_2O	2.5 µl
Total volume	20 µl

Reaction mixtures were mixed thoroughly, centrifuged briefly and incubated at 37°C for 60 min. The reaction was stopped by heating at 65°C for 15 min.

4.1.5 Ligation of DNA fragments

Vector and insert volumes required in a ligation reaction were calculated according to the following equations (Cranenburgh 2004):

$$V_v = \frac{T}{\left(\dfrac{V_c * I_l * I_r}{I_c * V_l}\right) + 1}$$

$$I_v = T - V_v$$

where:

I_l	insert length
V_l	vector length
I_c	Insert concentration
V_c	vector concentration
I_r	required insert-to-vector ratio
T	volume of total DNA solution component
V_v	vector volume
I_v	insert volume

The optimal vector:insert ratio (I_r) of 1:3 was determined by using the equation above.

Ligation reactions were performed with the following ingredients:

Vector	x µl
Insert	y µl (x+y = 8 µl)
10X ligase buffer	1 µl
T4 DNA ligase	0.25 µl
H₂O	0.75 µl
Total volume	10 µl

The ligation reaction was gently mixed by pipetting up and down, centrifuged briefly and incubated overnight at room temperature (RT). 5 µl of the ligation reaction was transformed into 50 µl chemically competent *E. coli* (DH5α^TM) cells.

4.1.6 Transformation of *E. coli* (DH5α[TM]) chemically competent cells

50 µl chemically competent *E. coli* (DH5α[TM]) (Life Technologies) cells were thawed on ice for 10 min. 50 ng of DNA was added, mixed gently and held on ice for additionally 10 min. Afterwards, *E. coli* cells were processed with a heat shock at 42°C for 1 min and then placed on ice for another 10 min. 800 µl LB medium was added to the *E. coli* cells and the mixture was incubated at 37°C with continuous shaking (300 rpm) for 180 min at room temperature for cell recovery and expression of antibiotic resistance. To select recombinant bacteria, 100 µl of the transformation mixture were spread onto selective LB agar containing the appropriate antibiotics. Plates were inverted and incubate at 37°C overnight.

Subsequently, colonies were picked, grown in 5 ml liquid LB with appropriate antibiotics overnight in 37°C and 180 rpm shaking. Plasmid DNA was isolated as described previously (alkaline lysis method) and controlled by restriction enzyme analysis and/or by sequencing (GATC biotech).

4.1.7 Control digest of DNA

Reaction conditions:

10X FastDigest Green Buffer	2µl
DNA	0.5 – 1µg
FastDigest restriction enzyme	0.5 µl
H_2O	up to 20 µl

The reaction was held 1h at 37°C and then was loaded on 1% (w/v) agarose gel electrophoresis.

4.1.8 Transformation of *Agrobacterium tumefaciens* (GV3101) chemically competent cells

200 µl chemically competent *A. tumefaciens* cells were thawed on ice for 90 min. Around 200 ng of plasmid DNA was carefully mixed with the competent bacteria and kept on ice for 10 min and then flash-frozen in liquid nitrogen for 5 min. The bacteria were heat shocked (37°C, 5 min) and afterwards recovered in 800 µl LB medium for 4 hours at 28°C. 100 µl of transformation reaction were spread onto a selection plate containing LB medium with rifampicin, gentamycin

and spectinomycin. Plates with bacteria were inverted and incubated at 28°C and resistant colonies were further analyzed after 2 to 3 days.

Subsequently, 3-5 colonies were picked, grown in 5 ml liquid LB with appropriate antibiotics overnight in 28°C and 180 rpm shaking. Plasmid DNA was isolated as described previously (alkaline lysis method). 50µl *E. coli* competent cells were transformed with 200 ng plasmid DNA extracted from *A. tumefaciens* cells as described in 4.1.6. Eventually plasmid DNA was controlled by restriction enzyme analysis (chapter 4.1.7.).

4.1.9 Concentration determination of nucleic acids (NanoDrop)

Nucleic acid (DNA, RNA) concentration and purity were measured using the NanoDrop ND-1000 spectrophotometer (Thermo Scientific).

The absorption of $1 - 1.5$ µl of a nucleic acids solution was measured at 260 nm against the solvent. The purity of a DNA or RNA was estimated using the absorbance ratio of 260 nm and 280 nm (260/280). The ratio of ~1.8 for DNA and ~2.0 for RNA was accepted as a "pure" nucleic acid ("Measure Nucleic Acids with NanoDrop Products" 2016).

4.2 Generation of transgenic bacteria

4.2.1 Making *E. coli* (DH5α^{TM}) chemically competent

Required solutions: LB

100 mM $CaCl_2$, autoclaved, ice cold

4:1 $CaCl_2$:Glycerol, autoclaved, ice cold

A fresh LB plate of *E. coli* cells was prepared by streaking out cells from a frozen stock and growing overnight at 37°C. An individual colony was picked and inoculated in 10 ml LB medium overnight. 5 ml overnight culture were inoculated into 500 ml LB medium and incubated at 37°C with continuous shaking until the culture reached 0.6-0.7 OD_{600}. *E. coli* cells were harvested by spinning at 3000 rpm for 10 min at 4°C. Supernatant was discarded and bacterial pellet was gently resuspended in 50 ml ice cold $CaCl_2$, with followed centrifugation at 3000 rpm for 10 min at 4°C. Bacterial pellet was resuspended in 5 ml ice cold 4:1 $CaCl_2$:Glycerol. 50µl aliquots of competent *E.coli* cells were frozen in liquid nitrogen and stored at -80°C.

4.2.2 Making *Agrobacterium tumefaciens* (GV3101) chemically competent

Required solutions: LB

150 mM NaCl

20 mM $CaCl_2$

A fresh LB plate (containing rifampicin and gentamicin) of *A. tumefaciens* cell was prepared by streaking out cells from a frozen stock and growing 3 days at 28°C. An individual colony was picked and inoculated in 5 ml LB medium for 24 hours at 28°C. 4 ml fresh *A. tumefaciens* culture was inoculated into 200 ml LB medium with appropriate amount of antibiotics (rifamycin + gentamicin) and incubated at 28°C on a shaker until the culture reached OD_{600} approximately 0.5 (about 7 hours). *A. tumefaciens* cells were harvested by centrifugation at 5000 rpm for 10 min at 4°C. The supernatant was discarded and the bacterial pellet was resuspended in 50 ml NaCl. After that bacterial cells were spun down at 5000 rpm for 10 min at 4°C. *A. tumefaciens* pellet was gently resuspended in 8 ml ice cold $CaCl_2$. Competent *A. tumefaciens* cells were aliquoted (200 µl), frozen in liquid nitrogen and stored at -80°C.

4.3   PCR reaction with Phusion polymerase

All PCR reactions in this study were done with Phusion High-Fidelity DNA polymerase. This polymerase was chosen due to ability to generate long templates with high accuracy and speed.

Reaction conditions:

Phusion HF buffer	10 µl
10 mM dNTPs	1 µl
FW primer (10 µM)	1 µl
FW primer (10 µM)	1 µl
DNA template (1-10 ng)	x µl
Phusion polymerase	0.5 µl
H_2O	up to 50 µl

Table 13: Phusion polymerase PCR conditions.

Cycle step	Temperature	Time	Cycles
Initial denaturation	98°C	30 s	1
Denaturation	98°C	10 s	
Annealing	*	20 s	30 – 35
Extension	72°C	30 s per 1 kb	
Final extension	72°C	5 – 10 min	1

* Annealing temperature (T_m) of primers was calculated with the nearest neighbor method ("Tools >> The Sequence Manipulation Suite" 2015). For primers ≤ 20nt the annealing temperature was equal to the T_m of the lower T_m primer. For primers >20nt the annealing temperature was +3°C to the T_m of the lower T_m primer.

4.4 Subcloning

All PCR products used in subcloning reactions were generated by Phusion polymerase in PCR reactions, described in Chapter 4.3. DNA was separated by agarose gel electrophoresis (Chapter 4.1.3), extracted from gel by NucleoSpin Gel and PCR Clean-up Kit (Macherey-Nagel) and cloned into *TOPO-blunt* vector (Life Technologies), according to the manual description. PCR products were full-length sequenced (GATC biotech, Germany).

4.4.1 Artificial microRNA

Artificial microRNA (5'-TAGCATAGCGAAGTCGGGCTG-3') targeting ammonium transporters (AMT1;1, AMT1;2, AMT1;3, and all AMT1 at once) was designed using the *amiRNA* designer interface WMD3 - Web MicroRNA Designer (Schwab et al. 2006).

The selected *amiRNA* sequence was introduced into the miR319a precursor by side-directed mutagenesis according to cloning protocol developed by (Schwab et al. 2006) (Fig. 12).
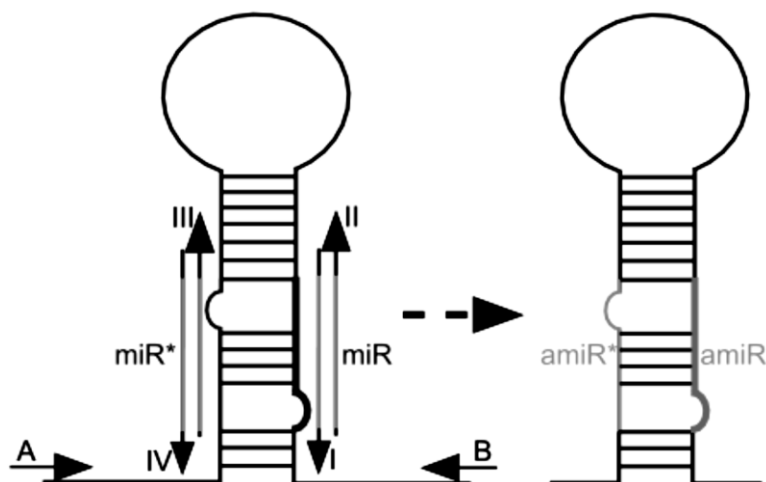
Figure 12: MicroRNA cloning strategy.
I: microRNA forward primer, II: microRNA reverse primer, III: microRNA* forward primer, IV: microRNA* reverse primer (primers' sequences listed in the Table 8).

The *amiRNA* (fragment d) containing precursor is generated by overlapping PCR. At first fragments (a) to (c) were amplified by PCR (Table 14).

Table 14: Primers in PCR reactions for *amiRNA* construction.

PCR fragment	FW primer	RV primer	Template
a	A	IV	pRS300
d	III	II	pRS300
c	I	B	pRS300
d	A	B	a+b+c

For the first 3 PCRs the template was the plasmid pRS300 with the Arabidopsis microRNA precursor miR319a (Schwab et al. 2006). The obtained *amiRNA* precursor was cloned from *TOPO-blunt* vector into *SalI – BcuI* sites of *pUTbar* vector containing the ubiquitin-10 promoter (UBQ10) promoter (Fig. 13).
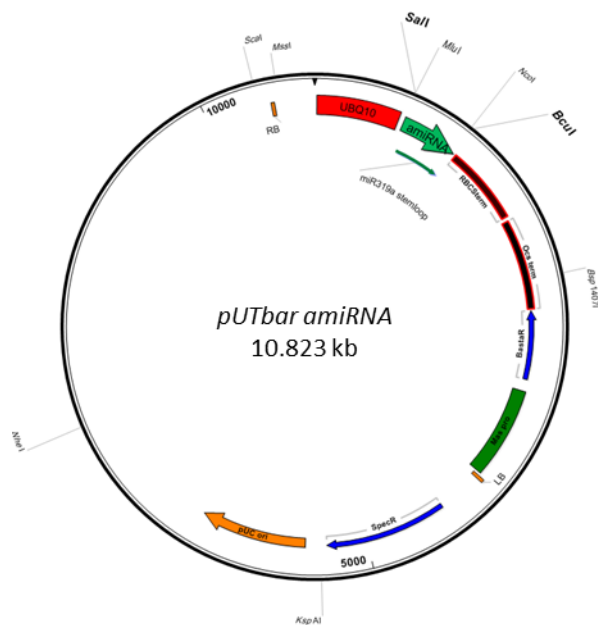
Figure 13: *pUTbar* vector containing *amiRNA* to silence *AMT1s*.

4.4.2 Generation of plasmids

4.4.2.1 AtAMT1;1-GFP, AtAMT1;2-GFP, AtAMT2;1-GFP

To localize AtAMT1;1, AtAMT1;2, AtAMT2;1 in *cipk23* mutant plants listed ammonium transporters were fused to GFP. The promoter and coding regions of AMT1;1 (At4g13510; 1503 bp), AMT1;2 (At1g64780; 3307 bp) and AMT2;1 (At2g38290; 3386 bp) were cloned from *pAMT1;1::AMT1;1-GFP pTkan*[+] (Mayer and Ludewig 2006), *pAMT1;2::AMT1;2-GFP pTkan*[+] (Neuhäuser et al. 2007) and *pAMT2;1::AMT2;1-GFP pTkan*[+] (Neuhäuser, Dynowski, and Ludewig 2009) vectors respectively into the plant transformation binary vector *pTbar-GFP* using the *MssI* and *XbaI* restriction sites (Fig 14).

Figure 14: *pTBar* vectors with AMT-GFP constructs under their own promoters.

4.4.2.2   Split YFP plasmid construction. pTkan⁺ YN 153stop, pTbar YC stop.

The YFP molecule was split between amino acids 153 and 154 (Ohad, Shichrur, and Yalovsky 2007). The N-terminal fragment (N-eYFP, 1-153 aa) and C-terminal fragment (C-eYFP, 154-239 aa). The PCR of the N-terminal fragment was performed with primers including *MluI-XhoI* restriction sites and of the C-terminal fragment with primers including *SalI-BcuI* restriction sites (Table 15).

39

Table 15: Primers for constructing split YFP vectors.

eYFP part	Forward Primer	Restriction site
N-eYFP	GCGCACGCGTTTATGGTGAGCAAGGGCGAG	*MluI*
C-eYFP	GCGCGTCGACTTGACAAGCAGAAGAAC	*SalI*

eYFP part	Reverse Primer	Restriction site
N-eYFP	GCGCCTCGAGTTTCAATAGACGTTGTGGCTG	*XhoI*
C-eYFP	GCGCACTAGTTTTTACTTGTACAGCTCGTC	*BcuI*

The reverse primer of N-eYFP was designed to establish translation termination after 152 aa to produce the N-eYFP fragment (Ohad, Shichrur, and Yalovsky 2007).

The eYFP fragments were individually inserted into the multiple cloning site of the *pTkan⁺* and *pTbar* vectors, N-eYFP using *MluI* and *XhoI* and C-eYFP into *SalI-BcuI* restriction sites. Thereby the *pTkan⁺ YN 153stop* and *pTbar YC stop* vectors were constructed (Fig. 15).
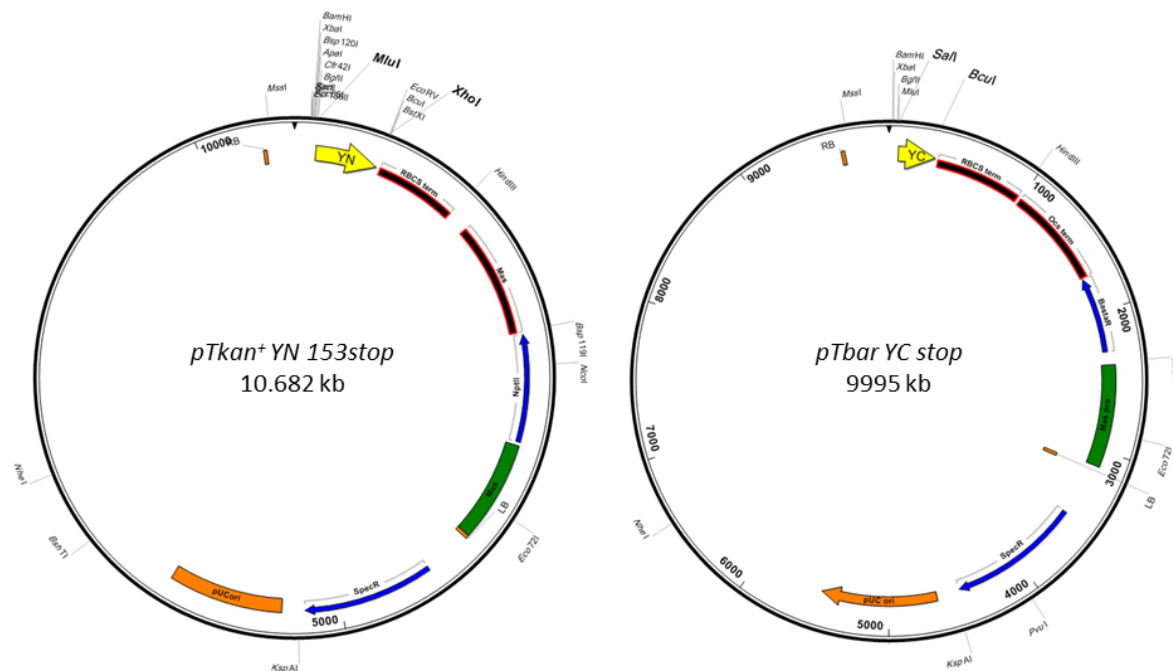
Figure 15: Split YFP vectors.
Left: *pTkan⁺ YN 153stop*, right: *pTbar YC stop*.

4.4.2.3   pTkan⁺ pCIPK23::CIPK23-NY, pTbar pCIPK23::CIPK23-CY

The sequence *pCIPK23::CIPK23* was amplified in a PCR reaction. Primers were constructed with cutting sites for following subcloning reactions.

pCIPK23::CIPK23 was inserted into *pTKan⁺ NY 153stop* vector by *KpnI-ApaI* restriction sites and into *pTbar CY stop* by *MluI-MluI* restriction sites. For *pTbar pCIPK23::CIPK23-CY* the right orientation of the pCIPK23::CIPK23 was checked by control digestion.

Table 16: Primers for CIPK23 split YFP constructs.

Vector	Forward Primer	Restriction site
pTKan⁺ NY 153stop	GCGCGGTACCAAGGTCATGTGTATGT	*KpnI*
pTbar CY stop	GCGCACGCGTAAGGTCATGTGTATGTAC	*MluI*
Vector	Reverse Primer	Restriction site
pTKan⁺ NY 153stop	GCGCGGGCCCGCTGTCGACTGTTTTG	*ApaI*
pTbar CY stop	GCGCACGCGTTGCTGTCGACTGTTTTGC	*MluI*

4.4.2.4   pTkan⁺ pCIPK23::NY, pTbar pCIPK23::CY

The promoter region (1500 bp) of *CIPK23* was amplified in a PCR reaction. Primers were constructed in a way to introduce *MluI-MluI* cutting sites at the beginning and at the end of the PCR product.

Primers:

pCIPK23 FW   GCGCACGCGTAAGGTCATGTGTATGTAC

pCIPK23 RV   ATACGCGTCTCTCTCTCTATATATATATC

Promoter *CIPK23* was inserted instead of *pCIPK23::CIPK23* into *pTkan⁺ pCIPK23::CIPK23-NY* and *pTbar pCIPK23::CIPK23-CY* by *MluI-MluI* cutting sites.

An ATG site at the beginning of C-eYFP fragment was created by a site-directed mutagenesis approached. C-eYFP in *TOPO* vector was used as a template in the PCR reaction (Phusion polymerase).

Primers:

C-eYFP + ATG FW   CTTGCGTCGACATGGACAAGCAGAAG

C-eYFP + ATG RV   CTTCTGCTTGTCCATGTCGACGCAAG

The sequence of the PCR product was checked by GATC sequencing and C-eYFP+ATG was cloned instead C-eYFP into *pTbar pCIPK23::CIPK23-CY* vector by *SalI-BcuI* restriction sites.

4.4.2.5   *pTkan⁺ pAMT1;1::AMT1;1-NY, pTkan⁺ pAMT1;2::AMT1;2-NY, pTkan⁺ pAMT2;1-NY; pTbar pAMT1;1::AMT1;1-CY, pTbar pAMT1;2::AMT1;2-CY, pTbar pAMT2;1::AMT2;1-CY*

N- and C-terminal fragments of eYFP were amplified by Phusion polymerase in PCR reactions and *PagI-SalI* linkers were introduced.

Table 17: Primers for AMTs split YFP constructs.

eYFP part	Forward Primer	Restriction site
N-eYFP (NY)	CCTTTCATGATTATGGTGAGCAAGG	*PagI*
C-eYFP (CY)	CCTTTCATGATTGACAAGCAGAAG	*PagI*
eYFP part	Reverse Primer	Restriction site
N-eYFP (NY)	GCGCGTCGACTCAATAGACGTTGTGGCT	*SalI*
C-eYFP (CY)	GCGCGTCGACTTACTTGTACAGCTCG	*SalI*

N-eYFP and C-eYFP fragments were inserted instead of GFP into *pAMTs::AtAMTs-GFP pTkan⁺* and *pAMTs::AtAMTs-GFP pTbar* vectors (described above) respectively using *PagI-SalI* restriction sites.

4.4.3   CIPK23 complementation line

To introduce the *CIPK23* gene in the *cipk23* mutant plants and create complementation lines, *cipk23* plants were transformed with the *pTbar-pCIPK23::CIPK23* vector (Chapter 4.6.4). *PromoterCIPK23::CIPK23stop* was amplified in a PCR reaction (Chapter 4.3). Following primers were used:

FW   GCGCACGCGTAAGGTCATGTGTATGTAC

RV   CGCGACTAGTTTATGTCGACTGTTTTGC

The forward primer harbors a *MluI* cutting site and the reverse primer a *BcuI* cutting site. The reverse primer additionally introduces a single nucleotide mutation to the TAA stop codon at the end of *CIPK23* CDS. *pCIPK23::CIPK23stop* was inserted by *MluI-BcuI* into the *pTbar* vector. The expression of the *CIPK23* gene was checked by qPCR (Chapter 4.5).

4.5   Expression analysis

4.5.1   Total RNA isolation from plants

To verify gene expression *Arabidopsis* plants were grown hydroponically as described in the chapter 4.6.3.

To analyze change in transcript levels after ammonium resupply, plants were grown 6 weeks in HL with 1000 µM NH_4NO_3, pH was adjusted to 6.0 with KOH. After 6 weeks plants were moved to HL without nitrogen for 4 days. Ammonium was resupplied to N-starved plants in the concentration of 2 mM NH_4^+ (HL with 1 mM $(NH_4)_2SO_4$) for 5, 15, 30, 60 and 120 min or for 30 min only.

After the treatment plants were removed from the solution and briefly dried with paper. Roots were separated from the shoots, immediately frozen in liquid nitrogen and stored at -80°C.

The frozen roots of minimum three plants were pooled and homogenized in liquid nitrogen. RNA was isolated from 100 mg of ground roots, according to the manufacturer's instructions of the RNA extraction kit (Analytik Jena). RNA concentration and purity was measured by NanoDrop (Chapter 4.1.9).

4.5.2   cDNA synthesis, reverse transcription of mRNA into cDNA

Amounts of 1 µg RNA were applied to a reverse transcription reaction. Reverse transcription has been done according to the manufacturer's instructions (Reverse transcription kit (Qiagen)) using a mix of oligo-dT and random oligomers (Qiagen).

4.5.3 Real time-quantitative PCR (RT-qPCR)

The cDNA was amplified using KAPA SYBR FAST qPCR kit (Peqlab) and the C1000 Thermo Cycler combined with a CFX 384 Real Time (BIO-RAD) system. Each RT-PCR reaction contained 0.05 µg of total RNA in a total volume of 15 µl. The cDNA was pipetted in duplicates, each 6 µl, into the wells of the 384-well qPCR plate (BIO-RAD). The qPCR mix was prepared with 200 nmol (final concentration) of each primer.

qPCR mix:

Supermix (2x)	7.5 µl
FW primer (10 µM)	0.3 µl
RV primer (10 µM)	0.3 µl
H_2O	0.9 µl
Total volume	9 µl

The PCR reaction was done with the following program:

Step	Temperature	Duration	Cycles
Initial denaturation	95°C	3 minutes	1
Denaturation	95°C	3 seconds	45 cycles
Annealing/ Elongation	60°C	20 seconds	
Melting curve	65°C to 95°C Increment 0.2°C		

To discriminate between specific and non-specific PCR products, the PCR reaction profile included a melting curve analysis. In this step, the temperature-dependent (from 65°C to 95°C) dissociation of the DNA product (double-stranded DNA) was measured. To control primer dimers formation, qPCR mix without DNA – a no template control (NTC), was included for each primer pair.

For each sample the CFX Manager 3.0 software (BIO-RAD) measured the threshold cycle (*Ct* value), a defined cycle, in which the fluorescence generated within a reaction has exceeded a

fluorescence threshold (the background fluorescence). The gene expression was normalized by the *ΔΔCt*-method (BIO-RAD software), in which the expression of the target gene was normalized to the expression levels of *PDF* and *SAND* reference genes. *PDF* and *SAND* expression stability values were below the quality thresholds for control (CV<0.25, M<0.5).

Acceptable values for stably expressed reference genes (Hellemans et al. 2007):

Sample	CV	M
Homogeneous	< 0.25	< 0.5
Heterogeneous	< 0.5	< 1

CV – Coefficient of Variation of normalized reference gene relative quantities; **M** – M-value, a measure of the reference gene expression stability.

Often one of the samples was set as a control sample. In this situation, the software normalized the relative expression of the target gene to the control gene expression (established at 1). This normalized expression is Relative Normalized Expression.

4.6 Plant methods

4.6.1 Verification of *k1* and *k2* homozygousy

Homozygousy of the *CIPK23* (*k1*, SALK_036154C) and the *lectin protein kinase* (*k2*, SALK_058928C) knock-out lines were verified by direct PCR (KAPA3G direct PCR Plant kit, PEQLAB Biotechnologie GmbH) using SALK designed primers (Table 7). The PCR was repeated two times to verify the result.

4.6.2 Plant growth on plates with MeA

Seeds were surface-sterilized with 70% ethanol, containing 0.001% Triton, germinated and grown for four days on modified Hoagland medium (HL) containing 2 mM KNO_3 as single nitrogen source. The growth medium was buffered with 20 mM MES (pH 6.0) and had 0.8% Agar. Afterwards seedlings were either transferred to the control medium (HL with 2 mM KNO_3) or to medium containing additionally 20 or 30 mM MeA. Plates were placed vertically in a plant growth chamber (Percival Scientific) for 10 days (short day: 8h/16h day/night; 22°C/18°C). Root

systems were scanned at a resolution of 400 dpi (Epson Expression 10000XL) and the root length was determined using ImageJ software (Schneider, Rasband, and Eliceiri 2012). Relative root length was calculated by dividing root length on MeA medium (HL 2 mM KNO_3, 20 mM MeA/30 mM MeA) after 10 days by the root length on the control medium (HL 2 mM KNO_3) after 4 days.

4.6.3 ^{15}N uptake test in hydroponic culture

Plants were grown for six weeks hydroponically in modified Hoagland medium (HL) with 1000 µM NH_4NO_3, pH was adjusted to 6.0 with KOH. When explicitly stated, hydroponic growth experiments were additionally supplemented with 2000 µM K_2SO_4, resulting in a total potassium concentration of 5 mM.

In the first two weeks the nutrient solution was replaced once a week, in week three and four twice a week and in the last two weeks every second day. Plants were grown in non-sterile hydroponics in a growth chamber under tightly controlled environment conditions (8h/16h day/night; light intensity 100-120 µmol $m^{-2} s^{-1}$; temperature 22°C/18°C and humidity range 50% to 60%).

After six weeks plants were cultivated for four days in the HL medium without nitrogen. The nitrogen starved plants were then divided into two tests: (1) some plants were immediately analyzed for their ^{15}N uptake and (2) some were transferred into HL solution containing 1 mM $(NH_4)_2SO_4$ for 30 min (ammonium shock) then the ^{15}N uptake was measured. For ^{15}N uptake tests, roots were washed twice in 1 mM $CaSO_4$ and incubated for 6 min (short-term uptake) or 30 min (long-term uptake) in HL solution containing 0.5 mM or 5 mM $^{15}NH_4^+$ followed by another two washing steps in 1 mM $CaSO_4$. Afterwards, roots were briefly dried, separated from shoots, both plant parts were immediately frozen in liquid nitrogen and cold-dried. Samples were ground, 1.0 mg (0.5 mM $^{15}NH_4^+$) or 0.5 mg (5 mM $^{15}NH_4^+$) powder was used for ^{15}N, total N and total C determination by isotope ratio mass spectrometry.

4.6.4 Plant Transformation

Arabidopsis thaliana plants were grown in soil and transformed by the floral dip method (Clough and Bent 1998) with transgenic *Agrobacterium tumefaciens* strain GV3101 harboring

the appropriate plasmid. Transgenic plant selection and segregation were performed on selective agar plates (1/2 MS with 4 µM MSX and/or 50 µM Kanamycin, Table 11).

For the split YFP approach plants (WT) at first were transformed with *pTkan⁺ pCIPK23::CIPK23-NY, pTbar pCIPK23::CIPK23-CY, pTkan⁺ pCIPK23::NY, pTbar pCIPK23::CY* constructs. Transgenic plants from T1 seeds were subjected to the next round of floral dip transformation with the required construct.

4.6.5 Fluorescence detection by laser scanning confocal microscope (LSM)

7-14 days old homozygous plants carrying a single T-DNA insertion were observed using a laser scanning confocal microscope (LSM700_ZEN_2010, Zeiss, Germany).

Table 18: LSM settings for GFP localization.

Objective	Plan-Apochromat 20x/0.8
Master gain	Ch2 755
	ChD 220
Pinhole	70 µm
Filters	453 – 1000
Laser	488 nm : 2%

Table 19: LSM settings for split eYFP localization.

Objective	Plan-Apochromat 20x/0.8
Master gain	Ch2 800
	ChD 230
Pinhole	70 µm
Filters	SP 555
Laser	488 nm : 2%

4.6.6   Potassium analysis

Roots and shoots of six week old plants intended for mineral analysis were dried individually at 60°C. Dried plant material was ground and ashed in a muffle furnace at 500°C for 4 hours. After cooling, the samples were treated two times with 2 ml of 3.4 M HNO_3 and subsequently evaporated to dryness. The ash was dissolved in 2 ml of 4 M HCl, diluted ten times with hot deionized water and boiled for 2 min. Potassium amount was determined by atomic absorption spectrometry (UNICAM 939, Offenbach / Main, Germany).

4.7   Protein biochemical methods

4.7.1   Microsomes preparation for the Western blot

For preparation of microsomes, plants were grown hydroponically as described in the Chapter 4.6.3. After ammonium shock (2 mM NH_4^+) roots were immediately harvested in liquid nitrogen. Samples were ground, 1.0 g powder was resuspended in 5 ml ice-cold extraction buffer and incubated with constant agitation for 15 min at 4°C.

Extraction buffer: 250 mM TRIS-HCl, pH 8.5

290 mM Sucrose

25 mM EDTA

2 mM DTT

5 mM   β-Me

Protease inhibitors (Chapter 3.1.2):   Aprotinin

Leupeptin

Pepstatin

PMSF

EGTA

Phosphatase inhibitor cocktail 2 (Sigma)

Phosphatase inhibitor cocktail 3 (Sigma)

Phosphatase inhibitor cocktail (Roche PhosSTOP)

Samples were proceeding with centrifugation 4500g for 15 min at 4°C. Supernatants were filtered through 4 layers of Miracloth (Calbiochem) and recentrifugated at 41000 g for 2h at 4°C. The pellets were resuspended in 100 µM of the ice-cold storage buffer.

Storage buffer:	400 mM Manitol
	10% (v/v) Glycerol
	6 mM MES-TRIS, pH 8.0
Protease inhibitors (Chapter 3.1.2):	Aprotinin
	Leupeptin
	Pepstatin
	PMSF
	EGTA

Phosphatase inhibitor cocktail 2 (Sigma)

Phosphatase inhibitor cocktail 3 (Sigma)

Phosphatase inhibitor cocktail (Roche PhosSTOP)

Protein concentration was measured by Nanodrop, A280 application. The Protein A280 application displays the UV spectrum, measures the protein's absorbance at 280 nm and does not require generation of a standard curve. 60 µg of the microsome preparation was loaded to the gel, Chapter 4.7.6 ("Measure Nucleic Acids with NanoDrop Products" 2016).

4.7.2 Microsome preparation for mass spectrometry

Arabidopsis plants were grown for 4 weeks as described in Chapter 4.6.3. Half of the nitrogen-starved plants (4 days, HL-N) were exposed to ammonium shock (2 mM NH_4^+). After the treatments (starvation or shock), roots were separated from shoots and immediately harvested in liquid nitrogen. Frozen roots (2 g per sample) were ground in a potter with Homogenisation Buffer (ratio 1:5). Homogenates were centrifuged at 7 500 g for 15 min at 4°C. Supernatants were collected and filtered through 4 layers of Miracloth (Calbiochem) and recentrifuged at 48000 g for 75 min at 4°C. Pellets containing microsomal membrane proteins were

resuspended in 8 M urea, 2 M thiourea, pH8 and sonicated 10 min for protein solubilization (Pertl et al. 2001).

Homogenisation Buffer: 330 mM sucrose

                                     100 mM KCl

                                     1 mM EDTA

                                     5 mM DTT

                                     50 mM MES-TRIS, pH 7.5

Protease inhibitor cocktail (Sigma)

4.7.3   In-solution trypsin digestion

Solubilized protein samples were centrifuged 10 min at 10 000 rpm to pellet any insoluble material. The pH of the final solutions was checked with pH strips. For every 50 µg of the protein sample 1 µL of Reduction Buffer (1 µg/µL DTT in water) was added and samples were incubated 30 min at room temperature (RT). After 30 min of incubation 1 µL Alkylation Buffer (27 mM iodoacetamide in water) was added for every 50 µg sample protein and incubated 20 min at RT. To cleave carboxyl sidegroup of lysine residues, LysC protease (isolated from *Lysobacter enzymogenes*) was used in 1:100 ratio (0.5 µL LysC per 50 µg sample protein) and incubate for 3 h at RT.

Due to trypsin is very sensitive to high salt concentrations, samples were diluted 4 times with 10 mM TrisHCl, pH8 and digested with 3 µL of trypsin overnight at RT. Finally, the samples were acidified (pH 2.0) with trifluoroacetic acid (TFA) to a final concentration of 0.2%.

4.7.4   Peptide desalting and concentration

Desalting and concentration of peptides were achieved in the same step using C_{18}-Stage Tips (Rappsilber, Ishihama, and Mann 2003).

Stage Tips were equilibrated two times with 100 µL of 0.5% acetic acid. 150 µL of the samples were loaded to Stage Tips and spun down. Afterwards Stage Tips were washed two times with 100 µL Buffer A (4000 rcf, 3 min). To elute peptides from the Stage Tips solutions A and B were

used in proportion 1:1. Next, samples were spun at 1000 g and immediately subjected to phosphopeptide enrichment.

Solution A: 0.1% TFA

                                 5% acetonitrile

Solution B: 0.1% TFA

                                 80% acetonitrile

4.7.5 Phosphopeptide enrichment

Phosphopeptides were enriched over TiO_2 (Larsen et al. 2005). Titanium enrichment was performed using 1 mg of TiO_2 powder per 100 μg of proteins. First, TiO_2 beads were equilibrated with 100 μL of Solution A. Then samples were loaded to TiO_2 columns and centrifuged at 1000 g for 5 min two times (flow-through was collected and loaded to the columns second time). TiO_2 beads were washed twice with 100 μL Solution A.

Phosphopeptides were eluted twice: with 50 μL of 5% ammonia and with of 50 μL of 5% piperidine. Both elutes were combined and immediately acidified using 50 μL of 20% phosphoric acid. Phosphopeptides were concentrated as described in Chapter 4.7.4 with exception that proteins were eluted by 40 μL of solution B (80% acetonitrile, 0.5% acetic acid) and concentrated in a speed vacuum concentrator.

For Mass Spectrometry analysis 8 μL of Resuspension Solution was added to each sample.

Solution A: 0.1% TFA

                                 5% acetonitrile

Resuspension Solution: 0.2% TFA

                                 5% acetonitrile

4.7.6 SDS-polyacrylamide gel electrophoresis (SDS-PAGE)

SDS-polyacrylamide gel electrophoresis (SDS-PAGE) technique was used to separate proteins in an electrical field according to their molecular weight. SDS gel consisted of staking gel (5%) and separation gel (12%) (Table 20).

Table 20: Composition of the separation and stacking gel used in SDS-PAGE.

Ingredient	Staking gel	Separation gel
TRIS-HCl 0.5 M, pH 6.8	1.5 ml	--
TRIS-HCl 1.5 M, pH 8.8	--	3 ml
Acrylamid, 40%	0.75 ml	3 ml
ddH$_2$O	3.68 ml	3.83 ml
SDS 20%	30 µl	60 µl
TEMED	15 µl	14 µl
APS 10%	20 µl	100 µl

Prior to load protein samples onto a SDS gel, each protein sample was mixed with 4x sample buffer and heated at 90°C for 15 min to denature the proteins.

10µl of the prepared protein samples were loaded into the pockets of a SDS gel. Additionally, 6 µl of the "PageRuler Prestained Protein Ladder" (Thermo Scientific) was loaded into the SDS gel (usually in lane 1) and served as molecular weight standard. The gel tank was filled up with 1x SDS running buffer. The gel was run: 40 V for 20 min (for better stacking of the proteins) and then 120 V until the dye front almost reached the gel bottom. After SDS-PAGE Western blot analysis (chapter 4.8) was performed.

4x sample buffer: 4% (w/v) SDS

                                 10% (v/v) β-Me

                                 40% (v/v) Glycerol

                                 0.5 M TRIS-HCl, pH 6.8

                                 0.004% (w/v) Bromphenol blue

1x SDS running buffer: 25 mM TRIS

                                192 mM Glycine

                                0.1% (w/v) SDS

4.8 Western blot

4.8.1 Transfer of proteins from SDS-PAGE on nitrocellulose membrane

Semi-Dry Electro Blotting System (Peqlab) was used to transfer proteins from a polyacrylamide gel on a nitrocellulose membrane (Peqlab) for later antibody detection.

The setup of a Western blot was as follows: 3 layers Whatman paper soaked in anode buffer ll, 3 layers Whatman paper soaked in anode buffer l, nitrocellulose (NC) membrane equilibrated in anode buffer l, SDS gel incubated 1 min in cathode buffer, 3 layers Whatman paper soaked in cathode buffer. The blotting duration was 2 hours at 10 volts and constant current settings.

Cathode buffer: 25 mM TRIS-HCl, pH 9.4

                                40 mM 6-aminocaproic acid

                                20% (v/v) Methanol

Anode buffer l: 25mM TRIS-HCl, pH 10.4

                                20% (v/v) Methanol

Anode buffer ll: 300 mM TRIS-HCl, pH 10.4

                                20% (v/v) Methanol

4.8.2 Visualization of proteins on the membrane, Ponceau Red

Visualization of protein bands after transferring on the nitrocellulose membrane was possible using the Ponceau Red method (Gallagher et al. 2008). This staining technique is used to check for success of transfer and estimate proteins in samples. After the blotting membrane was washed in TBST and incubated in staining solution for 10 minutes at continuous agitation, RT. The membrane was washed in ddH$_2$O until proteins bands were well defined and scanned at a resolution of 600 dpi (Epson Expression 10000XL). Before the next step membrane was destained in ddH$_2$O.

| Staining solution: | 0.1% (w/v) Ponseau S |
| | 5% (v/v) Acetic acid |

4.8.3 Immunodetection of proteins on nitrocellulose membranes

Immunodetection is a method used to identify a specific protein blotted to a membrane by using a primary antibody, which is directed against the target protein of interest.

To saturate unspecific binding sites on the nitrocellulose (NC) membrane, the membrane was agitated in TBST buffer with 1% (w/v) BSA for 1 hour, at RT, on a shaker. Then, the blot was incubated with primary antibody (Table 9) ON at 4°C with agitation. Before second antibody application, in order to remove primary antibody excess and to prevent nonspecific binding, the membrane was washed three times with TBST buffer each time 10 minutes at RT on a shaker. Afterwards the blot was incubated with HRP conjugated secondary antibody (Table 9) for 1 hour, at RT, with agitation. Prior the detection, unbound secondary antibody was removed by four washing steps, twice TBST and twice TBS (each 10 minutes, RT, shaker). The signal from horseradish peroxidase (HRP) was detected using ECL (enhanced chemi-luminescence). For this ECL solution was freshly mixed and poured on the membrane for 2 min.

HRP bounded to the secondary antibody. Luminol from ECL solution is oxidized by HRP in the presence of H_2O_2. The reaction is accompanied by light emission, which was detected by membrane exposure to X-ray film.

ECL solutions:	Solution A:	100 mM TRIS-HCl, pH 8.6
		2.5 mM Luminol
	Solution B:	11 mg para-Hydroxycoumarin acid
	H_2O_2	30%

ECL detection mix:	2 ml Solution A
	0.6 ml 30% H_2O_2
	200 µl Solution B

5 Results

5.1 Initial screen for kinases involved in AMT regulation

To identify kinases that potentially regulate ammonium transporters in *Arabidopsis thaliana,* a bioinformatics screen was performed. The analysis considered public available expression data of all putative genes annotated as kinases found in the *Arabidopsis* genome. A screen for genes expressed in the root and in the hypocotyl identified 52 kinase candidates. Up to two T-DNA insertion lines for each candidate kinase were ordered at the European Arabidopsis Stock Centre (NASC) and propagated. Due to the large number of lines, the verification of the T-DNA insertion and homozygosity was initially not performed. However, all lines were subjected to a physiological screen that is detailed below. In theory, the absence of a kinase (which inhibits AMTs) should result in hyper-active ammonium transporters (Fig. 16).
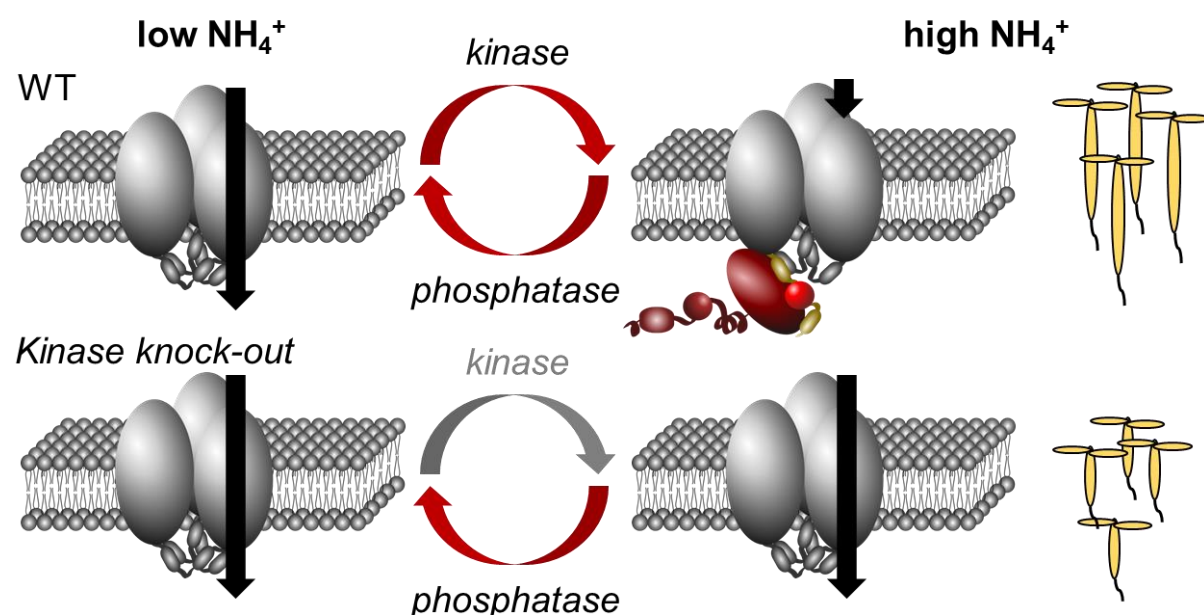
Figure 16: Screen for the AMT-regulating kinase using ammonium toxicicity in a hypocotyl growth test. High external ammonium concentration triggers AMT phosphorylation by a kinase that inhibits ammonium import. This mechanism minimizes ammonium toxicity (top), however, when that kinase is not functional, high ammonium concentrations inhibit hypocotyl growth in darkness (bottom).

Lines with hyper-active AMTs may consequently have a higher susceptibility to toxic concentrations of ammonium and are hyper-sensitive to the toxic ammonium analog,

methylammonium (MeA). Because high variability in the root establishment under high ammonium or methylammonium concentrations, a more robust screen with hypocotyl elongation in the dark was established. In dark-grown *Arabidopsis* seedlings, ammonium and MeA toxicities lead to reduced hypocotyl elongation. Essentially, disruption of the AMT regulating kinase should lead to shorter hypocotyls and increased sensitivity to ammonium toxicity. Only two T-DNA insertion lines, named *k1* and *k2*, showed the expected reduction in hypocotyl length (Fig. 17). The kinase genes targeted in these lines were therefore chosen as candidate genes and were further investigated.
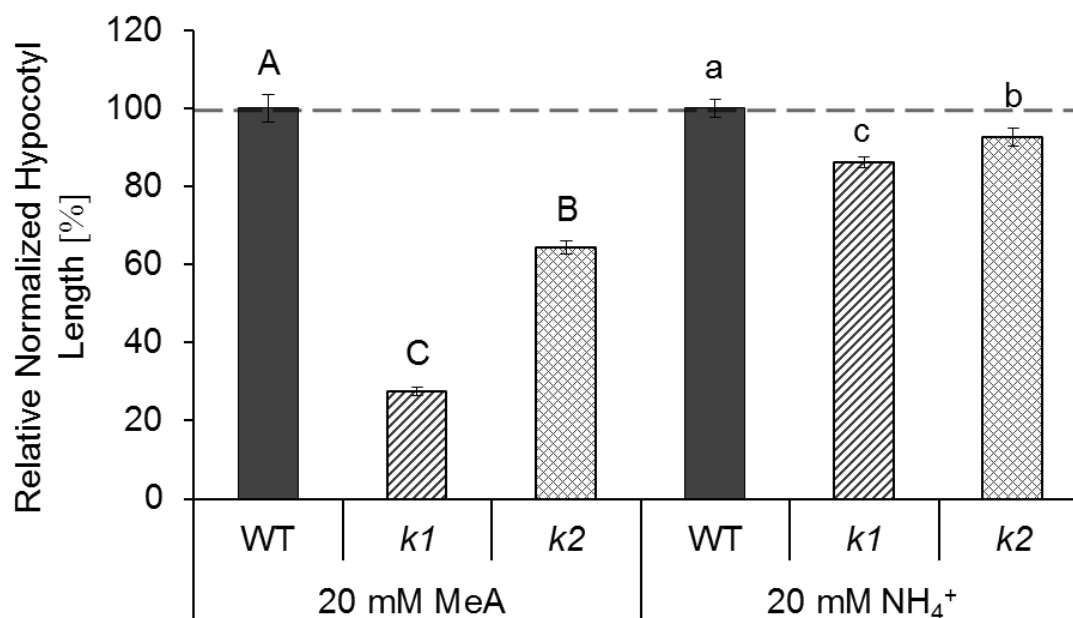

Figure 17: Hypocotyl length of wild type, *k1* and *k2* plants in the presents of 20 mM ammonium/methylammonium.
Hypocotyl length is normalized in percentage to wild type and relative to control conditions (0 mM MeA/NH$_4^+$). Two T-DNA insertion lines, *k1* and *k2*, showed increased sensitivity to toxic methylammonium (left) and ammonium (right). Significance was tested using SAS test, p≤0.001. Experiments were reproduced (n=3, plants ≥ 100) and representative data is shown ±SE. WT, wild type plants; *k1* plants, T-DNA insertion line SALK_036154C; *k2* plants, T-DNA insertion line SALK_058928C.

5.2 Characterisation of T-DNA insertion lines for zygousity and target gene expression

In order to test the allelic composition of individual plants for the T-DNA insertion, recommended SALK primers (BP+LP+RP) ("T-DNA Primer Design" 2015) were used in a PCR-based assay. The combination of left primer (LP) and right primer (RP) amplifies the wild type

allele, while the left T-DNA border primer (BP) and RP only raise a product from the mutant allele (Fig. 18B+C). Figure 18A shows the PCR results and verifies homozygous *k1* and *k2* plants.
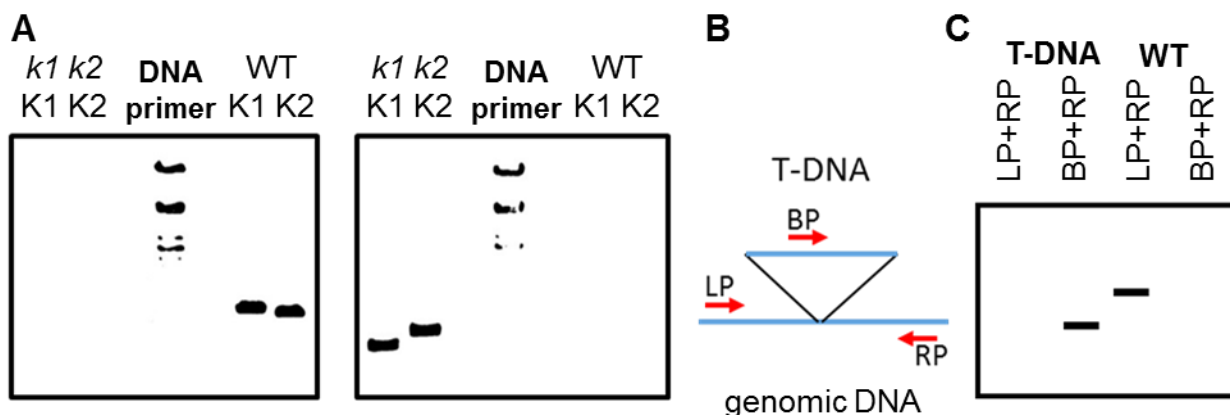

Figure 18: Test for zygousity of *k1* and *k2* plants.
(A) Agarose-gelelectrophoresis of homozygous *k1* and *k2* plant lines compared to wild type. (B) Overview of the primer location on genomic DNA and the T-DNA insertion. (C) Scheme of the outcome of the PCR and gelelectrophoresis of primer pairs shown in (B). B and C modified from ("T-DNA Primer Design" 2015). WT, wild type plants; *k1* plants, T-DNA insertion line SALK_036154C; *k2* plants, T-DNA insertion line SALK_058928C; LP, left primer; RP, right primer; BP, left T-DNA border primer.

Furthermore, the transcript abundance was tested in order to confirm whether the T-DNA insertion lead to the knock-out (KO) of the respective gene. *K1* mRNA was not detectable by RT-PCR in the *k1* line, while the *K2* transcript was strongly reduced in the *k2* line (Fig. 19). These results indicate that the T-DNA insertions effectively disrupt the respective kinase gene expression in the two lines. Therefore, *k1* was considered a real knock-out (*loss-of-function*) line, while *k2* was identified as knock-down mutant.

In the SALK_036154C (*k1*) line, the T-DNA insertion site is located in the 7th intron, 1655 bp downstream from the ATG. The *K2* gene consists of a single exon and the T-DNA insertion (SALK_058928C) is inside this exon, 426 bp downstream from the ATG (Fig. 20). Thus the *k2* line also probably represents a *loss-of-function* line, as the T-DNA disrupts the reading frame.

In summary, the homozygousity for the T-DNA insertion and its suppression of the transcription were confirmed for SALK_036154C (*k1*, CIPK23 KO) and SALK_058928C (*k2*, LECTIN PROTEIN KINASE KO). Consequently, further experiments were carried out with these two lines.
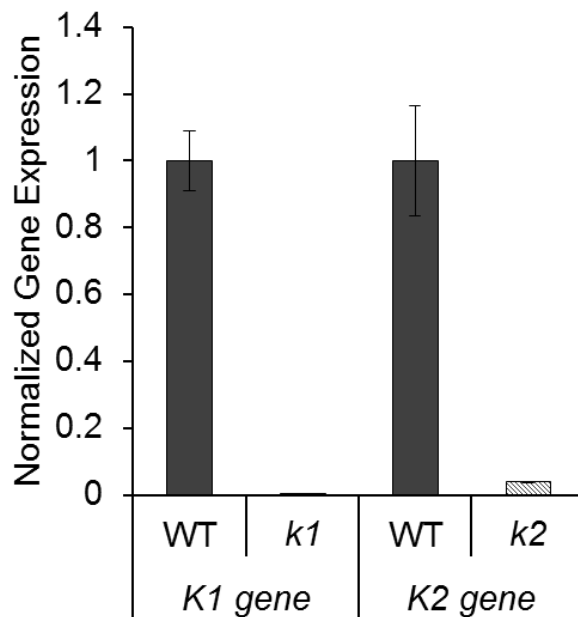
Figure 19: Kinase gene expression in *k1* and *k2* mutant lines.
Using quantitative PCR, two different T-DNA insertion lines (*k1* and *k2*) were tested for their expression of the respective gene (*K1* and *K2*) relative to wild type. Experiments were reproduced (n=4) and representative data is shown ± SD. WT, wild type plants; *k1* plants, T-DNA insertion line SALK_036154C; *k2* plants, T-DNA insertion line SALK_058928C.

CIPK23, AT1G30270, SALK_036154C

AT2G41890, SALK_058928C

Figure 20: Location of the T-DNA insertions in AT1G30270 (*k1*) and AT2G41890 (*k2*).
Red highlighted are the lines investigated in this study. Figure is taken from the Generic Genome Browser (v2.55) hosted by TAIR.

5.3 Ammonium uptake after ammonium shock

In order to test the importance of the kinases identified in the screen (Chapter 5.1) in respect to ammonium uptake *in planta*, the ability of the mutant plants to regulate ammonium uptake in their roots was investigated. If the candidate kinases phosphorylate and inhibit ammonium transporters, ammonium uptake should be decreased.

Plants starving for nitrogen have high AMT expression and show low or no AMT phosphorylation. Therefore, plants grown for six weeks with optimal ambient nutrient supply were then exposed to ammonium-depleted conditions. After 4 days, a subset of plants was exposed to a 30 minutes high ammonium shock to initiate phosphorylation and inhibition of ammonium uptake. Afterwards, plant roots were incubated for six minutes in low and high concentrations of ^{15}N-labeled ammonium sulfate. The abundance of heavy ^{15}N nitrogen isotopes was measured from dried plant material to calculate the ammonium uptake.
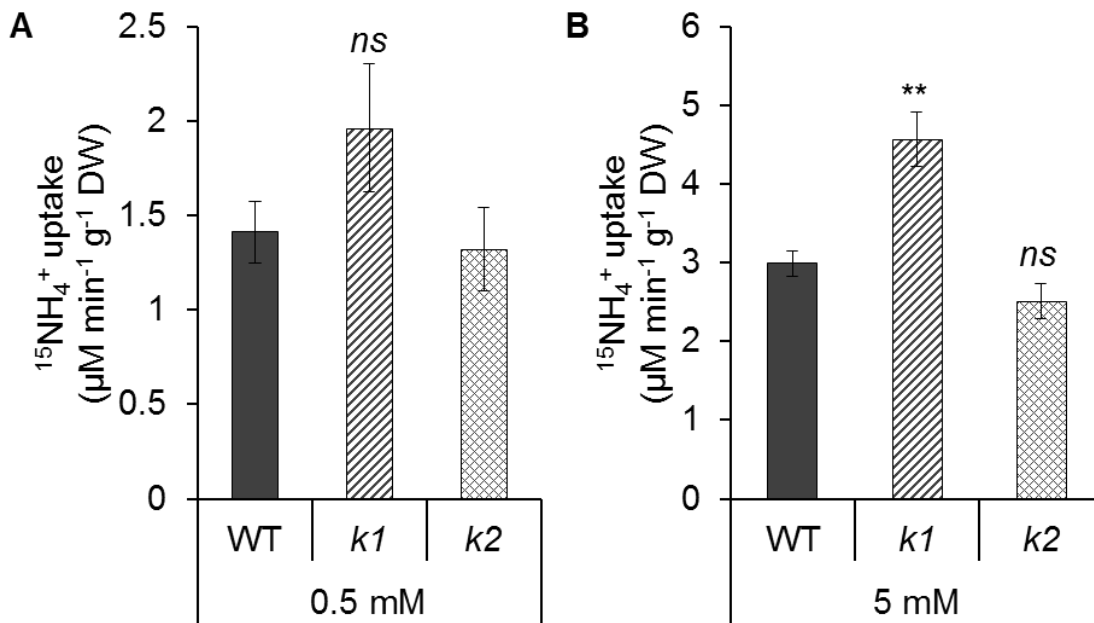

Figure 21: Uptake of ^{15}N-labeled ammonium into roots of wild type, *k1* and *k2* plants.
Six-week-old plants were grown hydroponically under continuous supply of 1 mM ammonium nitrate and then deprived of nitrogen for 4 days, after that plants were resupplied with 2 mM NH_4^+ [1 mM $(NH_4)_2SO_4$] for 30 min (ammonium shock). Plants after shock were moved to the HL solution containing 0.5 mM ^{15}N [0.25 mM $(^{15}NH_4)_2SO_4$] (A) or 5 mM ^{15}N [2.5 mM $(^{15}NH_4)_2SO_4$] (B) for 6 min. Significance was tested using T-test and indicated by stars; **, p≤0.01; ns, not significant. Experiments were reproduced (n=3) and representative data is shown ±SD. WT, wild type plants; *k1* plants, T-DNA insertion line SALK_036154C; *k2* plants, T-DNA insertion line SALK_058928C.

Mutant plant lines (*k1* and *k2*) showed no significant differences in ammonium uptake activity with 0.5 mM ammonium after six minutes uptake (Fig. 21 A). While wild type and *k2* plants had a very similar rate of ammonium uptake, the *k1* plant line had a trend to increase transport activity. After the exposure of the plant roots to 5 mM $^{15}NH_4^+$, *k1* plants accumulated significantly more labelled nitrogen in the roots compared to the wild type and the *k2* line (Fig. 21 B).

Since the *k2* line did not show a difference in ammonium uptake, the following experiments were concentrated on the *k1* line (from here on called *cipk23*) and the gene *CIPK23*.

5.4   Mutation in *CIPK23* gene causes plants growth limitations

Mutant plants (*cipk23*) grown hydroponically for the initial ammonium uptake tests (Chapter 5.3) were smaller in size and had less fresh and dry weight of shoot and root than wild type plants (Fig. 22). However, they were in a similar stage, judging from leaf numbers.
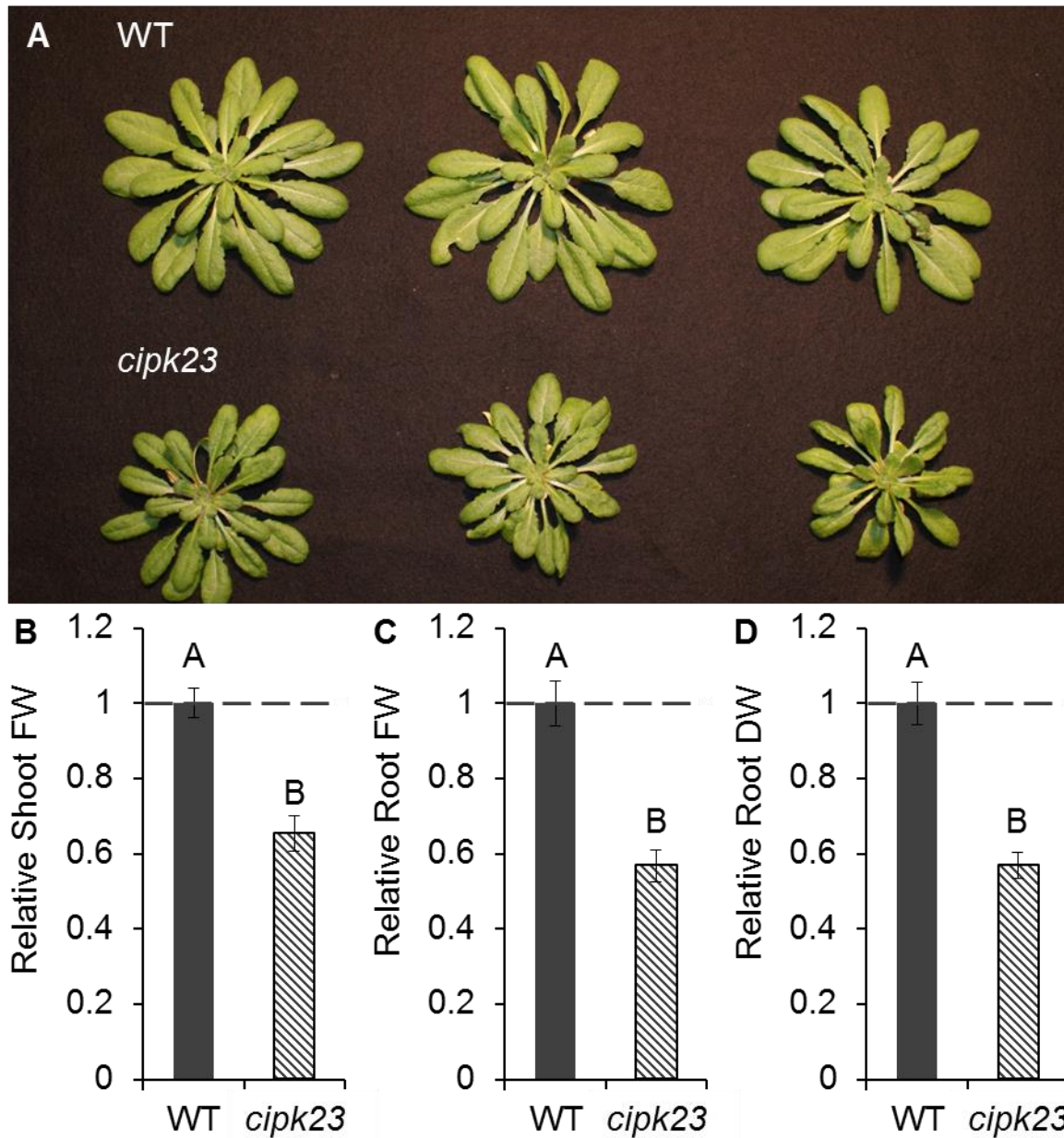
Figure 22: Phenotype of six weeks old wild type and *cipk23* plants.
Plants were grown hydroponically as described in methods. (A) Rosette size of WT and *cipk23* plants cultivated for 6 weeks in HL with 1 mM KNO_3 and 1 mM NH_4NO_3 hydroponically. Relative fresh shoot (B), fresh root (C) and dried root (D) biomass of 6 weeks old WT and *cipk23* plants. Significance was tested using T-test, p≤0.001. Experiments were reproduced (n=3) and representative data is shown ±SD. WT, wild type plants; *cipk23*, T-DNA insertion line SALK_036154C.

Additionally, the nitrogen and carbon content was measured. Despite the growth differences, nitrogen and carbon content in root and shoot of wild type and *cipk23* plants were not significant different (Fig. 23).
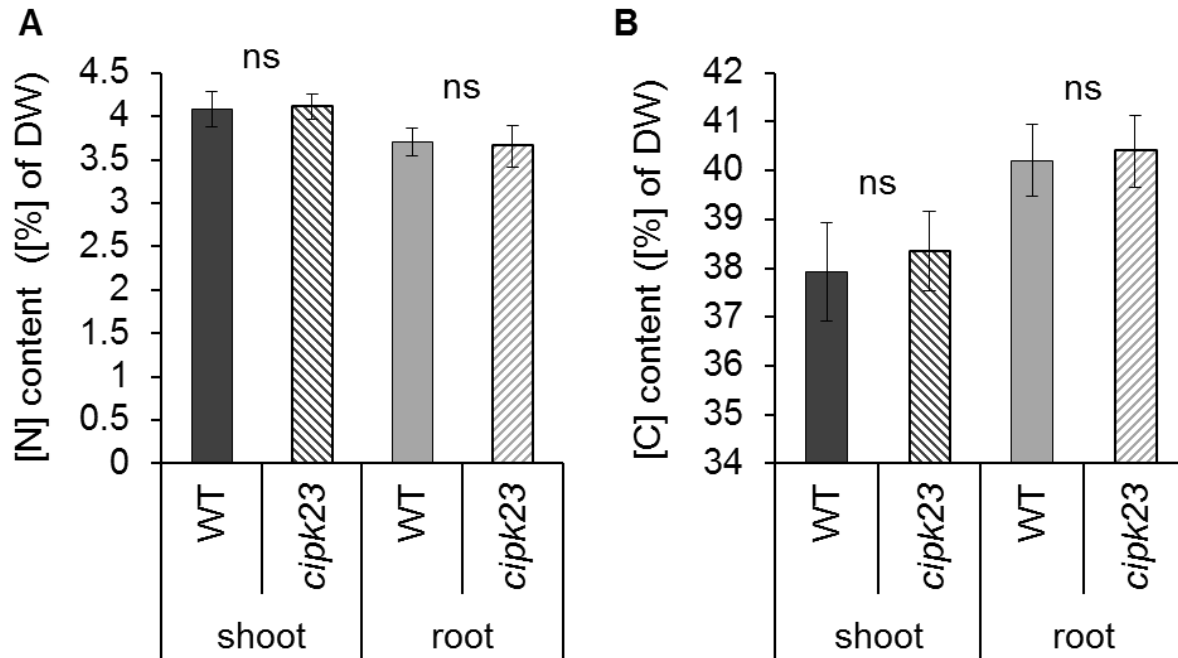
Figure 23: Nitrogen and carbon content in 6 weeks old wild type and *cipk23* plants.
Wild type and *cipk23* plants were similar in (A) nitrogen and (B) carbon content. Content in % of dry weight (DW). Significance was tested using T-test; ns, not significant. Experiments were reproduced (n=3) and representative data is shown ±SD. WT, wild type plants; *cipk23*, T-DNA insertion line SALK_036154C.

5.5 Complementation of *cipk23*

Another T-DNA insertion mutant in the *CIPK23* gene was ordered from the stock center, but this was not a complete loss-of-function line and only the above described homozygous plant line with T-DNA insertion in *CIPK23* gene resulted in total gene loss. The second *cipk23* line showed a minor reduction of *CIPK23* gene expression compared to the wild type plants (Fig. 24).

Figure 24: *CIPK23* gene expression in *CIPK23* T-DNA insertion lines.
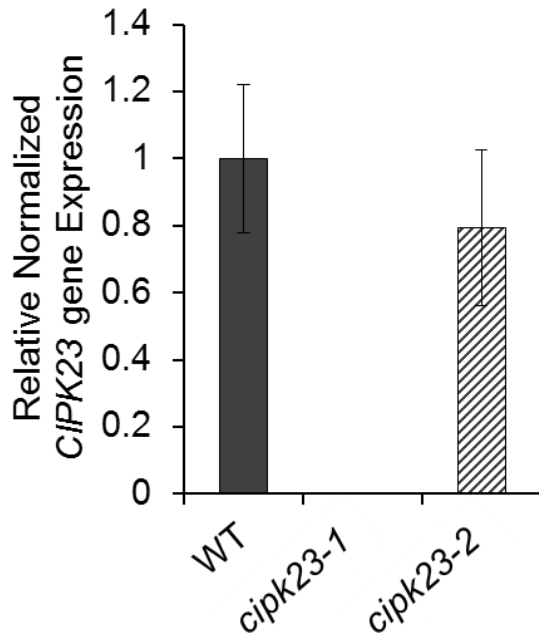Using quantitative PCR, two different T-DNA insertion lines (*cipk23-1* and *cipk23-2*) were tested for *CIPK23* gene expression relative to wildtype. Experiment was reproduced (n=2) and representative data is shown ±SD. WT, wildtype plants; *cipk23-1*, T-DNA insertion line SALK_036154C; *cipk23-2*, T-DNA insertion line, SALK_112091C.

Since no second independent *CIPK23* knock-out line was on hand, *cipk23* complementation lines were created. Complementation tests are required to confirm causal mutations by introducing a functional gene copy to counterpart a mutated allele. In order to confirm that only the *CIPK23* gene knock-out, and not another unexpected genomic event is responsible for the mutant phenotype, a construct encoding the *CIPK23* gene controlled by its own promoter was generated and transformed into *cipk23* plants. *CIPK23* expression was checked by the quantitative real time PCR method. Two independent complementation lines (*pCIPK23::CIPK23-1* and *pCIPK23::CIPK23-3*) showed comparable *CIPK23* gene expression to wild type plants (Fig. 25). These plant lines were selected for further experiments. In the first instance, complementation lines were grown for ^{15}N uptake experiments (Chapter 5.6), the results are discussed in the following chapter. However, the insertion of the functional *CIPK23* allele in knock-out plants restored normal root and shoot growth. Both complementation lines had significantly more root and shoot biomass relative to *cipk23* and were comparable to WT (Fig. 26). Therefore, the T-DNA insertion in the *CIPK23* gene was confirmed as the causal mutation.
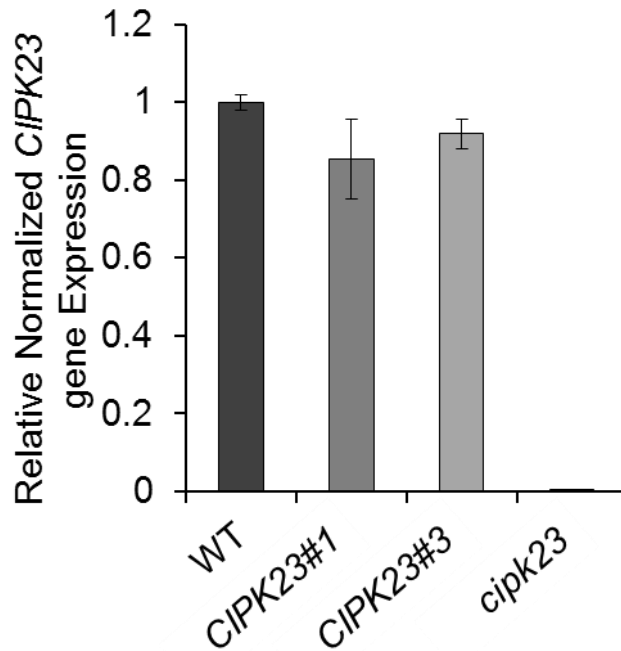
Figure 25: *CIPK23* gene expression in wild type, *cipk23*, and two complementation lines (*pCIPK23::CIPK23-1* and *pCIPK23::CIPK23-3*). Using quantitative PCR, *CIPK23* gene expression in complementation plant lines was tested relative to expression in WT. Experiment was reproduced (n=2) and representative data is shown ±SD. WT, wildtype plants; *CIPK23#1*, complementation line *pCIPK23::CIPK23-1*; *CIPK23#3*, complementation line *pCIPK23::CIPK23-3*; *cipk23*, SALK_036154C.
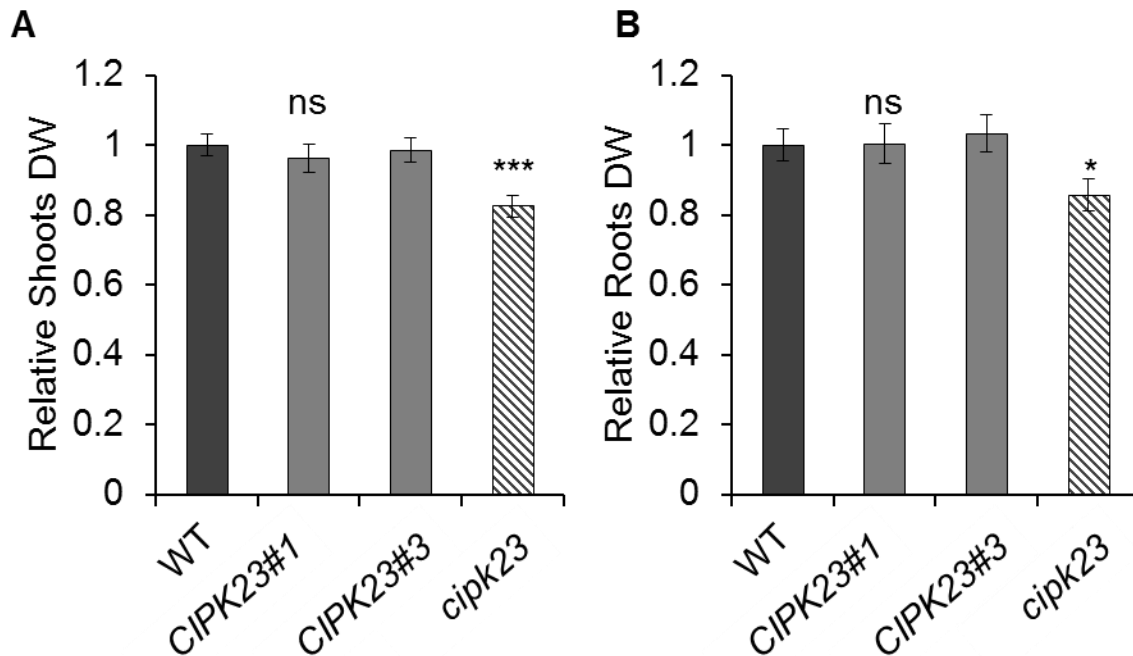
Figure 26: Shoot and root dry weight of wild type, *cipk23*, and two complementation lines (*pCIPK23::CIPK23-1* and *pCIPK23::CIPK23-3*).
(A) shoot, (B) root dry weight (DW) of WT, *cipk23*, *pCIPK23::CIPK23-1* and *pCIPK23::CIPK23-3* plant lines. Plants were grown hydroponically (5 mM potassium in HL) and harvested after 6 weeks. Significance was tested using T-test and indicated by stars; *, p≤0.05; ***, p≤0.001; ns, not significant. Experiments were reproduced (n=2, plants≥40) and representative data is shown ±SD. WT, wild type plants; *CIPK23#1*, complementation line *pCIPK23::CIPK23-1*; *CIPK23#3*, complementation line *pCIPK23::CIPK23-3*; *cipk23*, T-DNA insertion line SALK_036154C.

5.6 Ammonium uptake after and before ammonium shock

As described above, *cipk23* plants had reduced shoot and root biomass compared to wild type in hydroponic culture (Chapter 5.4). Reduced root length of *CIPK23* knock-out mutants under low-potassium conditions was also reported by Cheong and colleagues (Cheong et al. 2007). Only increasing potassium concentration (until the potassium level reached 5 mM) rescued the *cipk23* plants and restored root growth. While the potassium concentration in the growth medium (1 mM) was limiting in Cheong's experiments, to eliminate influence of potassium shortage on ammonium uptake, plants were additionally supplemented with additional 2 mM K_2SO_4 that resulted in a total potassium concentration of 5 mM in the growth solution.

Lanquar and colleagues revealed that 30 min of ammonium shock leads to complete phosphorylation of ammonium transporters (inactive AMTs), while under nitrogen starvation AMTs, stay non-phosphorylated and active. Plant lines with a disrupted kinase that regulates ammonium transport activity should therefore exhibit similar ammonium uptake after nitrogen starvation and ammonium shock. In order to test this hypothesis, roots of nitrogen starved and NH_4^+ shocked plants were incubated for six or thirty minutes in nutrient solution containing 0.5 mM or 5 mM $^{15}NH_4^+$. Nitrogen isotope uptake was measured in dried plant root material and the ammonium uptake was calculated.

All plant lines showed no major differences in ammonium uptake activity with 0.5 mM ammonium after six minutes (Fig. 27). Wild type and complementation lines (*pCIPK23::CIPK23-1*, *pCIPK23::CIPK23-3*) had very similar ammonium uptake, while *cipk23* had overall slightly increased transport activity, compared to wild type treatments.
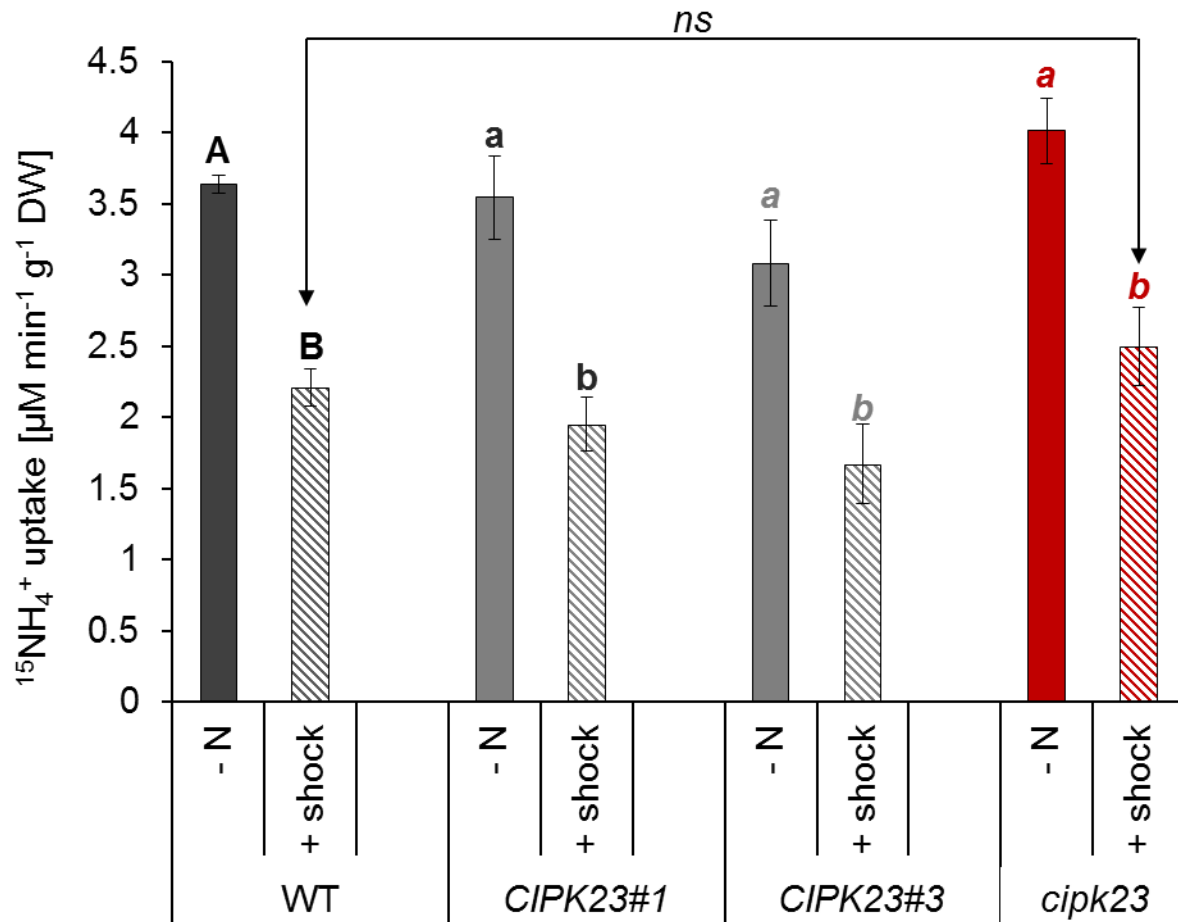
Figure 27: Uptake (6 min) of ^{15}N-labeled ammonium (0.5 mM) into roots of wild type plants, complementation lines (*CIPK23#1* and *CIPK23#3*) and *cipk23* plant line.
Six-week-old plants were grown hydroponically under continuous supply of 1 mM ammonium nitrate and then deprived of nitrogen for 4 days (−N), after 4 days half of the plants were resupplied with 2 mM NH$_4^+$ [1 mM (NH$_4$)$_2$SO$_4$] for 30 min (+ shock). N-starved plants and plants after shock were moved to the HL solution containing 0.5 mM ^{15}N [0.25 mM (^{15}NH$_4$)$_2$SO$_4$] for 6 min. Significance was tested using T-test, p≤0.001; ns, not significant. Experiment was reproduced (n=2) and representative data is shown ±SD. WT, wild type plants; *CIPK23#1*, complementation line *pCIPK23::CIPK23-1*; *CIPK23#3*, complementation line *pCIPK23::CIPK23-3*; *cipk23*, T-DNA insertion line SALK_036154C.

After 30 minutes feeding with 0.5 mM ammonium, all plant lines were similar in their ammonium uptake activity without ammonium shock (Fig. 28). However, the *cipk23* plant line showed significantly higher ammonium uptake after shock than wild type plants. The reduction in ammonium uptake activity with ammonium shock was approximately half compared to the wild type, however, uptake differences between treatments were still significant in *cipk23*.
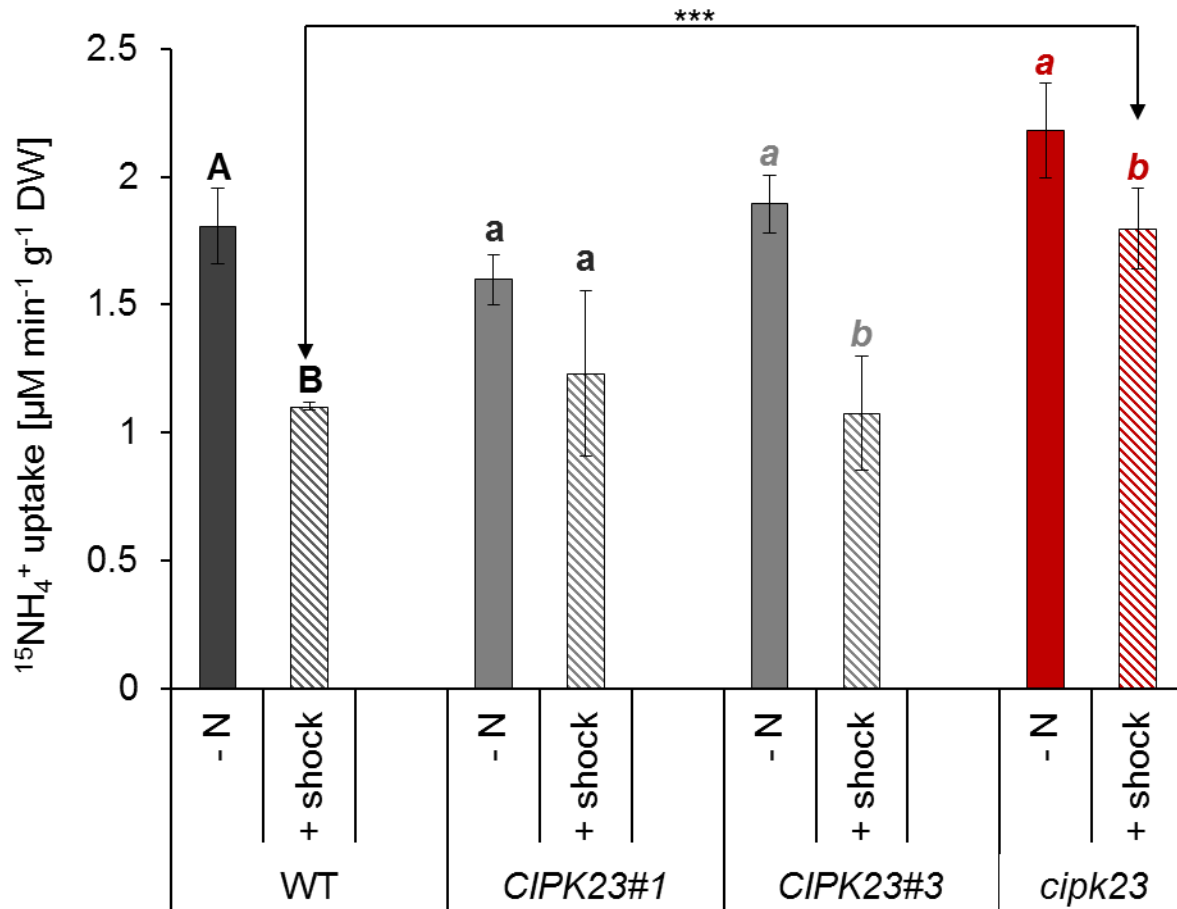
Figure 28: Uptake (30 min) of ^{15}N-labeled ammonium (0.5 mM) into roots of wild type plants, complementation lines (CIPK23#1 and CIPK23#3) and *cipk23* plant line.
Six-week-old plants were grown hydroponically under continuous supply of 1 mM ammonium nitrate and then deprived of nitrogen for 4 days (−N), after 4 days half of the plants were resupplied with 2 mM NH_4^+ [1 mM $(NH_4)_2SO_4$] for 30 min (+ shock). N-starved plants and plants after shock were moved to the HL solution containing 0.5 mM [15]N [0.25 mM $(^{15}NH_4)_2SO_4$] for 30 min. Significance was tested using T-test, $p \leq 0.001$; ***, $p \leq 0.001$. Experiment was reproduced (n=2) and representative data is shown ±SD. WT, wild type plants; *CIPK23#1*, complementation line *pCIPK23::CIPK23-1*; *CIPK23#3*, complementation line *pCIPK23::CIPK23-3*; *cipk23*, T-DNA insertion line SALK_036154C.

In the initial uptake experiments (Chapter 5.3), *cipk23* plants accumulated significantly more labelled ^{15}N then WT plants, when ammonium was resupplied to N-deprived seedlings at a concentration of 5 mM ammonium. In order to test whether higher concentrations of ammonium during uptake might increase differences in the investigated lines, 5 mM ammonium was used in the following experiments. Ammonium was fed for six minutes and the uptake was strongly reduced in all lines subjected to ammonium shock, except for *cipk23* (Fig.

29). In the absence of CIPK23 kinase activity, the regulation (inhibition) of ammonium transport activity was apparently lost and no significant differences were measured in samples with and without ammonium shock.

Figure 29: Uptake (6 min) of ^{15}N-labeled ammonium (5 mM) into roots of wild type plants, complementation lines (*CIPK23#1* and *CIPK23#3*) and *cipk23* plant line.
Six-week-old plants were grown hydroponically under continuous supply of 1 mM ammonium nitrate and then deprived of nitrogen for 4 days (−N), after 4 days half of the plants were resupplied with 2 mM NH$_4^+$ [1 mM (NH$_4$)$_2$SO$_4$] for 30 min (+ shock). N-starved plants and plants after shock were moved to the HL solution containing 5 mM ^{15}N [2.5 mM (^{15}NH$_4$)$_2$SO$_4$] for 6 min. Significance was tested using T-test, p≤0.001; ***, p≤0.001. Experiment was reproduced (n=2) and representative data is shown ±SD. WT, wild type plants; *CIPK23#1*, complementation line *pCIPK23::CIPK23-1*; *CIPK23#3*, complementation line *pCIPK23::CIPK23-3*; *cipk23*, T-DNA insertion line SALK_036154C.

Furthermore, all plant lines except *cipk23* showed significant uptake reductions after 30 minutes of 5 mM ammonium uptake. On average, *cipk23* plants transported the same amount of ammonium during the uptake experiment, regardless of the treatment (Fig. 30). Under these

conditions, the ability to regulate ammonium transport was lost completely in *CIPK23* knock-out mutants.
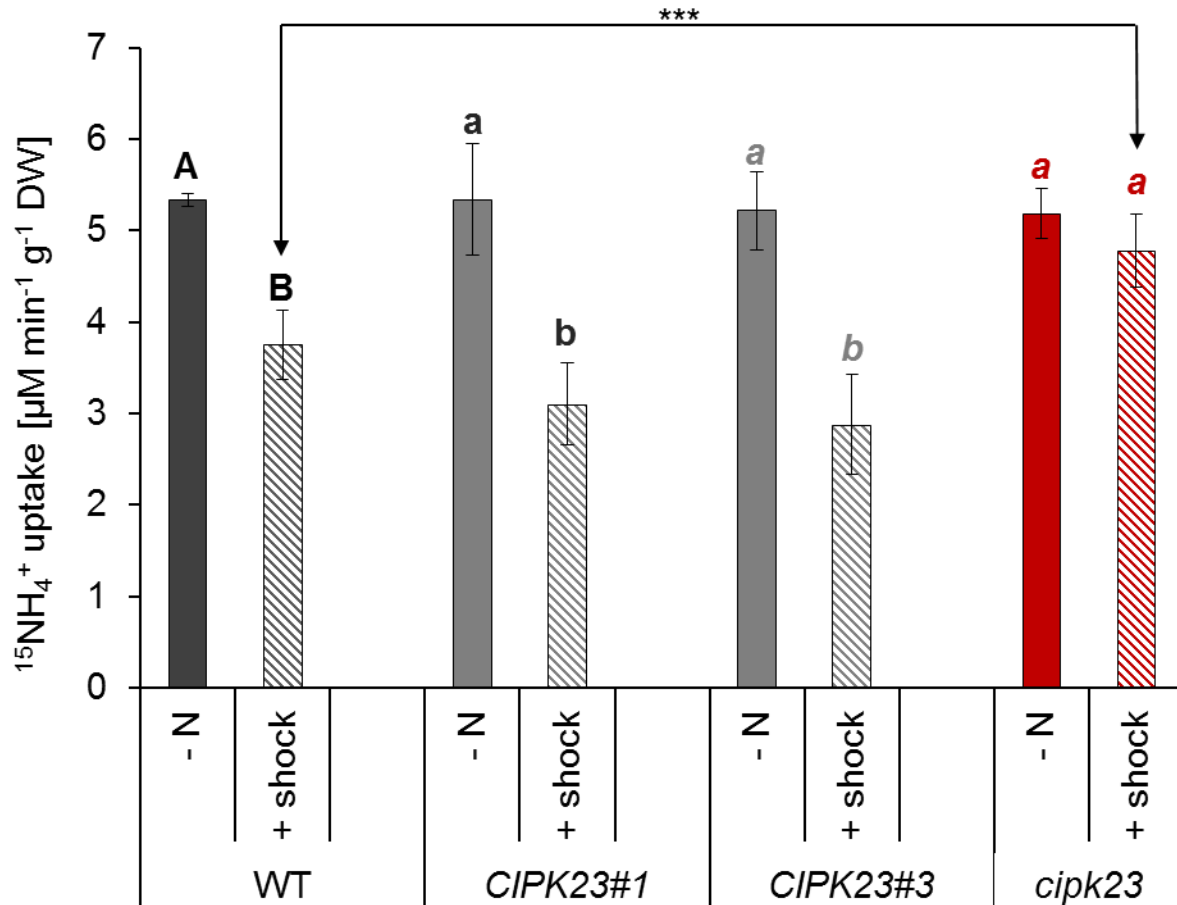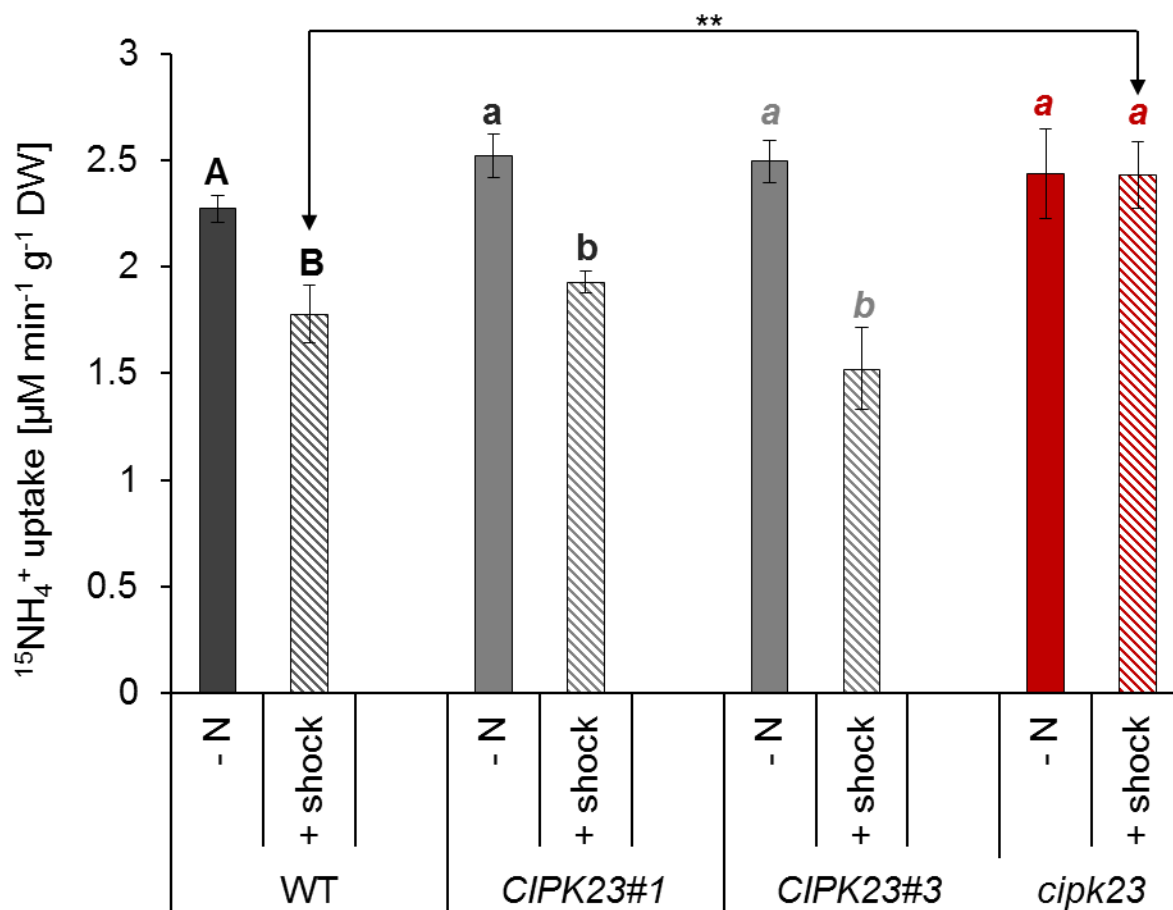

Figure 30: Uptake (30 min) of ^{15}N-labeled ammonium (5 mM) into roots of wild type plants, complementation lines (*CIPK23#1* and *CIPK23#3*) and *cipk23* plant line.
Six-week-old plants were grown hydroponically under continuous supply of 1 mM ammonium nitrate and then deprived of nitrogen for 4 days (−N), after 4 days half of the plants were resupplied with 2 mM NH$_4^+$ [1 mM (NH$_4$)$_2$SO$_4$] for 30 min (+ shock). N-starved plants and plants after shock were moved to the HL solution containing 5 mM ^{15}N [2.5 mM (^{15}NH$_4$)$_2$SO$_4$] for 30 min. Significance was tested using T-test, p≤0.001; **, p≤0.01. Experiment was reproduced (n=2) and representative data is shown ±SD. WT, wild type plants; *CIPK23#1*, complementation line *pCIPK23::CIPK23-1*; *CIPK23#3*, complementation line *pCIPK23::CIPK23-3*; *cipk23*, T-DNA insertion line SALK_036154C.

In table 21, the before mentioned uptake experiments are summarized and only the reduction values of ammonium uptake of plants after ammonium shock are compared to plants without shock treatment. In all experimental settings, wild type plants and *cipk23* complementation lines were able to reduce ammonium uptake after ammonium shock to a similar extent. When

a low concentration of ammonium (0.5 mM) was offered during the uptake experiment, *cipk23* lines were also able to reduce ammonium uptake. However, *cipk23* plants slightly reduced ammonium transport activity after ammonium shock when fed with 5 mM ammonium for six minutes. No reduction at all was seen after half an hour of ammonium shock. With increasing ammonium concentration in uptake experiments and increasing incubation time, differences in ammonium transport regulation became more and more prominent and significant.

Table 21: Reduction of ammonium uptake after ammonium shock in wild type (WT), complementation lines (*CIPK23#1* and *CIPK23#3*) and *CIPK23* knock-out plants (*cipk23*). This table summarizes data underlying beforehand figures.

^{15}N concentration	Uptake duration	Genotype	Reduction (%)
0.5 mM ^{15}N	6 min	WT	39
		CIPK23#1	45
		CIPK23#3	46
		cipk23	38
	30 min	WT	39
		CIPK23#1	23
		CIPK23#3	43
		cipk23	18
5 mM ^{15}N	6 min	WT	30
		CIPK23#1	42
		CIPK23#3	45
		cipk23	8
	30 min	WT	22
		CIPK23#1	23
		CIPK23#3	39
		cipk23	0.2

5.7 Potassium nutrition has a minor effect on *cipk23* plants

As explained in Chapter 5.6, plants for the second round of uptake experiments were grown under high-potassium supply (5 mM). Such increased potassium concentration should eliminate growth differences between mutant plants (*cipk23*) and wild type plants (Chapter 5.4). Indeed, root and shoot dry weights were less reduced in *cipk23* plants, however, the differences were

still significant (Fig. 31 B). Wild type and mutants also were still very different in rosette leaf size (Fig. 31A).
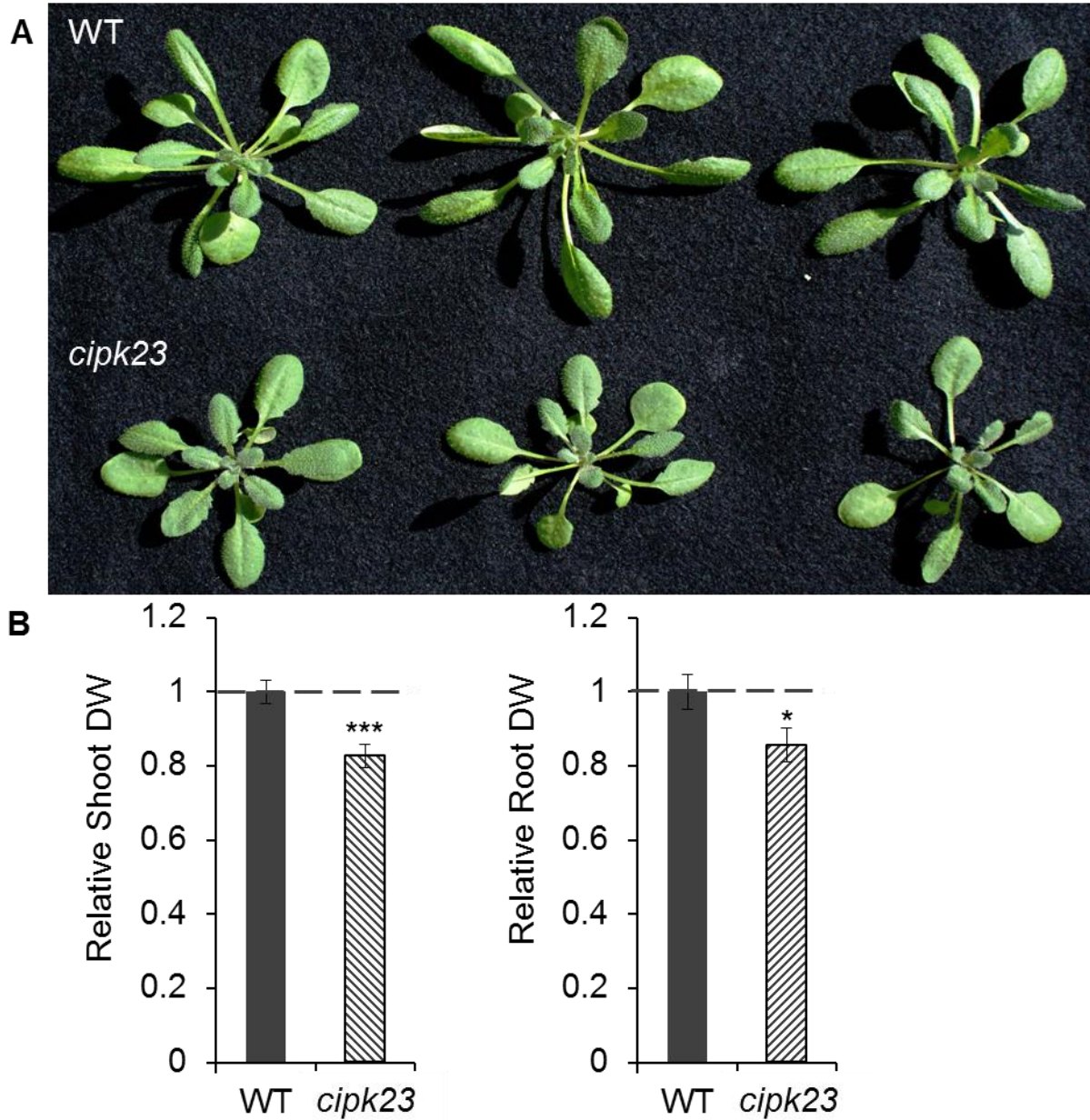
Figure 31: Wild type and *cipk23* plants growth under elevated potassium nutrition (5 mM potassium). (A) Phenotype of wild type (top) and *cipk23* (bottom), *cipk23* showed smaller rosettes after 4 weeks. (B) Root and shoot dry weight (DW) of 6 week old plants. Significance was tested using T-test and indicated by stars; *, p≤0.05; ***, p≤0.001. Experiment was reproduced (n=2) and representative data is shown ±SD. WT, wild type plants; *cipk23*, T-DNA insertion line SALK_036154C.

Cheong with colleagues (2007) demonstrated that potassium acquisition and accumulation were altered in *cipk23* plants and were correlated with root length. Compared to WT plants, *cipk23* seedlings had decreased potassium uptake from the medium and significantly lower potassium content (Cheong et al. 2007). To determine whether hydroponically grown *cipk23* plants were limited in potassium here, the potassium content in plant shoots was measured (Fig. 32A).
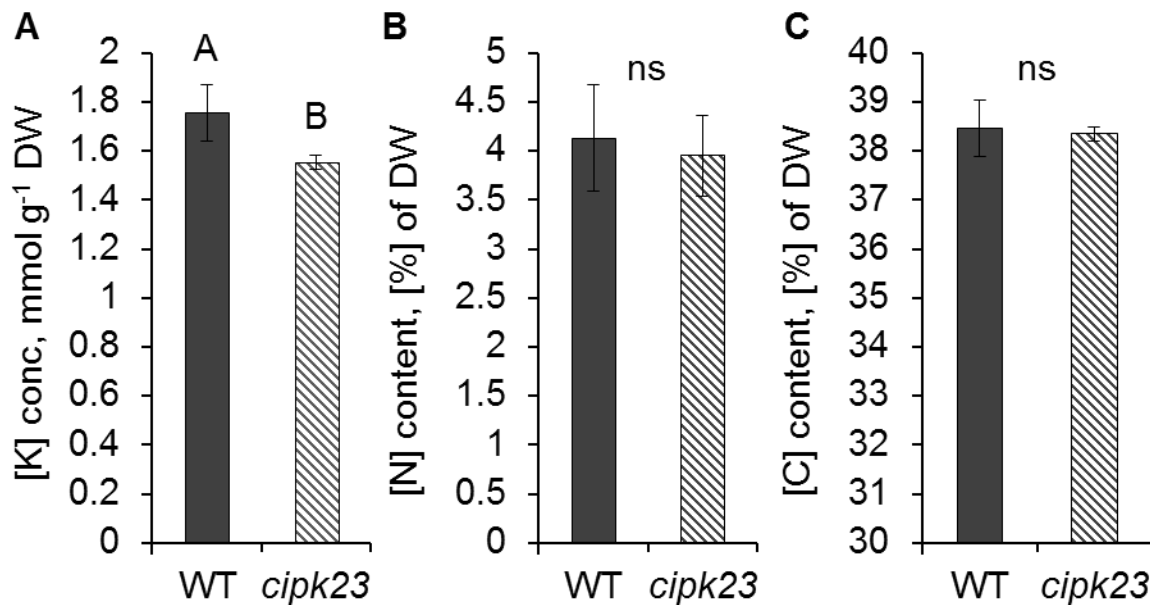
Figure 32: Potassium (A), nitrogen (B) and carbon (C) contents in the shoots of wild type and *cipk23* plants under elevated potassium nutrition.
Plants were grown hydroponically in HL solution under high-potassium conditions (5 mM) for 6 weeks. Significance was tested using T-test, p≤0.001; ns, not significant. Experiments were reproduced (n=3) and representative data is shown ±SD. WT, wild type plants; *cipk23*, T-DNA insertion line SALK_036154C.

Nitrogen and carbon content was similar in wild type and mutant plants (Fig. 32B+C), however potassium content was approximately 10% less abundant in *cipk23* (Fig. 32A). Thus, potassium accumulation in *cipk23* plant leaves was significantly less efficient than in control plants, even when plants were cultured in the medium with elevated potassium.

5.8 Characterization of *cipk23* and *amt1* knock-out plants

As apparent from the previous experiments, *cipk23* plants had more ^{15}N accumulation in the roots then WT, particularly when plants were supplied with 5 mM labelled ammonium. Under this ammonium concentration, HATS and LATS are involved in ammonium uptake. Interestingly, nitrate starvation induces transcription of the *HAK5* gene, which encodes HIGH AFFINITY K$^+$ TRANSPORTER 5, but this does not result in higher potassium uptake (Rubio et al. 2014). However, an increase in ammonium uptake might be explained by additional potassium/cation transport system activity, but additional potassium supply did not completely eliminate the difference in the potassium concentration between WT and *cipk23* plants (see previous chapter 5.7). In order to exclude that changes in the potassium transport system caused the elevated ammonium uptake, it was decided to test *cipk23* plants on plates with methylammonium (MeA). MeA is a non-metabolizable analogue of ammonium and at high levels severely inhibits plant root growth (Yuan et al. 2007). Potassium channels, that are partially permeable to ammonium, do not transport the bigger MeA ion (Moroni, Bardella, and Thiel 1998).

Already the initial screening for kinase candidates (changes in hypocotyl length) was performed under toxic concentrations of ammonium or methylammonium (Chapter 5.1). Even if CIPK23 phosphorylates (and inhibits) all AMT1s, ammonium transporters AMT1;3 and AMT1;5 were not targeted by this hypocotyl approach, as these two *AMTs* are not expressed in the hypocotyl. Therefore, plants were grown at high level of MeA and the root length was measured. If CIPK23 inactivates AMTs, then *cipk23* mutants with hyper-active ammonium transporters should be more sensitive to MeA than WT. In case CIPK23 activates the potassium transport system, MeA uptake is not affected and *cipk23* plants should have similar reduction in root length as wild type plants.

Root growth of *cipk23* plants was tested on vertical agar plates supplemented with two MeA concentrations: 20 mM and 30 mM. *A. thaliana* Col-0 ecotype and the AMT quadruple knock-out (*qko*, obtained from the von Wiren lab) served as controls (Yuan et al. 2007). Yuan with colleagues showed that *qko* mutants, where *AMT1;1, AMT1;2, AMT1;3* and *AMT2;1* are not expressed, were unaffected on agar plates supplemented with 20 mM or 50 mM MeA, while

growth of Col-0 plants was strongly inhibited. As expected, *qko* plants that lack MeA transport activity showed significantly less MeA sensitivity, relative to WT plants (Fig. 33).
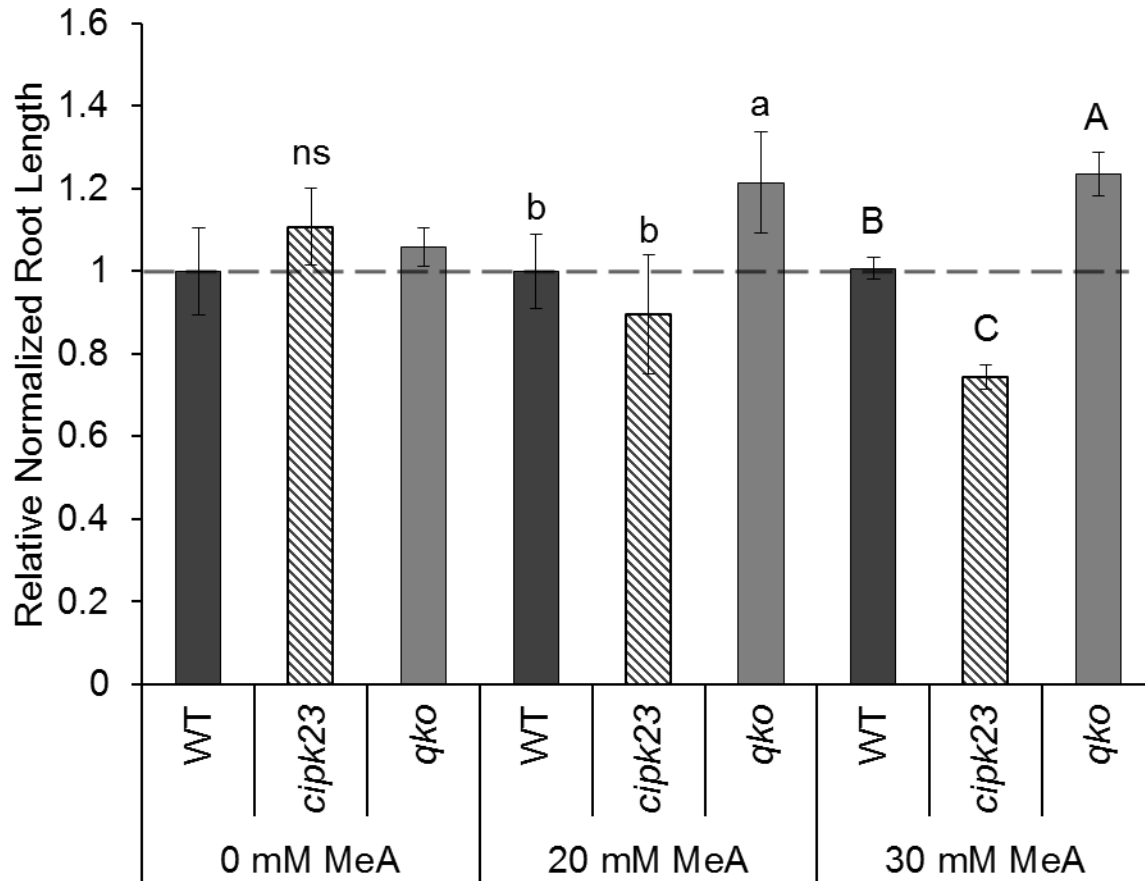
Figure 33: Primary root length relative to wild type of *cipk23* and *qko* plants grown on 0/20/30 mM MeA.
Plants were germinated and grown for 4 days on HL medium with 2 mM KNO_3, after 4 days plants were moved to the fresh agar plates with HL 2 mM KNO_3 (0 mM MeA), HL 2 mM KNO_3 + 20 mM MeA (20 mM MeA) or HL 2 mM KNO_3 + 30 mM MeA (30 mM MeA). Normalized root length was calculated by dividing the root length after 10 days of growth on the fresh agar plates by the root length on the HL medium with 2 mM KNO_3 after 4 days. Significance was tested using ANOVA test, $p \leq 0.001$; ns, not significant. Experiments were reproduced (n=3) and representative data is shown ±SD. WT, wild type plants; *cipk23*, T-DNA insertion line SALK_036154C.

Figure 34: Growth of the wildtype, *cipk23* and *qko* plants grown on 0/20/30 mM MeA.
Plants were precultured on HL medium containing 2 mM potassium nitrate as sole nitrogen source for 4 days and then transferred on agar plates containing 0, 20, or 30 mM MeA in the presence of 2 mM KNO_3 for 10 days. WT, wild type plants; *cipk23*, T-DNA insertion line SALK_036154C.

By contrast, *cipk23* plants exhibited an enhanced MeA toxicity, when grew with 30 mM MeA. In comparison with WT and *qko* plants, the *cipk23* line showed a strong reduction of the primary root length, when subjected to 30 mM MeA (Fig. 33, Fig. 34C). Furthermore, after 2 weeks growing in the presence of MeA, wild type, *qko* and *cipk23* plants differed in their lateral root density. In plants grown with 20 mM MeA, the lateral root density was reduced by around 50% and 80% in WT and *cipk23* plants, respectively. However, lateral density was not affected in *qko*. Increased MeA concentration (30 mM) strongly inhibited lateral root density in WT and *cipk23*, while *qko* mutants developed only 13% less lateral roots per cm of main root compared with the medium without MeA (Fig. 35).

Taken together, excess of MeA in the growth medium had a dramatic effect on WT and *cipk23*, but this was not observed in plants lacking four AMTs (*qko*). MeA caused strong inhibition of primary root elongation and lateral root formation, especially pronounced in *cipk23*. In

summary, the increased ammonium uptake and MeA sensitivity of *cipk23* plants was the result of an altered activity of ammonium transporters, rather than that of potassium transporters.

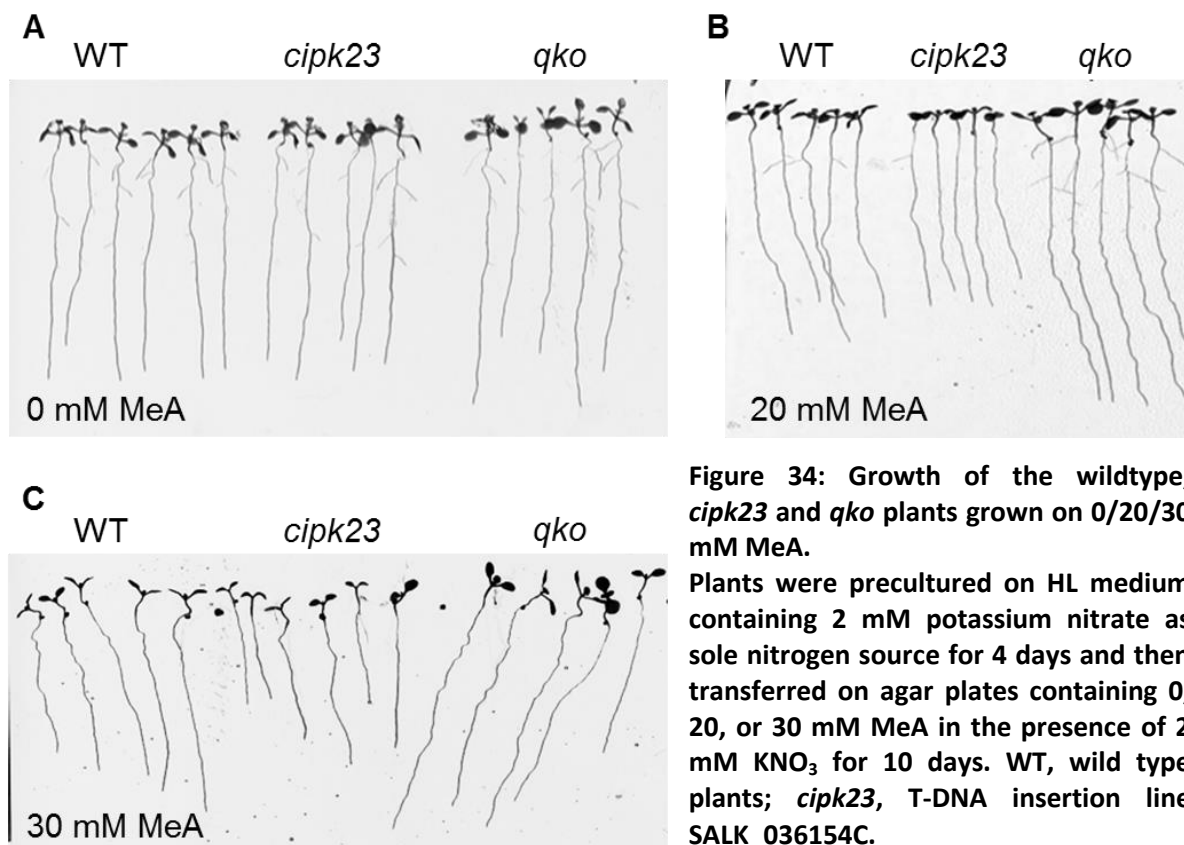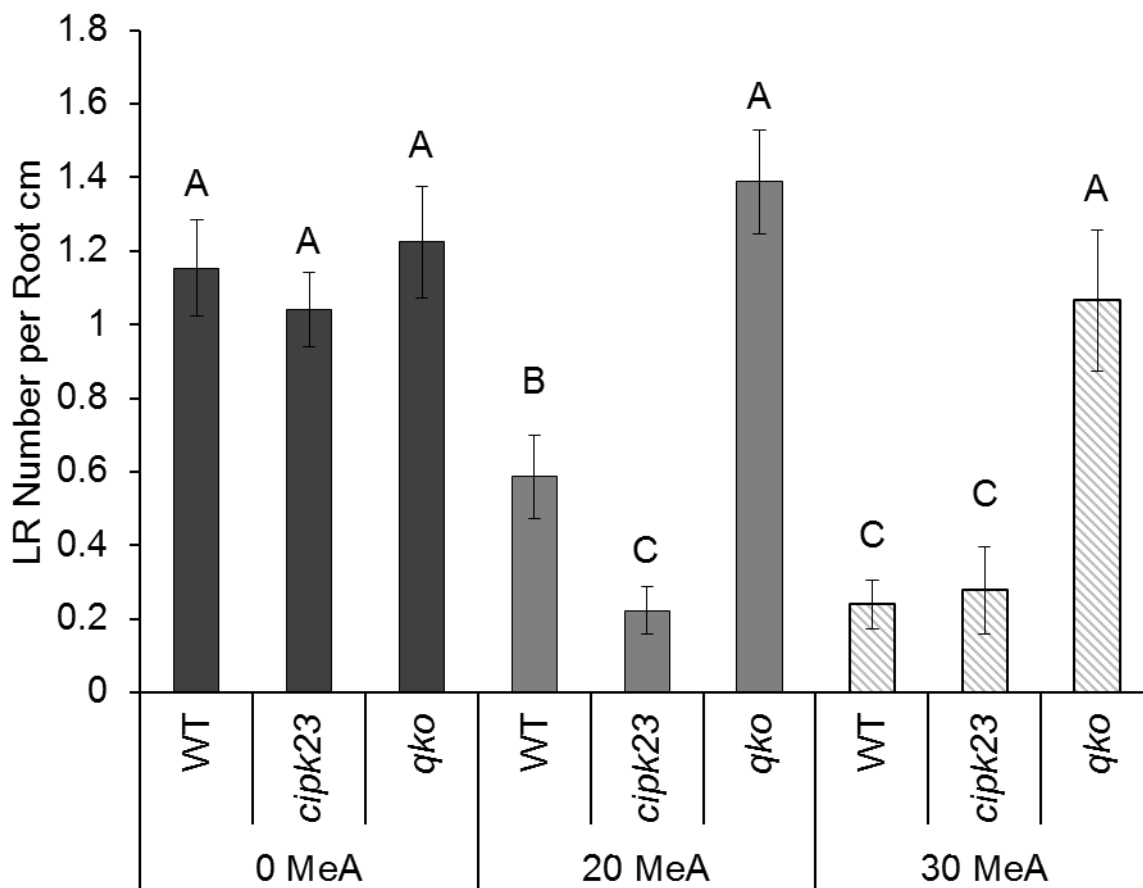**Figure 35: Number of the first order lateral roots relative to the primary root length of the wild type, *cipk23* and *qko* plants grown on 0/20/30 mM MeA.**
Plants were pre-cultured on HL medium containing 2 mM potassium nitrate as sole nitrogen source for 4 days and then transferred on agar plates containing 0, 20, or 30 mM MeA in the presence of 2 mM KNO$_3$ for 14 days. Significance was tested using ANOVA test, p≤0.001. Experiment was reproduced (n=3) and representative data is shown ±SD. WT, wild type plants; *cipk23*, T-DNA insertion line SALK_036154C.

5.8.1 Rescue of *cipk23* by reduced *AMT1* expression

Taken together, the data suggest that *cipk23* plants are characterized as plants with higher activity of ammonium transport. *Cipk23* is more sensitive to MeA, which is independent of the potassium transport system (Chapter 5.8). The absence of ammonium transporters should thus rescue *cipk23* plants from MeA toxicity, if no other systems were altered by the knock-out of

the *CIPK23* gene. Yuan and colleagues showed that the expression of the *AMT2;1* gene in *qko* line revealed no increase in the MeA sensitivity relative to *qko* (Yuan et al. 2007). Therefore a *cipk23* plant line with suppressed *AMT1* expression was initiated. Because the identification of multi-T-DNA insertion lines from crossings is challenging, because of the same resistance markers a strategy with artificial *microRNAs* targeting multiple *AMTs* in the *cipk23* background was used.

As a first step, artificial *microRNA* constructs to suppress all *AMT1*'s simultaneously were created and transformed into *cipk23*. The expression of the individual *AMTs* was checked and verified by RT-PCR (Fig. 36).
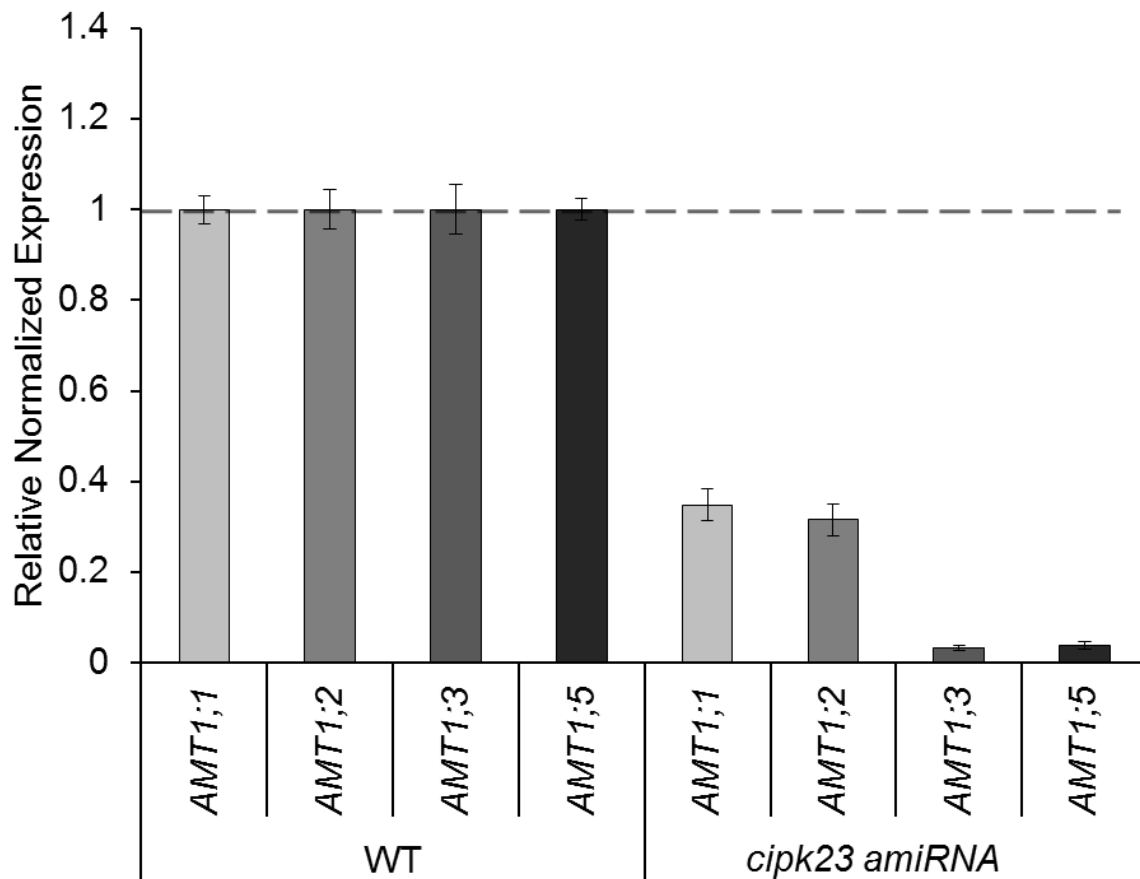

Figure 36: Relative normalized expression of *AMT1;1*, *AMT1;2*, *AMT1;3* and *AMT1;5* in wild type and *cipk23-amiRNA* plants.
Plants were grown for 14 days on solid agar plates containing ½ MS. Representative data of three replicates is shown with values ± SD. WT, wild type plants; *cipk23*, T-DNA insertion line SALK_036154C.

In the *cipk23-amiRNA* line, the expression of *AMT1;3* and *AMT1;5* were strongly reduced, but *AMT1;1* and *AMT1;2* transcripts were still detectable at around 30% of the wild type expression. Despite that, when *cipk23-amiRNA* plants were grown on sterile agar medium supplemented with 30 mM MeA (as described in Chapter 5.8), phenotypic analysis revealed no elevated MeA sensitivity compared to WT (Fig. 37). The loss of *CIPK23* was thus compensated by partial loss of AMT activity. In contrast to the *qko* mutant, *cipk23-amiRNA* plants failed to grow longer primary roots compared to the WT (Fig. 37).
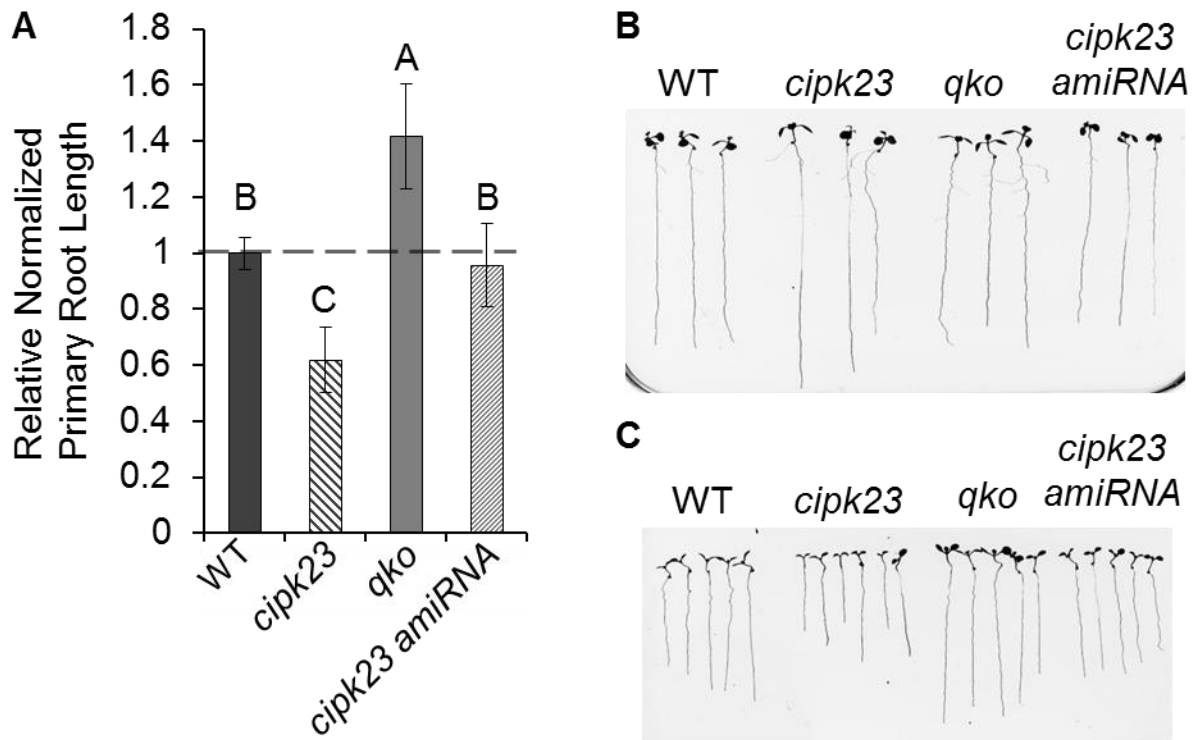
Figure 37: Growth of the wild type, *cipk23*, *qko*, and *cipk23-amiRNA* plants on agar with 30 mM MeA.
(A) Growth on HL medium containing 30 mM MeA and 2 mM KNO$_3$ for 10 days after preculture on HL medium with 2 mM KNO$_3$ for 4 days. (B) Growth on control plates: plants were germinated and grown on HL medium with 2 mM KNO$_3$, after 4 days plants were transferred to the fresh plates with HL medium containing 2 mM KNO$_3$ for 10 days. (C) Growth on selective plates: plants were germinated and grown on HL medium with 2 mM KNO$_3$, after 4 days plants were transferred to the fresh plates with HL medium containing 30 mM MeA and 2 mM KNO$_3$ for 10 days. Primary root length after 10 days of growth was normalized to the initial root length after 4 days of growth on agar with 2 mM KNO$_3$. Significance was tested using T-test, p$\leq$0.001. Experiment was reproduced (n=2) and representative data is shown ±SD. WT, wild type plants; *cipk23*, T-DNA insertion line SALK_036154C.

In conclusion, genetic suppression of *AMT1* transcripts by *amiRNA* in *cipk23* plants reduced *cipk23* MeA sensitivity to wild type level. Because *AMT1* transcripts are rather divergent, it was not possible to completely silence all *AMT1s* with one *amiRNA* precursor. However, AMTs are more than any other potential modifications in *cipk23* plants responsible for the different MeA sensitivity.

5.9   Localisation of AMTs. Expression of *AMTs*, *CIPK23* and *CBLs* after ammonium resupply

The hypocotyl assays and growth tests indicated that loss of *CIPK23* dramatically influenced the sensitivity to ammonium and it's toxic analog methylammonium. The following experiments exclude that differences in ammonium transporter expression or localisation are responsible for this hyper-sensitivity in *cipk23* plants.

5.9.1   Expression of ammonium transporters

Generally, the expression of ammonium transporter genes was rapidly down-regulated after 30 minutes of high ammonium treatment. In wild type and *cipk23* plants, the expression of *AMT1;1* and *AMT2;1* decreased about 40%. *AMT1;2*, *AMT1;3* and *AMT1;5* were repressed by approximately 50 to 70% after ammonium shock, compared to the expression under nitrogen starvation conditions (Fig. 38).

Wild type and *cipk23* plants had similar, but not exactly the same expression pattern of *AMT1;2*. After ammonium shock, in wild type, *AMT1;2* expression was significantly more reduced than in *cipk23* (T-test, $p \leq 0.05$).

In summary, WT and *cipk23* plants had an overall similar, but not identical, response to ammonium shock on the transcriptional level of ammonium transporters.
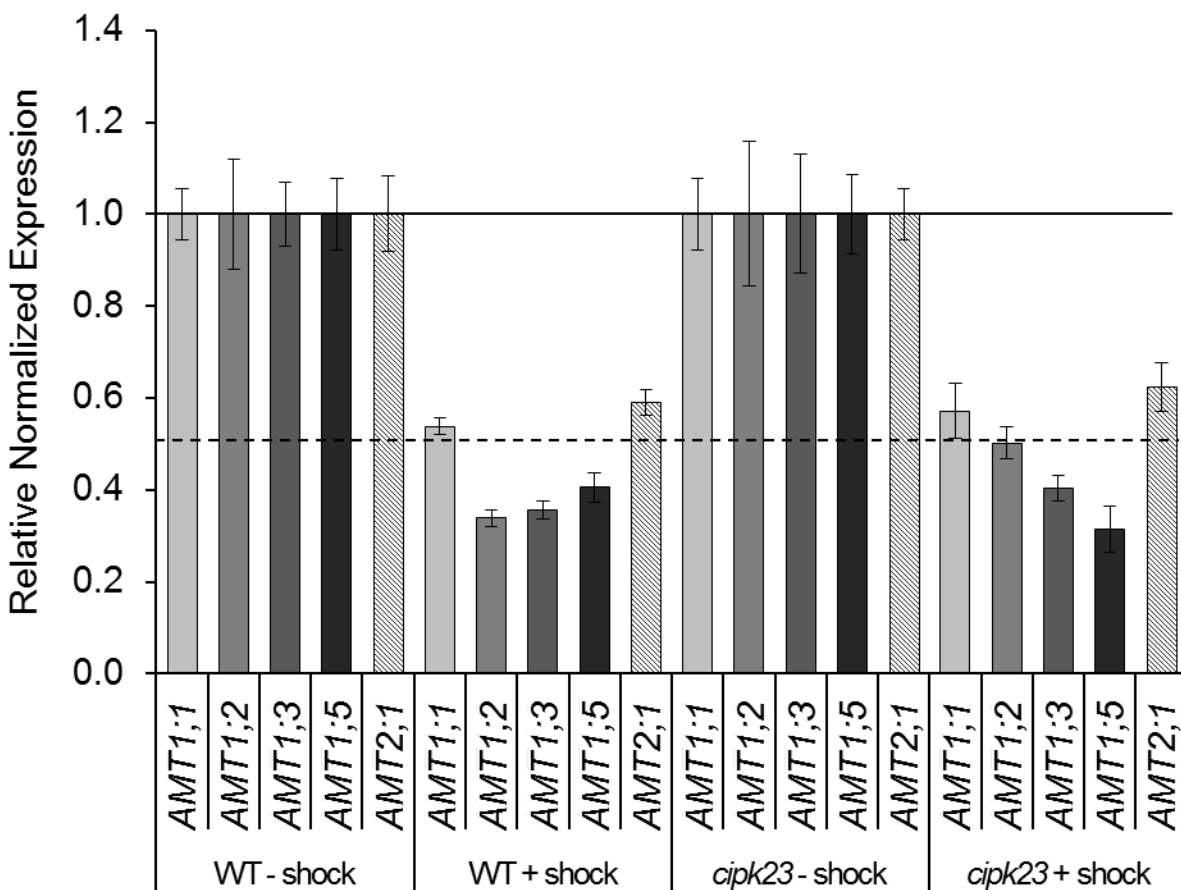
Figure 38: Relative normalized expression of ammonium transporters in wild type and *cipk23* plants after nitrogen starvation and after subsequent ammonium shock.
Plants were grown hydroponically in HL solution (as described in methods) for 6 weeks and then transferred in HL solution without nitrogen. After 4 days of nitrogen starvation (WT - shock; *cipk23* - shock) part of the plants were subjected to HL with 1mM $(NH_4)_2SO_4$ for 30 min – ammonium shock (WT + shock; *cipk23* + shock). Experiment was reproduced (n=3) and representative data is shown as the mean ±SD. WT, wild type plants; *cipk23*, T-DNA insertion line SALK_036154C.

5.9.2   Localization of AMT1;1, AMT1;2 and AMT2;1

Next, it was investigated whether the localisation of ammonium transporters had been changed in the absence of *CIPK23*. The localisation of AMT1;1, AMT1;2 and AMT2;1 was studied in the background of the *cipk23* line. Therefore, *cipk23* plants expressing AMT1;1, AMT1;2 or AMT2;1 fused to green fluorescent protein (GFP) driven under the respective native promoters (*pAMT::AMT-GFP*), were generated.
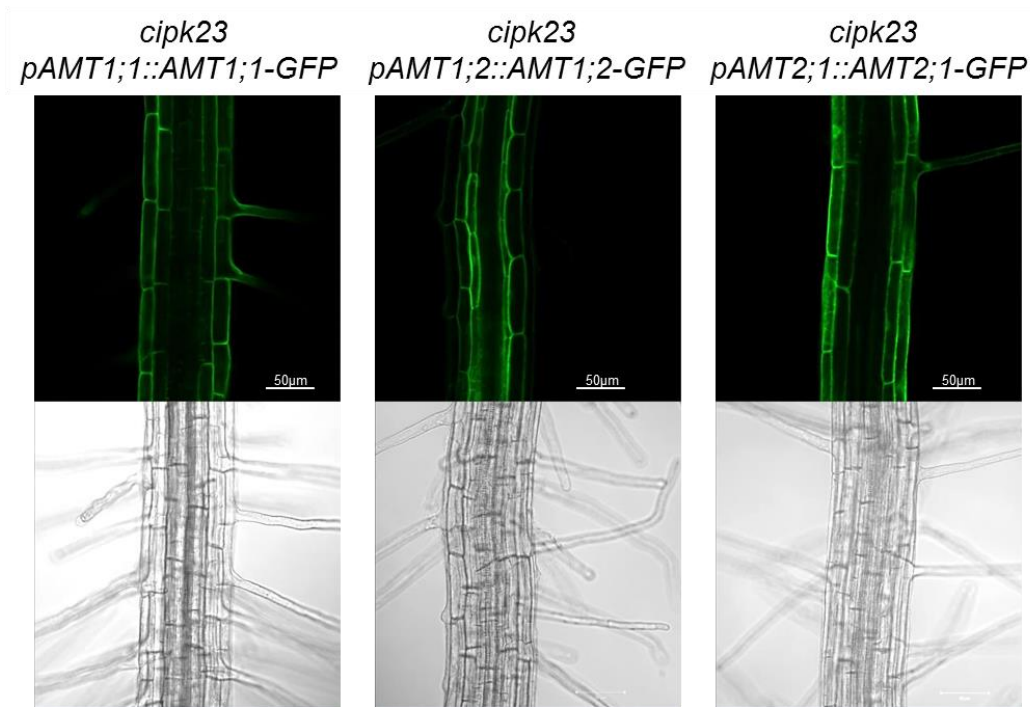
Figure 39: Localization of AMTs in *cipk23* background in *A. thaliana* roots.
AMT1;1 (left) and AMT2;1 (right) are expressed in root cortex and epidermis, while AMT1;2 (middle) is found in the endodermal and cortical cells. *cipk23*, T-DNA insertion line SALK_036154C.

Figure 40: AMT localisation in *Arabidopsis thaliana*, ecotype Col-0.
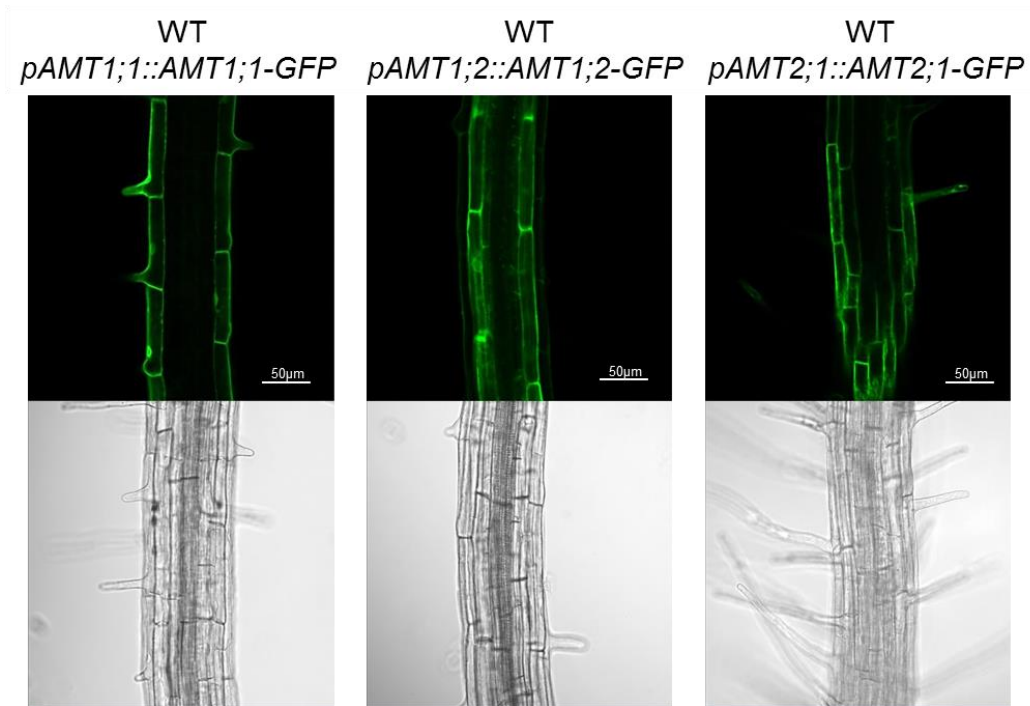AMT1;1 (left) and AMT2;1 (right) are expressed in root cortex and epidermis, while AMT1;2 (middle) is found in the endodermal and cortical cells. WT, wild type plants.

GFP fluorescence was detected in *cipk23* plants grown at low nitrogen using laser scanning confocal microscopy. The fusion proteins *AMT1;1-GFP* and *AMT2;1-GFP* were localized in the root cortex and epidermis plasma membrane, while *AMT1;2-GFP* was localized and expressed in the endodermal and cortical cell plasma membrane (Fig. 39).

Localisation of ammonium transporters in the *cipk23* mutant background followed the localisation of plants without the T-DNA insertion in the *CIPK23* gene (Fig. 40). Therefore, the disruption of *CIPK23* did not influence the organ-specific localisation of ammonium transporters in roots.

5.9.3 Expression of potassium transporters as potential ammonium LATS members

Potassium channels are potential candidates responsible for the low affinity transport system (LATS) of ammonium. CIPK23 activates potassium channel AKT1 (Xu et al. 2006; Cheong et al. 2007) and high-affinity potassium transporter HAK5 by phosphorylation (Ragel et al. 2015). AKT1 and HAK5 are the two major potassium uptake transporters in the plant roots (Alemán et al. 2011). When CIPK23 kinase is disrupted, both remain non-functional. Nevertheless, in the absence of HAK5 and AKT1, other potassium uptake systems, like KUP/HAK/KT transporters, provide potassium to support plant growth and development under sufficient potassium supply (Pyo et al. 2010). It has been demonstrated that the presence of ammonium inhibits potassium uptake mediated by KUP/HAK/KT transporters (Santa-María et al. 1997; Spalding et al. 1999; Pyo et al. 2010). This inhibition might indicate a partial ammonium uptake by KUP/HAK/KT transporters. In order to examine whether the transcript level of KUP/HAK/KT transporters were elevated in *cipk23*, expression of *KUP4* and *KUP8* genes was measured by RT-PCR. Additionally, the expression of *AKT1* was analysed to reveal if the expression was induced by ammonium resupply.
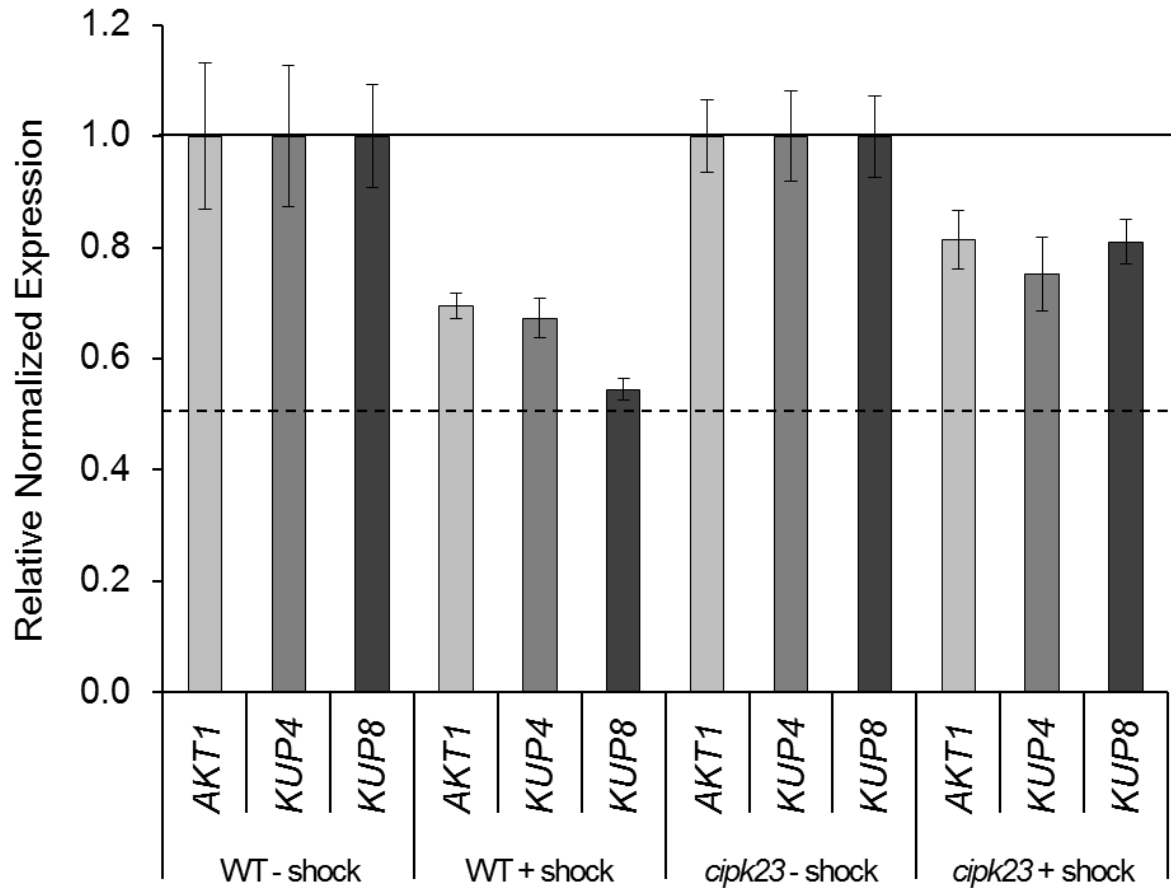
Figure 41: Relative normalized *AKT1*, *KUP4* and *KUP8* expression in wild type and *cipk23* plants after nitrogen starvation and after subsequent ammonium shock.
Plants were grown hydroponically in HL solution (as described in methods) for 6 weeks and then transferred in HL solution without nitrogen. After 4 days of nitrogen starvation (WT - shock; *cipk23* - shock) part of the plants were subjected to HL with 1mM $(NH_4)_2SO_4$ for 30 min – ammonium shock (WT + shock; *cipk23* + shock). The relative expression is the expression normalized independently to that in wild type or *cipk23* plants under N-starvation conditions. Experiment was reproduced (n=3) and representative data is shown as the mean ±SD. WT, wild type plants; *cipk23*, T-DNA insertion line SALK_036154C.

In general, *AKT1*, *KUP4* and *KUP8* were transcriptionally repressed in response to ammonium resupply, both in WT and *cipk23* plants. These data correspond with a mRNA array experiment, where the addition of nitrate to nitrogen-deprived plants decreased *HAK5* mRNA levels (Wang, Garvin, and Kochian 2001). However, the transcript levels of *AKT1* and *KUP4* decreased by 30% and *KUP8* to 50% after ammonium shock in wild type plants, but only by around 20% in *cipk23* (Fig. 41).

In summary, *AKT1* and *KUP4* expression levels were similar in wild type and *cipk23* plants. However, *KUP8* was expressed significantly higher in *cipk23* after ammonium shock (T-test, p≤0.05, Fig 41).

5.9.4   Expression of *CIPK23*, *CBL1* and *CBL9* genes after ammonium resupply

In order to shut down ammonium transport efficiently via phosphorylation, the responsible kinase is expected to be regulated by ammonium availability. In line with that, *CIPK23* expression increased with time under ammonium resupply. Nevertheless, in the first 15 min no increase in *CIPK23* mRNA level was detected compared to untreated plants (4 days HL-N). However, after 30 minutes, *CIPK23* transcripts reached twice the initial amount. Even after one and two hours, the *CIPK23* mRNA levels were still increasing, but not as strong as in the first 30 minutes, indicating an advancing expression peak (Fig. 42).

CIPK23 phosphorylation activity is dependent on CBL calcium sensors. Since CIPK23 regulates AKT1 (Xu et al. 2006; Cheong et al. 2007) and NRT1;1 (Ho et al. 2009) activity in complex with CBL1 and CBL9, *CBL1* and *CBL9* expression was also investigated. The expression of *CBL1* was increased in high ammonium conditions and its peak was detected after 30 minutes of ammonium resupply, with five times more transcripts compared to plants in nitrogen starvation. However, after one and two hours of ammonium supply, *CBL1* transcripts were roughly half, relative to the measurement before. The expression of *CBL9* also increased after 30 min of ammonium availability. Nevertheless, further ammonium resupply did not alter *CBL9* mRNA (Fig. 42).

Figure 42: Relative normalized expression of *CIPK23*, *CBL1* and *CBL9* genes in 6 weeks old wild type plants after 4 days of nitrogen starvation (-N) and after 5, 15, 30, 60, 120 min of 2mM NH$_4^+$ (as 1mM (NH$_4$)$_2$SO$_4$) shock.
Plants were grown hydroponically and subjected to high ammonium concentration, as described in the methods. Significance was tested using ANOVA Turkey test, p≤0.1. Experiment was reproduced (n=3) and representative data is shown as the mean ±SD.

In summary, *CIPK23* transcription increased after 15 minutes and increased steadily, while the transcript levels of *CBL1* increased more rapidly and peaked already after 30 minutes. *CBL9* expression appeared to be regulated not as strong as the *CBL1* gene and therefore might not play a role in the repression of ammonium transport activity.

5.9.5 Expression of *CBL1* and *CBL9* genes in *cipk23* plants

To investigate whether *CBL1* and *CBL9* expression in *cipk23* followed that of wild type plants, *CBL1* and *CBL9* transcript levels were also measured with RT-PCR. Because ammonium uptake

experiments were done 30 minutes after ammonium resupply, *CBL1* and *CBL9* transcription was determined at the same time points.

Essentially, *CBL1* and *CBL9* transcripts were regulated in the same way in *cipk23* and wild type plants. *CBL9* transcript levels were unchanged and *CBL1* showed an almost five times higher expression 30 minutes after ammonium shock (Fig. 43).

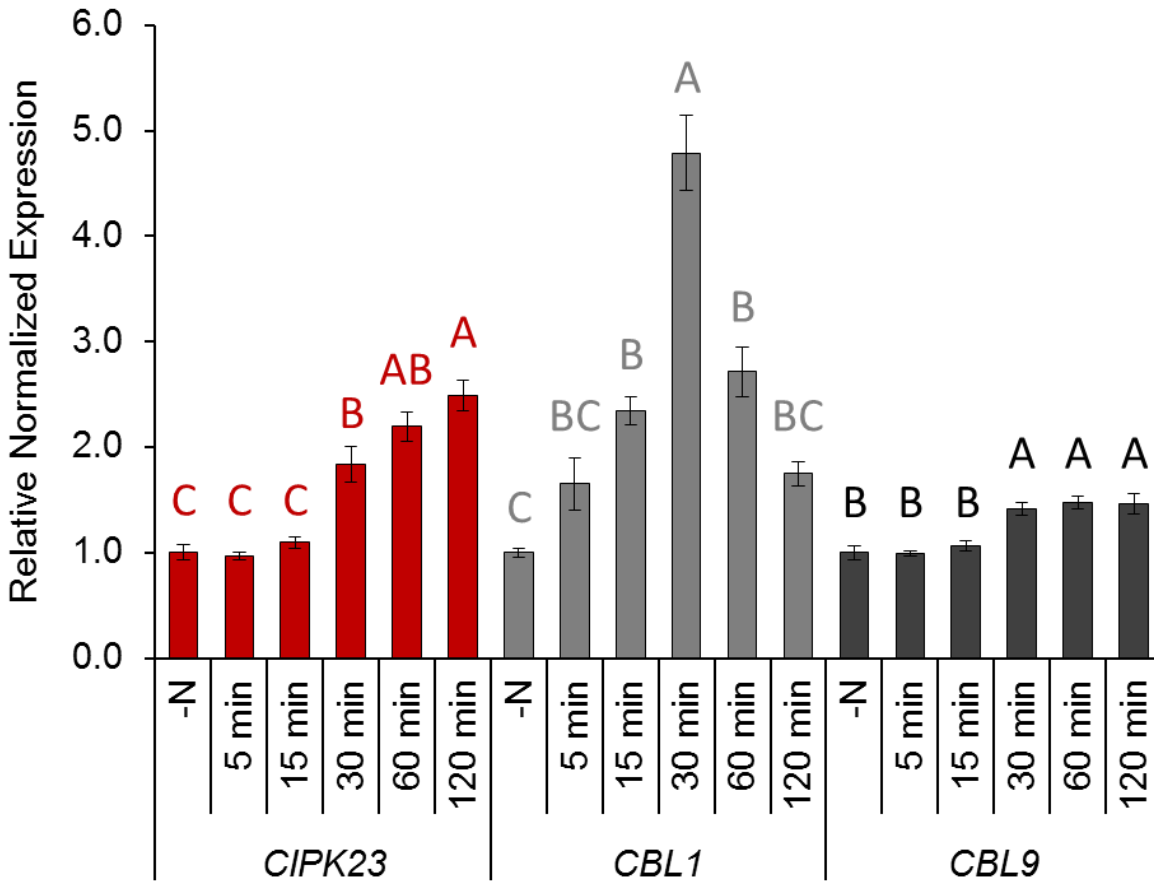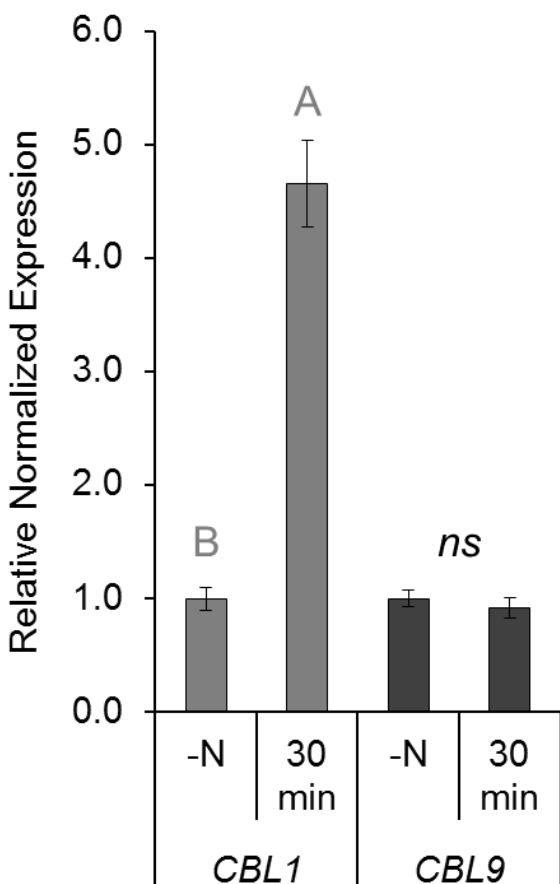**Figure 43: Relative normalized expression of *CBL1* and *CBL9* genes in 6 weeks old *cipk23* plants after 4 days of nitrogen starvation (-N) and after 30 min of 2mM NH_4^+ (as 1mM $(NH_4)_2SO_4$) shock.**
Significance was tested using students T-test, p≤0.001. Experiment was reproduced (n=2) and representative data is shown as the mean ±SD.

5.10 Knock-out of *CBL1* gene mimics knock-out of *CIPK23*

To stimulate CIPK23 kinase activity, the kinase has to interact with either CBL1 or CBL9 protein. As the expression experiments (Chapter 5.9.1) revealed an ammonium-dependent regulation of *CBL1* and *CBL9*, *cbl1* and *cbl9* mutant plants were ordered, homozygotes were isolated and subjected to ^{15}N uptake experiments, as described in Chapter 5.3.

The repression of the respective transcripts in T-DNA insertion lines (*cbl1*, SALK_110426C; *cbl9*, SALK_142774C) of *CBL1* and *CBL9* genes was analysed and confirmed by RT-PCR assay (Fig. 44).
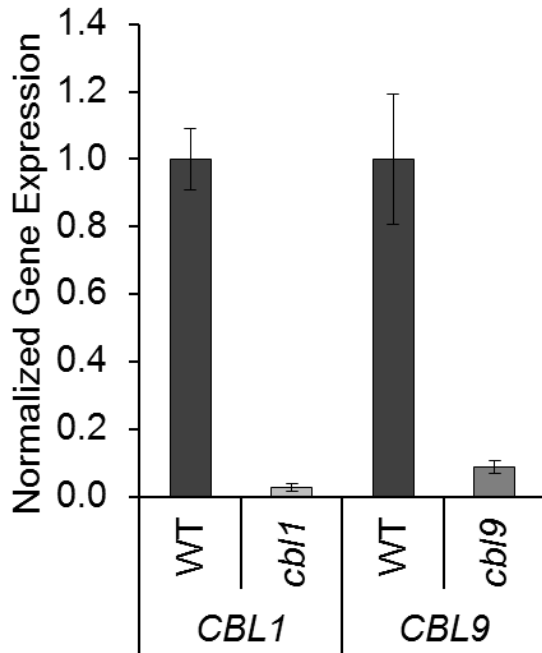
Figure 44: *CBL1* and *CBL9* genes expression in *cbl1*, *cbl9* mutant lines.
Using quantitative PCR, two different T-DNA insertion lines (*cbl1* and *cbl9*) were tested for their expression of the respective gene relative to wild type (WT). Experiment was reproduced (n=2) and representative data is shown ± SD. *cbl1*, T-DNA insertion line SALK_110426C; *cbl9*, T-DNA insertion line SALK_142774C.

Strongly reduced levels of CBLs were encountered, suggesting that both lines were true *loss-of-function* lines. If CBL1 and CBL9 were redundant, no ammonium hyper-sensitivity would be expected. However, if the hyper-sensitivity was associated with a single CBL, the respective mutant line should at least partially impair CIPK23 activity and therefore increase ammonium uptake after ammonium shock.

In ammonium uptake experiments, *cbl1* performed similar to *cipk23* plants. Ammonium uptake after ammonium shock was significantly increased in *cbl1* mutants, however, at 5 mM ^{15}N-labelled ammonium not as strong as in *cipk23*. In contrast, c*bl9* plants did not show any difference in ^{15}N uptake compare to wild type plants (Fig. 45).

This result pinpoints to the relevance of CBL1 in the regulation of AMTs by CIPK23. The combination of the transcriptional regulation of *CBL1* and the similar ammonium uptake of *cipk23* and *cbl1* plants suggest the requirement of these two components in AMT regulation and that CBL1 and CBL9 perform non-redundant functions.
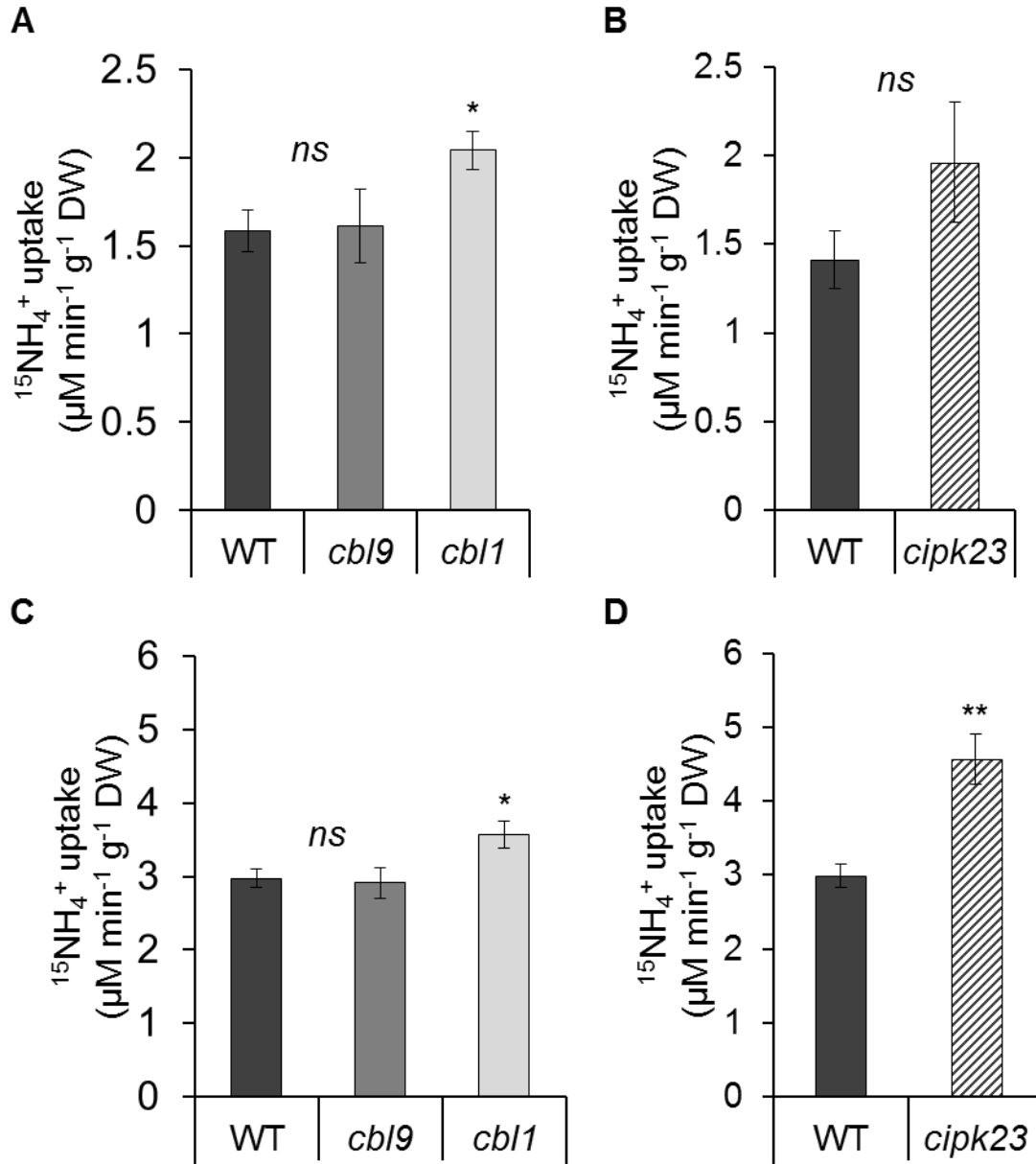
Figure 45: Ammonium uptake after ammonium shock in wild type, *cipk23*, *cbl1* and *cbl9* plants.
Uptake (6 min) of ^{15}N-labeled ammonium (0.5 mM) into roots of wild type plants (WT), *cbl1* and *cbl9* plants (A); wild type plants (WT) and *cipk23* plants (B). Uptake (6 min) of ^{15}N-labeled ammonium (5 mM) into roots of wild type plants (WT), *cbl1* and *cbl9* plants (C); wild type plants (WT) and *cipk23* plants (D). Plants were grown hydroponically for 6 weeks with 1 mM potassium, as previously described. For uptake experiments plants were moved to the HL solution containing 0.5 mM ^{15}N [0.25 mM (^{15}NH$_4$)$_2$SO$_4$] (A, B) or 5 mM ^{15}N [2.5 mM (^{15}NH$_4$)$_2$SO$_4$] (C, D) for 6 min. Significance was tested using students T-test and indicated by stars; *, p≤0.05; ** p≤0.01; ns, not significant. Experiment was reproduced (n=2) and representative data is shown ±SD. WT, wild type plants; *cbl1*, T-DNA insertion line SALK_110426C; *cbl9*, T-DNA insertion line SALK_142774C; *cipk23*, T-DNA insertion line SALK_036154C.

However, to confirm that CBL1 is involved in ammonium regulation and to exclude that the impaired potassium accumulation influences ammonium uptake, the experiments could be reproduced with elevated potassium concentration, as described in Chapter 5.6.

5.11 AMT-CIPK23 interaction analysis *in planta*

Despite strong genetic evidence for the interaction of CIPK23 with ammonium transport, it was unclear whether it directly or indirectly regulated AMTs. If CIPK23 regulates the activity of ammonium transporters by phosphorylation, direct physical interaction between AMT and kinase is inevitable. To examine a potential protein-protein interaction, bimolecular fluorescence complementation assays (BiFC) in plants (*in situ*) were used. The BiFC system *in planta* benefits from the presence of further possible required interaction partners: as the activity and localisation of CIPK23 kinase depends on the presence of CBLs, this additional interaction partner is thus available for the physical interaction in plant cells. By contrast, in heterologous systems, such as two-hybrid systems with yeast, CBLs might be not present and the CIPK23-AMT interaction might not take place.

Phosphorylation of the cytosolic carboxyl termini of AMT1;1 and AMT1;2 transporters has been demonstrated or predicted (Marini et al. 2000; Neuhäuser et al. 2007; Severi, Javelle, and Merrick 2007; Lanquar et al. 2009), while it is unknown whether AMT2;1 is also modified by phosphorylation. Therefore, the *AMT1;1*, *AMT1;2* and *AMT2;1* genes under their endogenous promoters were cloned into the BiFC vector system. For control constructs, the *CIPK23* promoter region (1500 bp upstream of the gene) was cloned in front of the N-terminal fragment of YFP and served as negative control to determine background fluorescence. Co-expression of ammonium transporters fused with N- or C-fragments of YFP was used as a positive control. Different combinations of YN (N-terminal sequence of YFP) and YC (C-terminal sequence of YFP) fusion pairs were stably expressed in plants (Fig. 46) and representative pictures from the roots are shown below (Fig. 47-49).

Figure 46: BiFC configurations for testing the AMT-CIPK23 interaction.
Yellow-shaded squares symbolize fluorescence from protein-protein interaction. YN, N-terminal fragment of YFP; YC, C-terminal fragment of YFP. Based on (Ohad, Shichrur, and Yalovsky 2007).
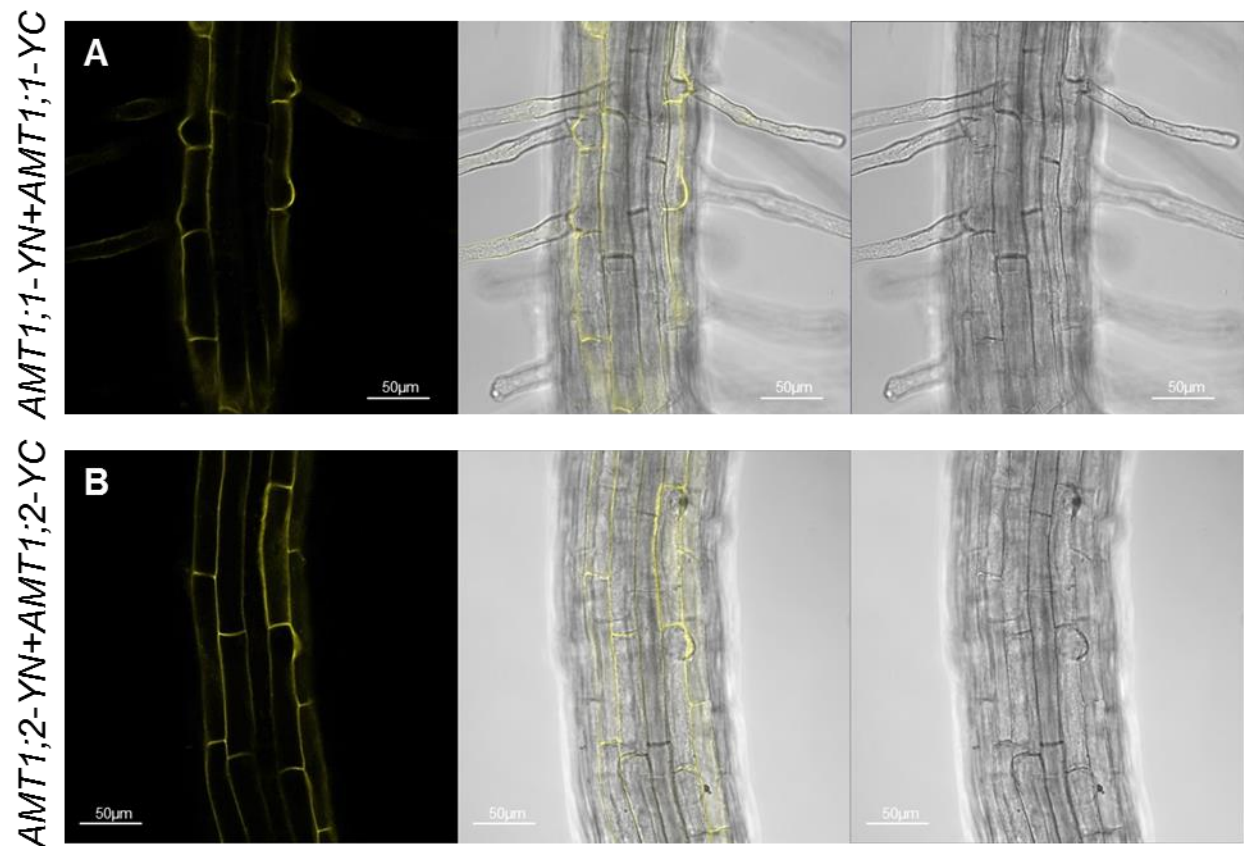
Figure 47: Ammonium transporters interaction in Arabidopsis root cells, bimolecular fluorescence complementation (BiFC) assay.
(A) *pAMT1;1::AMT1;1-YN* co-expressed with *pAMT1;1::AMT1;1-YC*. (B) *pAMT1;2::AMT1;2-YN* co-expressed with *pAMT1;2::AMT1;2-YC*.

Ammonium transporters localize in the plasma membrane as trimers, thus, plants expressing two AMTs fused with N- or C-parts of YFP (*AMT1;1-YN + AMT1;1-YC*; *AMT1;2-YN + AMT1;2-YC*), YFP should come in close proximity. Consequently, the functional YFP should be reconstructed and fluorescence detected. This experiment served as positive control of the BiFC system and was successful (Fig. 47).

Co-expression of tagged CIPK23 together with AMT1;1 or AMT1;2 (fused with complemental halves of YFP) generated functional YFP molecules (Fig. 48), indicating a direct interaction for these CIPK23-AMT pairs. The strongest BiFC signals were obtained with AMT1;1 and CIPK23 (Fig. 48A). In contrast, co-expression of CIPK23 kinase and AMT2;1 transporter did not restore YFP and no fluorescence was detected.
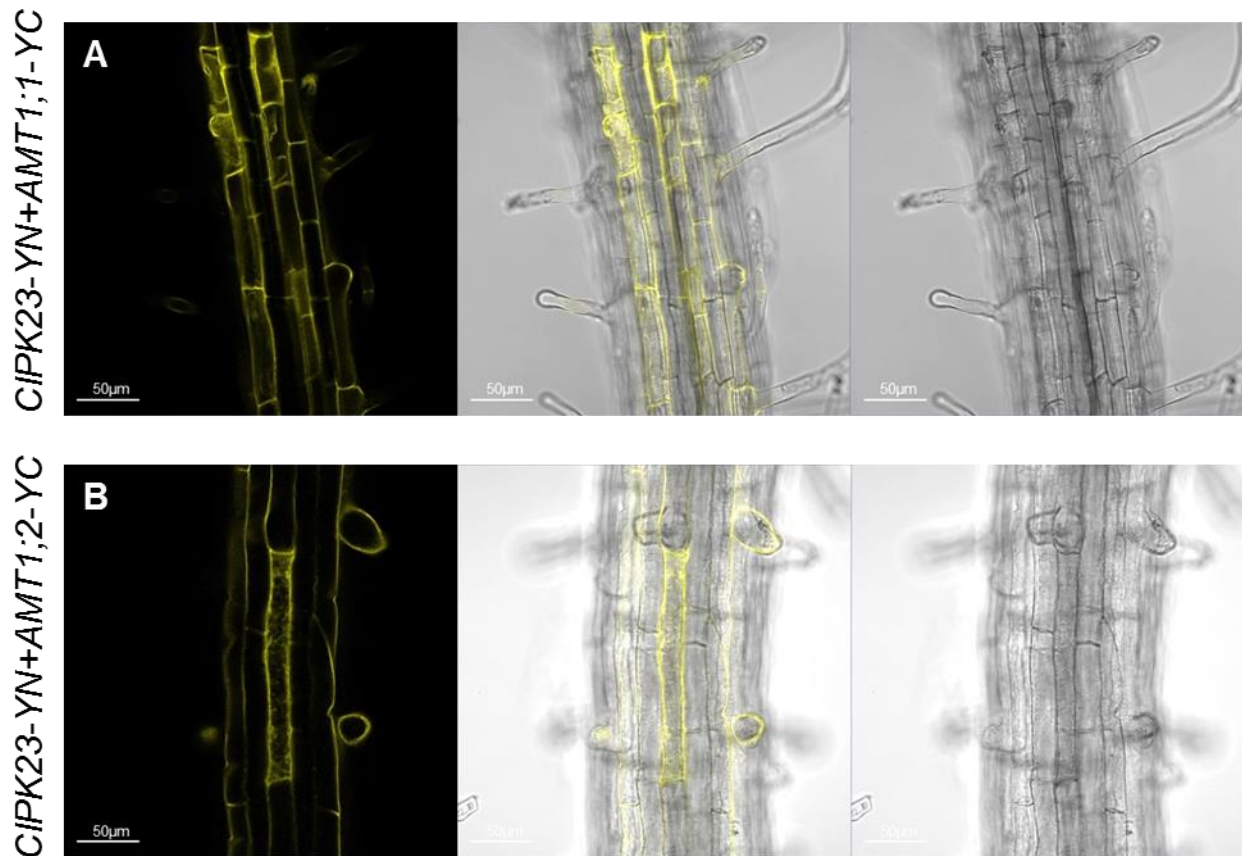
Figure 48: CIPK23 interacts with AMT1;1 and AMT1;2.
(A) *pCIPK23::CIPK23-YN* **coexpressed with** *pAMT1;1::AMT1;1-YC.* **(B)** *pCIPK23::CIPK23-YN* **coexpressed with** *pAMT1;2::AMT1;2-YC.*

To exclude the possibility that the detected fluorescence resulted from coincidental protein-protein proximity that restored YN and YC to fluorescing YFP, without real interactions of CIPK23 and AMTs, *pAMT1;1::AMT1;1-NY* or *pAMT1;2::AMT1;2-NY* were co-expressed with the C fragment of YFP under the *CIPK23* endogenous promoter. Reconstitution was observed neither with *AMT1;1-YN,* nor with *AMT1;2-YC* (Fig. 49). Only a very weak background signal was visible, that was easily distinguishable from real YFP fluorescence (Fig. 47-48).

Additional, the spectral signature and an estimate of the maximum emission of the reconstructed YFP protein was recorded using lambda stacks. The emission maximum obtained from λ stack corresponds to the maximum emission of enhanced YFP, which is around 530 nm ("Learn How to Analyze Emission Fingerprinting with Lambda Stacks" 2016) (Fig.50).

pCIPK23-YN+AMT1;1-YC
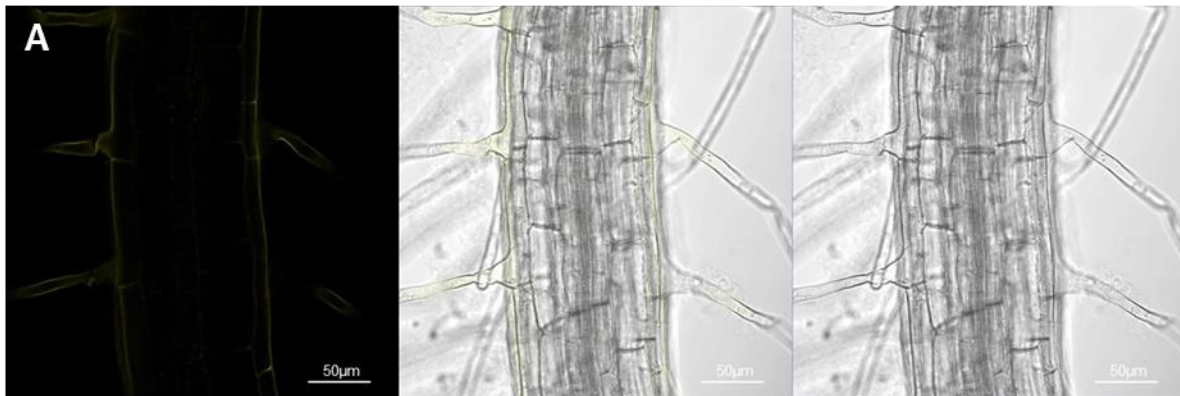
pCIPK23-YN+AMT1;2-YC
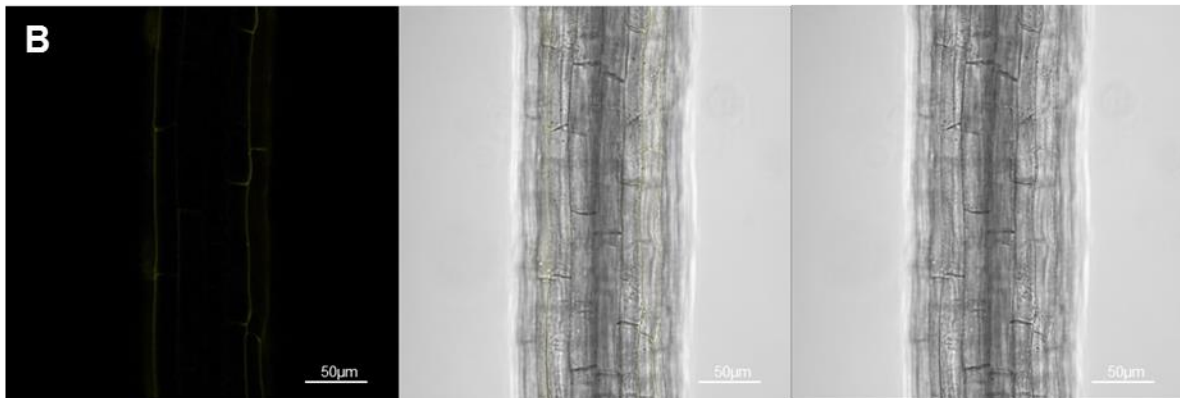
Figure 49: Coexpression of N fragment of YFP under *CIPK23* promoter with *pAMT1;1::AMT1;1-YC* (A) and *pAMT1;2::AMT1;2-YC* (B).
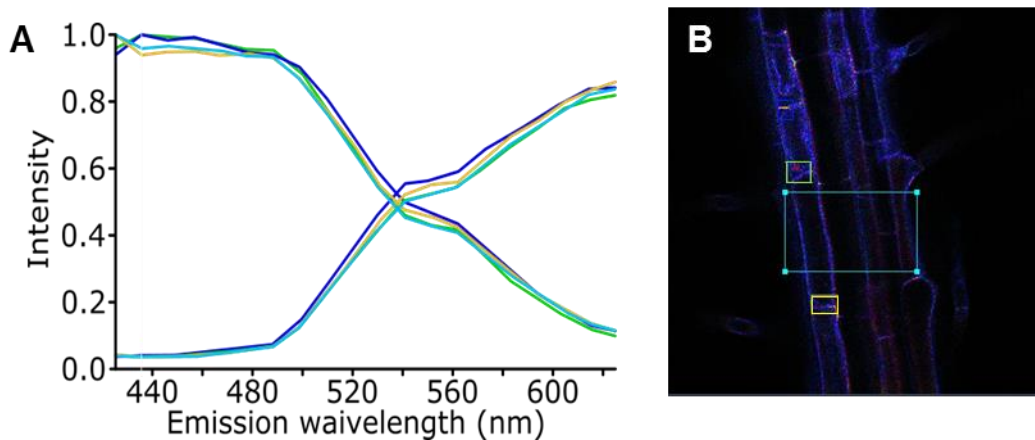
Figure 50: Lambda stack from reconstructed YFP protein.
(A) Reconstructed YFP maximum emission is at approximately 530 nm. Four emission measurements were taken at locations shown in B (corresponding colours). (B) Lambda encoded confocal picture with *pCIPK23::CIPK23-YN* coexpressed with *pAMT1;1::AMT1;1-YC*. nm, nanometers.

The results gained from BiFC experiments in *Arabidopsis* roots suggested direct protein-protein interaction between CIPK23 kinase and AMT1;1 or AMT1;2 transporters, but not with AMT2;1, which lacks relevant similar phosphorylation sites in the C-terminus. Because no specific YFP signal was obtained between AMT2;1 and CIPK23, the following experiments focussed on AMT1;1 and AMT1;2 phosphorylation by CIPK23 kinase.

5.12 Phosphorylation state of AMT1;1 and AMT1;2

At this point, the influence of CIPK23 in ammonium transport and the direct interaction with AMT1;1 and AMT1;2 was evident. However, the function of CIPK23 in ammonium transport system was not clarified. In order to test whether the CIPK23 might directly act as a kinase that phosphorylates ammonium transporters (AMTs), the phosphorylation state of AMTs was measured.

Ammonium resupply of nitrogen-starved seedlings induces phosphorylation of residues in the C-terminus of ammonium transporters (Lanquar et al 2009). Using Western blot (WB) with phosphorylation-specific antibodies, the phosphorylation state of AMTs after 30 min of ammonium shock was examined. Plants were grown and treated as described in Chapter 5.3. Membrane proteins were extracted from 6 weeks-old plant roots by microsome preparation,

separated by dodecyl sulfate polyacrylamide gel electrophoresis, transferred to a nitrocellulose membrane, bound by antibodies and detected using spectrophotometric methods.

Since the C-terminus of AMT1s is highly conserved, a phospho-specific antibody (anti-P) raised against the phosphorylated threonine in peptide: CG-Nle-D-Nle-**pT**-RHGGFA-amide of AMT1;1 was expected to additionally detect phosphorylated AMT1;2 and AMT1;3 proteins; but not the weakly expressed AMT1;4 or AMT1;5. Previous YFP complementation experiments demonstrated that AMT1;1 and AMT1;2 are direct targets for CIPK23 kinase. To specifically examine the phosphorylation state of AMT1;1 or AMT1;2 proteins in wild type and *cipk23* plants, plants stably expressing *pAMT1;1::AMT1;1-GFP* or *pAMT1;2::AMT1;2-GFP* were used. In transgenic lines with GFP-fused ammonium transporters, two bands corresponding to AMTs are expected to be detected by the anti-P antibody. The first band is a pool of phosphorylated monomers from AMT1;1, AMT1;2 and AMT1;3 proteins in SDS-PAGE. The expected molecular mass of monomeric AMT proteins is around 33-55 kDa (Blakey et al. 2002; Ludewig et al. 2003; Lanquar et al. 2009; Yuan et al. 2013). The second band corresponds to phosphorylated GFP-tagged monomers of *AMT1;1-GFP* or *AMT1;2-GFP*. with a shift in the band size due to increased molecular weight by GFP (~27 kDa) fusion. In addition, this band must be detected in the protein gel blot analysis with anti-GFP antibody. Importantly, the anti-GFP antibody detects *AMT1;1-GFP* or *AMT1;2-GFP* proteins irrespective of their phosphorylation status and thus serves as a control for protein quantification. Presumably, the intensity of the band identified by anti-GFP antibody represents the total amount of *AMT1;1-GFP* proteins (*AMT1;1-GFP + AMT1;1-GFP~P*) or *AMT1;2-GFP* proteins (*AMT1;2-GFP + AMT1;2-GFP~P*) in the samples. Thus, the intensity of the bands identified by anti-P antibody were normalised to the intensity of total *AMT1;1-GFP* or *AMT1;2-GFP* proteins, detected by anti-GFP antibody.

In wild type plants expressing *pAMT1;1::AMT1;1-GFP*, phosphorylated AMT1;1 proteins were detected after the treatment with 1 mM $(NH_4)_2SO_4$ for 30 min (Fig. 51A). As expected, using the anti-P antibody, two bands differing in molecular weight were detected: at around 45 and 80 kDa. The band at around 80 kDa, in my opinion, is likely representing *AMT1;1-GFP~P* proteins, as in previous studies (Yuan et al. 2007), while the 45 kDa band represents phosphopeptides of AMT1;2, AMT1;3 and AMT1;1 that are not fused to GFP. In contrast to WT plants, in *cipk23*

expressing *pAMT1;1::AMT1;1-GFP,* phosphorylation of *AMT1;1-GFP* was strongly reduced (Fig. 51D), while phosphorylation of other AMT1s was almost undetectable (Fig. 51C). Despite these differences in phosphopeptides, the amount of proteins (*AMT1;1-GFP + AMT1;1-GFP~P*) identified by the anti-GFP antibody in *cipk23* plants was comparable to the amount in Col-0 plants (Fig. 51B). Evaluation of WB staining revealed that *cipk23* plants exhibited around 50% decrease in *AMT1;1-GFP* phosphorylation compared to the control plants (wild type) after 30 min of ammonium shock.

The phosphorylation state of ammonium transporters in wild type and *cipk23* plants expressing *AMT1;2-GFP* protein was tested with the same experimental scheme. Similar to the previous results for *AMT1;1-GFP*, ammonium transporters (AMT1;1, AMT1;2 and AMT1;3) in WT were more phosphorylated after ammonium resupply than in *cipk23* (Fig. 52). Unfortunately, the level of *AMT1;2-GFP* phosphorylation apart from other AMTs could not be convincingly detected, possibly due to lower expression levels. In plant roots, AMT1;2 protein is expressed in lower levels than AMT1;1 and was undetectable in the Western blot. Optimization attempts like increased antibody concentration and/or exposure time resulted in too strong background.

In summary, ammonium resupply triggers phosphorylation of ammonium transporters in wild type plants in a larger scale than in *cipk23*. Nevertheless, also in *cipk23,* a certain degree of phosphorylation was detectable in response to ammonium treatment.

Figure 51: Ammonium transporters phosphorylation in wild type and *cipk23* plants expressing *pAMT1;1::AMT1;1-GFP* after ammonium shock.
Plants were grown hydroponically for 6 weeks (as described in methods). 4 days nitrogen starved wild type (WT) and *cipk23* plants were exposed to 2 mM NH_4^+ [1 mM $(NH_4)_2SO_4$] for 30 min. (A) Western blot of wild type (WT) and *cipk23* plants containing *AMT1;1-GFP* using the anti-P antibody (n=2). (B) Western blot of wild type (WT) and *cipk23* plants containing *AMT1;1-GFP* using the anti-GFP antibody (n=2). (C) Relative intensity of the band at 45 kDa using anti-P antibody (AMT1s phosphopeptide). (D) Relative intensity of the band at 80 kDa using anti-P antibody (*AMT1;1-GFP* phosphopeptide). Intensity values from the bands at 45 kDa and 80 kDa from blot A were normalized to the intensities of the band at 80 kDa from the blot B.
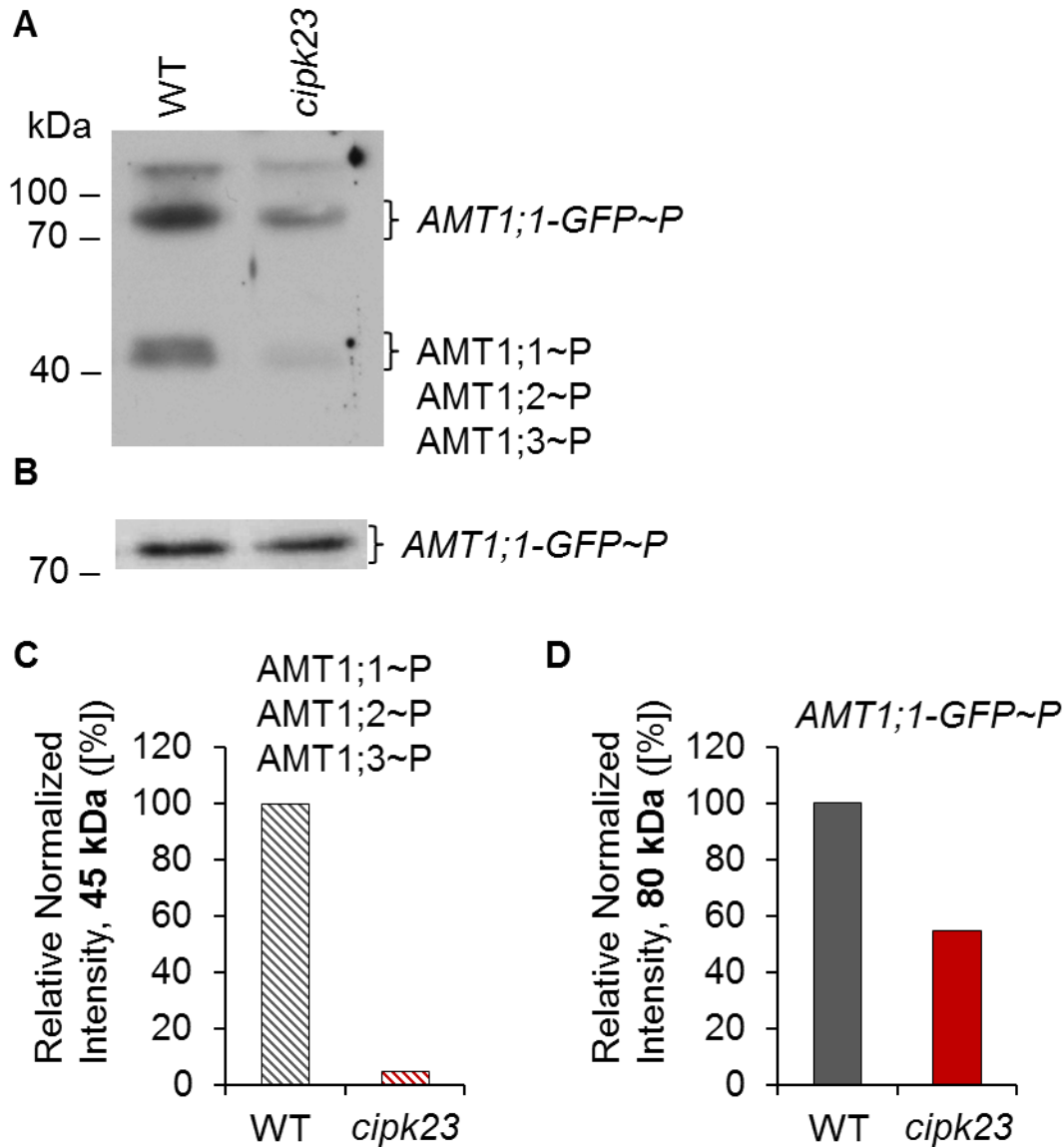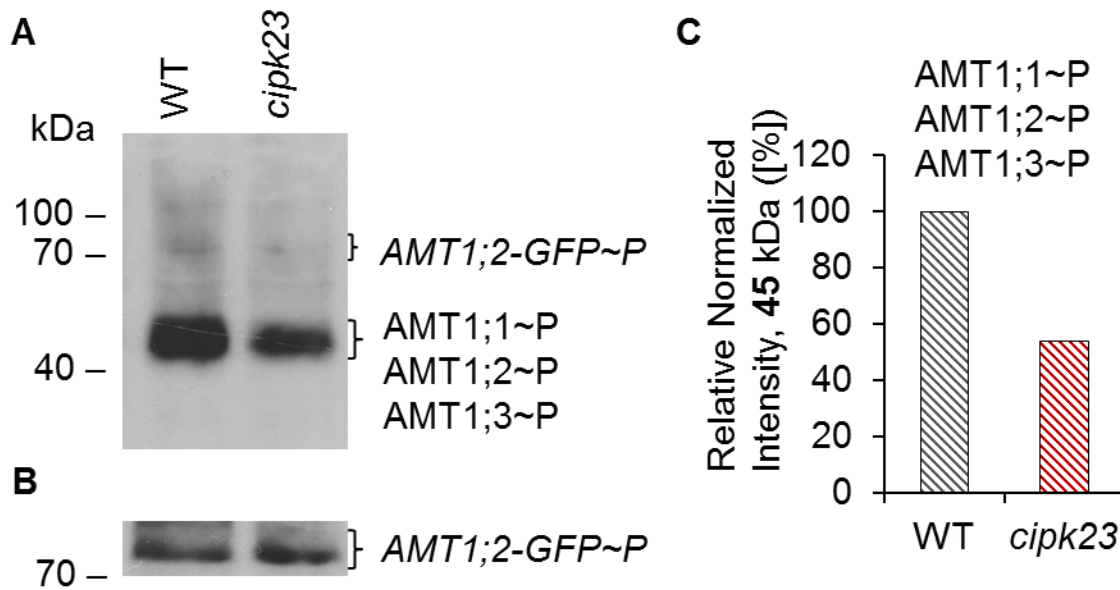
Figure 52: Ammonium transporters phosphorylation in wild type and *cipk23* plants expressing *pAMT1;2::AMT1;2-GFP* after ammonium shock.
Plants were grown hydroponically for 6 weeks (as described in methods). 4 days nitrogen starved wild type (WT) and *cipk23* plants were exposed to 2 mM NH_4^+ [1 mM $(NH_4)_2SO_4$] for 30 min. (A) Western blot of wild type (WT) and *cipk23* plants expressing *AMT1;2-GFP* using the anti-P antibody (n=3). (B) Protein extracts of WT and *cipk23* plants containing *AMT1;2-GFP* using the anti-GFP antibody (n=3). (C) Relative intensity of the band at 45 kDa using anti-P antibody (*AMT1;2-GFP* phosphopeptide). Intensity value from the band at 45 kDa from blot A was normalized to the intensities of the band at 80 kDa from the blot B.

Despite the lack of the CIPK23 kinase, a low level of ammonium transporter phosphorylation was detected in *cipk23* plants. Previously, Lanquar with colleagues showed that phosphorylation of T460 in AMT1;1 protein was time dependent (Lanquar et al. 2009). To analyze the time dependence of ammonium-triggered phosphorylation in WT and *cipk23* plants, two time points of ammonium resupply to nitrogen-deprived plants were analyzed in the following experiment.

Similar to the results obtained by Lanquar, after 4 days of nitrogen depletion, ammonium transporters were non-phosphorylated in WT and *cipk23* plants (Fig. 53A). Ammonium resupply (2 mM NH_4^+) for 15 min was sufficient to trigger AMT1s phosphorylation in WT and, surprisingly, in mutant plants nearly to the same level. Nevertheless, in WT plants, AMT phosphorylation strongly increased between 15 and 30 min of ammonium resupply. For *cipk23*

plants, the phosphorylation status of ammonium transporters remained approximately constant during the treatment (Fig. 53A and 53C). To control total protein levels in the samples, the nitrocellulose membrane was stained with Ponceau-S after the proteins from microsomal preparations were transferred to the membrane. In WT and *cipk23* plants, total protein levels remained constant during the treatment (Fig. 53B).
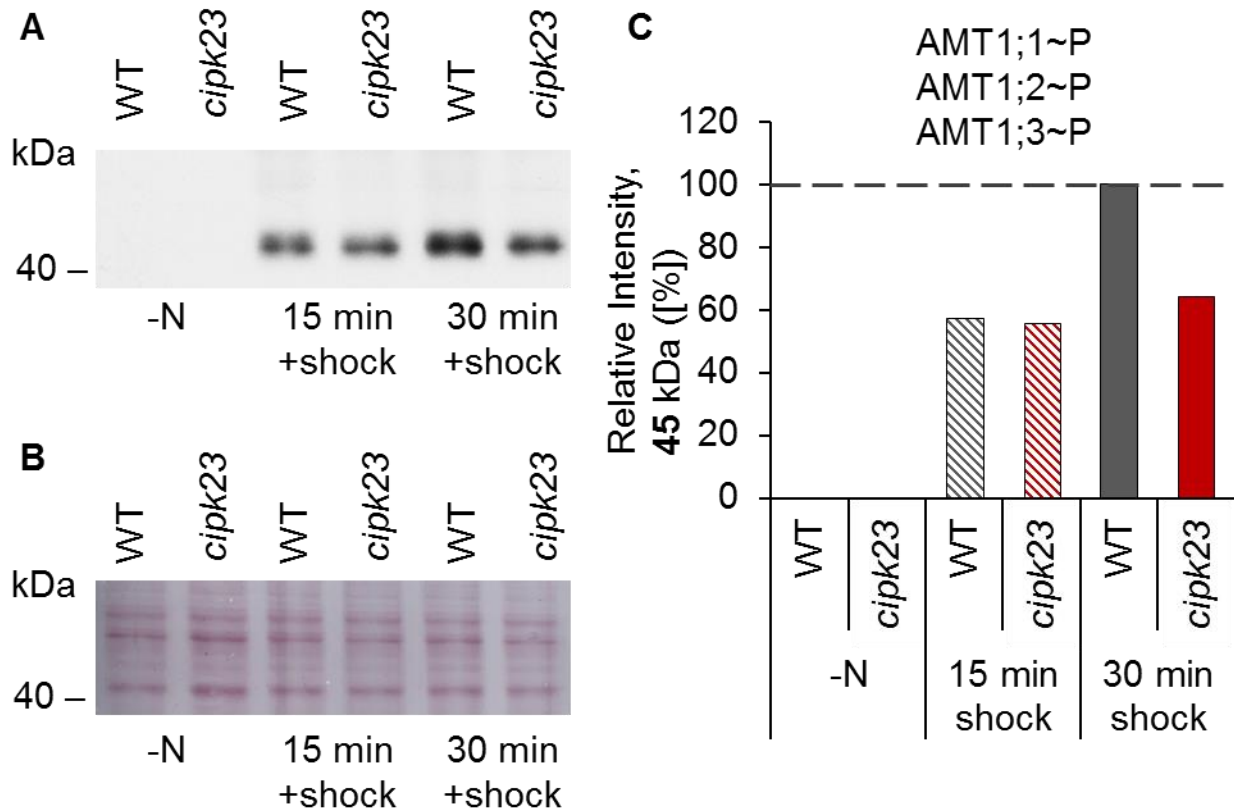
Figure 53: Time dependent phosphorylation of ammonium transporters in wild type and *cipk23* plants.
Plants were grown hydroponically for 6 weeks (as described in methods). 4 days nitrogen starved wild type (WT) and *cipk23* plants were exposed to 2 mM NH_4^+ [1 mM $(NH_4)_2SO_4$] for 15 and 30 min. (A) Protein gel blot analysis using anti-AMT1-P antibody (n = 1). (B) Ponceau staining of the nitrocellulose membrane. (E) Relative intensities of the 45 kDa bands using anti-AMT1-P antibody.

Taken together, WT plants showed ammonium-dependent AMT phosphorylation increased over time. In *cipk23* plants, ammonium resupply triggered AMT phosphorylation to a certain level, which was not significantly changed with time.

5.13 Phosphorylation state of ammonium transporters

Finally, using phosphoproteomics of microsomal fractions, potential differences in phosphorylated peptides were analysed from wild type and *cipk23* mutants. In both wild type and the mutant line, phosphorylated peptides of the ammonium transporter AMT C-termini were identified, but the amount of phosphorylated peptides was low and inconsistently detected. Figure 54 shows data of one selected experimental dataset with the highest coverage of phosphopeptides and lowest variation between biological replicates. The total amount of ammonium transporters (irrespective of the phosphorylation or oxidation status) was adequately high (around 1%) in all samples (Fig. 54D), but quite some variation was identified in the replications. Importantly, the results confirm that ammonium transporters (AMT1;1, AMT1;2 and AMT1;3) were still phosphorylated in the *cipk23* background, in agreement with the previous results. Surprisingly, after ammonium shock, AMT1;1 peptides with the relevant phosphorylated threonine (T460) were more abundant in *cipk23* than in wild type plants (Fig. 54A). In contrast, in *cipk23* plants, phosphorylation of the C-terminal serine (S488) was invariably low, independent from treatments (Fig. 53B). However, disruption of the CIPK23 kinase negatively affected phosphorylation of the AMT1;3 transporter at the position of threonine 464, the homologous position to T460 in AMT1;1 (Fig. 54C). Phosphopeptides of AMT1;2 were identified at very low levels in this experiment, as in two other experiments. Because the high variation among experiments the phosphoproteomics data were considered as premature and are therefore not further discussed.
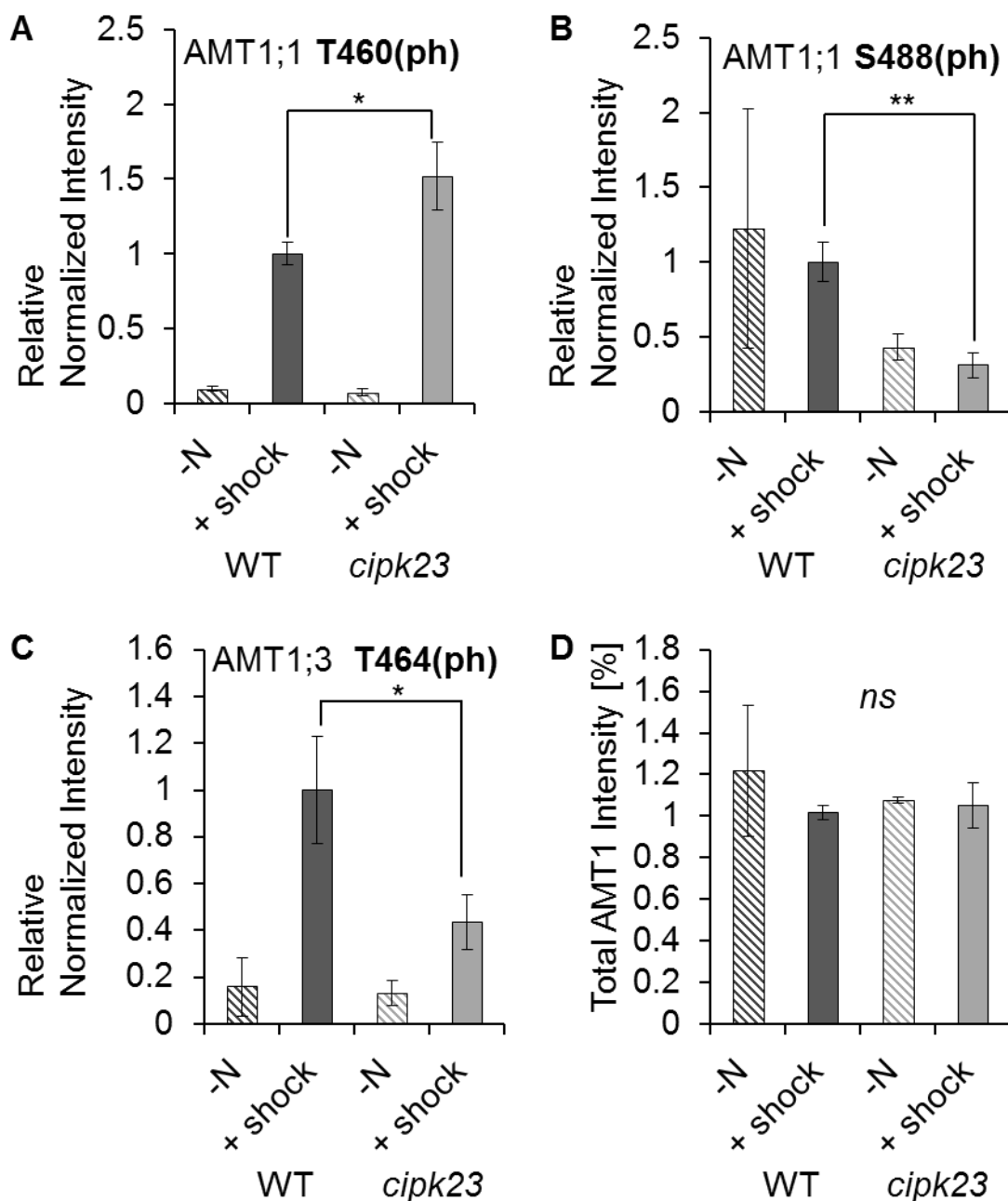
Figure 54: Relative normalized AMT1;1 and AMT1;3 phosphorylation in wild type and *cipk23* plants.
Plants were grown hydroponically for 4 weeks (as described in methods). Subsequently plants grew 4 days without nitrogen (-N) and then half of the plants were exposed to 2 mM NH_4^+ [1 mM $(NH_4)_2SO_4$] for 30 min (+ shock). Relative normalized intensity of ISSEDEMAGMDMT(ph)R from AMT1;1 protein (A), RVEPRS(ph)PSPSGANTTPTPV from AMT1;1 protein (B), ISEQHEMQGMDMT(ph)R from AMT1;3 protein (C), total normalized intensity of ammonium transporters (D). Intensities of phosphopeptides (irrespective of the oxidation level) were normalized to the total peptides intensity in the same sample. Significance was tested using T-test; *, p≤0.05, **, p≤0.01, ns, not significant. Experiments were repeated (n=3), data is shown ±SD

6 Discussion

For plants, ammonium (NH_4^+) is an important inorganic nitrogen source, and its assimilation requires less energy compared to nitrate (Mehrer and Mohr 1989). To uptake ammonium over a wide range of concentrations, plants developed low- and high-affinity ammonium transport systems (Kronzucker, Siddiqi, and Glass 1996; Wang et al. 1993). However, high ammonium levels repress plant growth (Chen et al. 2013; Li, Shi, and Su 2010; Li et al. 2011). It was demonstrated that high-affinity ammonium transporter *At*AMT1;1 was phosphorylated in response to ammonium resupply (Lanquar et al. 2009). This phosphorylation prevents further ammonium transport by allosteric inactivation of the AMT trimer and ensures fast reaction to high, potentially toxic ammonium concentrations. This work identified a kinase which is responsible for a fair amount in the rapid reduction of ammonium transport activity.

6.1 CIPK23 integration in ammonium regulatory network

In a bioinformatics screen, 52 kinases were identified as potential kinase candidates that could regulate ammonium transporter activity in *Arabidopsis thaliana*. Initial experiments were based on the hypothesis that lack of the functional kinase in the ammonium regulatory pathway would lead to uncontrolled ammonium uptake through not phosphorylated and thus hyper-active ammonium transporters (Fig. 16). Accordingly, plants devoid of the kinase accumulate more ammonium over time and are expected more susceptible to toxic concentrations of ammonium/methylammonium than WT.

Plant lines with a T-DNA insertion in the *AT1G30270* (*k1*, *CIPK23*) gene and in the *AT2G41890* (*k2*) gene showed increased sensitivity to elevated concentrations of ammonium and methylammonium (Fig. 17). However, disruption of only one kinase resulted in increased ammonium uptake after ammonium shock. *Cipk23* mutants were isolated and had a severely reduced ability to decrease ammonium uptake, when subjected to 5 mM ammonium. Complementation of ammonium transport activity was achieved when the *cipk23* mutant was transformed with the *CIPK23* wild type allele (Fig. 29 – 30, and Table 21).

Surprisingly, short-term uptake showed that *cipk23* did not significantly differ in ^{15}N accumulation at low (0.5 mM) ammonium concentration (Fig. 27 and Table 21). Nevertheless,

prolonging the incubation time to 30 min revealed that ammonium import in wild type and *cipk23* plants occurred with diverse capacity (Fig. 28 and Table 21). This is likely explained by the differential effect of phosphorylation on differently localized AMTs: AMT1;1 in the epidermis and AMT1;2 in inner cortical and endodermal cells, where ammonium later reaches high levels.

Ammonium resupply to N-deprived roots triggers complex plant responses including reduction of ammonium transporter gene expression (Fig. 38, Rawat et al. 1999; Straub, Ludewig, and Neuhäuser 2014) and phosphorylation of ammonium transporter C-termini (Fig. 52, Lanquar et al. 2009). These changes on transcriptional and post-transcriptional levels aim to rescue the plant from accumulation of potentially toxic ammonium amounts.

However, dysfunction of the CIPK23 kinase did not result in complete reduction of AMT phosphorylation and activity. Importantly, a *loss-of-function* mutation in the *CIPK23* gene did not influence AMT (AMT1;1, AMT1;2, AMT2;1) protein amount or localization (Fig. 39–40). After 30 min of ammonium shock, phosphorylated ammonium transporters were detected in *cipk23* plants (Fig. 51–53). This certain phosphorylation level of AMTs in *cipk23* mutants is evidently responsible for the detected reduction of ammonium uptake at 0.5 mM ammonium in the medium.

However, longer ammonium resupply and/or higher ammonium concentrations lead to further increase in AMT phosphorylation in the wild type (Fig. 53, Lanquar et al. 2009), but not in *cipk23* plants (Fig. 53). Lanquar and colleagues showed that *At*AMT1;1 phosphorylation occurred already at very low ammonium concentration such as 50 µM – a potentially not toxic condition (Lanquar et al. 2009). Presumably, some other kinase is additionally involved in this response to ammonium resupply, while a further reaction to elevated ammonium is mediated by the CIPK23 kinase. This hypothesis is supported by the transcriptional regulation of the CIPK23 kinase in response to ammonium availability. When ammonium was added to N-starved plants, the amount of *CIPK23* transcript remained unchanged for the first 15 min. However, 30 min of ammonium supply to the roots was accompanied by strong induction of *CIPK23* gene expression. Even after two hours, *CIPK23* mRNA levels were still increasing, but not as strong as in the first 30 minutes (Fig. 42). Notably, *CIPK23* transcript reached a maximum level also after

30 min in response to nitrate resupply to N-starved plants, but in contrast, after 2 hours *CIPK23* mRNA decreased almost to the initial amount (Ho et al. 2009).

Alternatively, high ^{15}N uptake in *cipk23* mutants reflects ammonium LATS in addition to HATS. Potassium channels/transporters might permeate NH_4^+ and were speculated as part of ammonium LATS, but the molecular identity of LATS remains elusive (Schachtman et al. 1992; Bertl et al. 1997; Hoopen et al. 2010). Moreover, the expression of the high-affinity potassium transporter HAK5 is induced by nitrate starvation and its activity is repressed by ammonium ions (Hoopen et al. 2010; Rubio et al. 2014). Indeed, in the hydroponic growth experiments, nitrogen limitation induced *AKT1*, *KUP4*, and *KUP8* transcription. However, under ammonium-replete conditions, *KUP8* was transcriptionally repressed in WT to a larger extend than in *cipk23* mutants (Fig. 41). Presumably the KUP8 transporter is not regulated by CIPK23, but a potential target for the SRK2E kinase, and functionally involved in the potassium efflux (Osakabe et al. 2013). Potassium efflux might be necessary to balance cation homeostasis in root cells when ammonium is extensively taken up by AMTs in the absence of functional CIPK23. Indeed, *cipk23* plants accumulate less potassium compared to WT (Fig. 32A). An alternative explanation for relatively high *KUP8* expression is that KUP8 transporters commit an active extrusion of excess NH_4^+ taken up by hyper-active AMTs in *cipk23* mutants. It was hypothesized that high ammonium supply results in NH_4^+ cycling across the plasma membrane, where ammonium uptake is followed by active ammonium efflux (Britto et al. 2001). Overall, the interference between ammonium and potassium uptake and accumulation always occurs in plants, consequently, modifications in one system affect the other system.

However, the impaired growth of *cipk23* mutants upon the toxic non-metabolizable analogue of ammonium, methylammonium (MeA) (Fig. 33) was directly linked to ammonium, instead of potassium transport. So far, it is postulated that MeA can be transported into the plant root only by ammonium transporters (Moroni, Bardella, and Thiel 1998; Gazzarrini et al. 1999). In comparison to wild type and *qko* plants, *cipk23* mutants were limited in main root elongation and lateral root formation (Fig. 33–35). Moreover, modification of *AMT1* transcription by an *amiRNA* in *cipk23* mutants alleviated *cipk23* growth suppression induced by MeA (Fig. 37). Since AMT1;4 is a pollen-specific ammonium transporter (Yuan et al. 2009) and AMT2;1 is not

responsible for MeA sensitivity in *Arabidopsis* (Yuan et al. 2007), it was aimed to knock-out AMT1;1, AMT1;2, AMT1;3 and AMT1;5 ammonium transporters. Unfortunately, due to the diversity in *AMT1* sequences, complete silencing of all *AMT1*s with one *amiRNA* precursor was not accomplished (Fig. 30). Nevertheless, a *cipk23-amiRNA* plant line restored primary root length to the level of WT plants when exposed to 30 mM MeA (Fig. 37). The quadruple knock-out (*qko*) *Arabidopsis thaliana* line, which is defective in AMT1;1, AMT1;2, AMT1;3 and AMT2;1 transporters, had superior root growth compared to WT and *cipk23-amiRNA* plants. Such result can be explained by residual expression of *AMT1;1* and *AMT1;2* in *cipk23-amiRNA* plants (Fig. 30) that might result in some MeA accumulation in the plant root.

Interestingly, *cipk23* phenotypic alterations partially correspond to the phenotype of the ammonium hypersensitive *amos2* mutant (Li et al. 2011). Moreover, T-DNA insertion in the *amos2* mutant is localised into a 16-cM region at the top of chromosome 1 (Fig. 55), covering the position of the *CIPK23* gene.

Similar to the growth on MeA of the *cipk23* plants, *amos2* mutants showed almost complete cessation of lateral root emergence under high ammonium concentrations (Li et al. 2011).
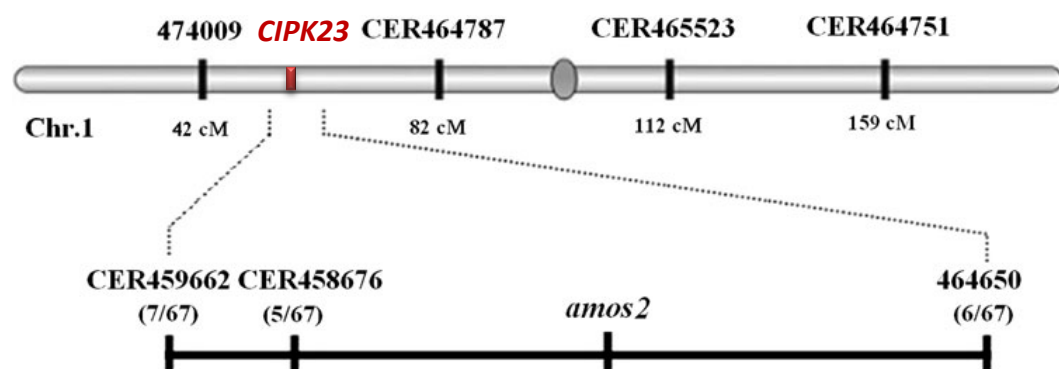

Figure 55: Genetic map of the amos2 locus.
CIPK23 position is close to the center of the identified region. Modified from (Li et al. 2011).

Based on the above, the knock-out of the *CIPK23* gene refrains AMTs from being completely phosphorylated and thus has strong influence on ammonium/methylammonium transport in the plant root.

Physical interaction between the CIPK23 kinase and ammonium transporters AMT1;1 and AMT1;2 (Fig. 48) was obtained by bimolecular fluorescence complementation assays (BiFC) *in situ*. This supports the idea that CIPK23 directly phosphorylates ammonium transporters. Interaction between CIPK23 kinase and AMT2;1 was not detected. Ammonium transporter AMT2;1 is less than 25% identical to proteins of the *At*AMT1 family at the amino acid level and, in fact, more closely related to the bacterial AMTs (Sohlenkamp et al. 2002). Importantly, AMT2;1 C-terminus does not have a certain threonine residue which is phosphorylated in AMT1 proteins to regulate their activity (Neuhäuser et al. 2007; Lanquar, et al. 2009). However, two serine and four threonine in the AMT2;1 cytosolic carboxyl terminus might be phosphorylated. Interestingly, *At*AMT2 is partially co-localized with *At*AMT1 transporters in the plant root (Neuhäuser, Dynowski, and Ludewig 2009) and under N-starvation transcriptionally up-regulated, similar to other *AMTs* (Fig. 38). Additionally, when *At*AMT2;1 was expressed in *Xenopus* oocytes, ammonium was transported without charge movement, indicating rather NH_3 then NH_4^+ transport (Neuhäuser, Dynowski, and Ludewig 2009). Because the gradient at the root plasma membrane for NH_3 is under most conditions outward, it might be proposed that *At*AMT2;1 contributes to NH_3 efflux, although this was never shown. Taken together, AMT1 transporters, which transfer NH_4^+ (or NH_3/H^+) through the plasma membrane, have different post-translational regulation in contrast to AMT2;1, which might transport NH_3.

A protein-protein interaction between CIPK23 kinase and AMT1;3 or AMT1;5 transporters was not investigated. In the future perspective, such experiments are desired. It was demonstrated that AMT1 transporters are able to form functional homo- and heterotrimers (Ludewig et al. 2003; Graff et al. 2011; Yuan et al. 2013). Until now, the impact of AMT1 hetero-oligomerization on ammonium uptake regulation remains unknown. Potentially, one phosphorylated AMT species could inhibit other AMT species by changing the trimer composition and forming heterotrimers with non-phosphorylated AMTs. The combination of hetero-oligomerization and C-terminus as *trans*-regulators might broaden the impact of the phosphorylation of only one kind of AMT and possibly adds new ways of signal integration.

6.2 Transcriptional regulation of AMTs

AMT1;1, AMT1;3, AMT1;5, AMT2;1 transcripts were all less abundant after ammonium shock, irrespective of the *CIPK23* allele (Fig. 38). However, in *cipk23* plants, *AMT1;2* was less repressed compared to WT. Dissimilarly to other AMT1s, AMT1;2 localizes in the root endodermal and cortical cells (Neuhäuser et al. 2007) and is important for ammonium passage over the Casparian strip. Thus, when AMTs cannot be phosphorylated and their transcription is not strongly down regulated, ammonium continuously enters plant roots. Usually, ammonium is assimilated to glutamine in the roots (Lea and Miflin 2003). However, at very high ammonium levels in roots, ammonium may be transported to the shoot. Likewise, under elevated external ammonium concentrations, *amos2* mutants accumulated excessive ammonium amounts in the shoots, exceeding the ammonium concentrations found in root tissue (Li et al. 2011). To avoid accumulation of ammonium at toxic levels, excess ammonium might move to the shoot by AMT1;2 transporters, where ammonium can be assimilated by glutamine synthetase.

In conclusion, AMTs are similarly regulated on transcriptional level in wild type and *cipk23* plants in response to ammonium resupply. Higher expression of AMT1;2 might help mutant plants to cope with increasing amounts of ammonium.

6.3 The CIPK23-CBLs interaction network

Activity and cellular localization of CIPKs (CBL-interacting protein kinases) depend on interacting CBL proteins (Xu et al. 2006; Cheong et al. 2007; Batistic et al. 2010; Hashimoto and Kudla 2011). The CIPK23 kinase regulates activity of potassium transporter AKT1 (Xu et al. 2006; Cheong et al. 2007) and nitrate transporter NRT1.1 (Ho et al. 2009) in a complex with CBL1 and CBL9 proteins. Data from this study suggests that CBL1, rather than CBL9, is involved in the regulation of ammonium uptake in a complex with CIPK23 kinase. Expression of *CBL9* and *CBL1* in roots was regulated by ammonium supply (Fig. 42). However, in contrast to *CBL9,* the amount of *CBL1* transcripts increased instantly in response to high ammonium in wild type and *cipk23* plants. Maximum *CBL1* gene expression was observed in roots of plants subjected to ammonium for 30 min (Fig. 42, Fig. 43). This peak of *CBL1* expression is overlapping with the rapid increase of *CIPK23* transcripts at the same condition (Fig. 42). Moreover, in ^{15}N uptake

experiments, *cbl1* mutants performed similar to *cipk23* mutants while knock-out of *CBL9* gene did not alter ammonium uptake capacity (Fig. 45).

6.4 Plants mutated in *CIPK23* gene have impaired growth

Plant lines with malfunction of the CIPK23 kinase showed growth limitations when cultivated hydroponically. In ambient nutrient conditions of 2 mM nitrogen and 1 mM potassium, *cipk23* mutants developed significantly smaller shoots and roots (Fig. 22). Similar differences were seen in experiments of Cheong and colleagues in 2007. They demonstrated that root growth of *cipk23* mutants was strongly inhibited under low potassium supply. Moreover, *cipk23* plants were less efficient in potassium uptake. Under low-potassium conditions, *cipk23* seedlings accumulated around 25% less potassium compared to the wild type. However, the difference in potassium uptake and root growth of mutant and wild type plants became insignificant when the growth medium contained potassium in concentration of 5 mM (Cheong et al. 2007). Nevertheless, increasing the potassium concentration to 5 mM in this study did not rescue mutant plants from the growth limitation (Fig. 31). However, *cipk23* and WT plants grew more equally. While with 1 mM of available potassium *cipk23* plants developed about 45% less roots compared to WT, with 5 mM K^+ the difference did not exceed 20%. Cheong determined root length and potassium content in 7 days old *Arabidopsis* seedlings. Interestingly, in our hydroponic growth experiments with 5 mM potassium, *cipk23* plants did not have any visible growth limitation for the first 2 weeks. Growth reduction of *cipk23* plants became significant after 4 weeks and correlated with a decrease in potassium leaf content (Fig. 32A). Reduction of potassium transport is a well-known effect of ammonium disorder (Kronzucker, Szczerba, and Britto 2003; Santa-María et al. 1997; Spalding et al. 1999; Pyo et al. 2010). Notably, 6 weeks old *cipk23* plants accumulated less potassium than WT, but potassium contents in *cipk23* leaves were far from critical levels ("Plant Analysis" 2015).

Disruption of the CIPK23 kinase did not only affect regulation of potassium uptake, but also keeps ammonium transporters permanently active, therefore N assimilation and the equilibrium in ammonium and nitrate uptake should be affected. WT and *cipk23* plants did not differ in nitrogen content (Fig. 23A, Fig. 32B), however, it is possible that *cipk23* mutants accumulated more ammonium than nitrate compared to wild type plants. Lack of NO_3^- anion

might limit leaf development, because NO_3^- is an important osmotic anion for leaf cell expansion (Raab and Terry 1994). There are various reports postulating that growth on ammonium as exclusive nitrogen source negatively affects plant total leaf surface area (Walch-Liu et al. 2000; Helali et al. 2010). Furthermore, ammonium assimilation in roots requires sufficient supply with carbon skeletons from leaves. A decrease in carbohydrates augments specific ammonium toxicity and causes dramatic reduction in plant biomass (Claussen and Lenz 1999; Schortemeyer, Stamp, and Feil 1997). Irrespective to potassium availability in the growth medium in our experiments, root and shoot carbohydrate concentrations did not differ in wild type and mutant seedlings (Fig. 23B, Fig. 32C). Accordingly, *cipk23* plants should have a sufficient amount of carbohydrates for ammonium assimilation.

Taken together, the observed growth restrictions of *cipk23* plants might partially occur due to limitation of potassium uptake. The growth reductions of *cipk23* plants were directly correlated with the concentration of free potassium in the growth medium. Increased potassium supply improved growth of mutant plants, but not to the level of WT plants. It is therefore possible that *cipk23* growth limitations were coupled effects from reduced potassium acquisition and increased ammonium uptake.

7 Conclusion

Lanquar and colleagues proposed two models for ammonium sensing and signaling: a transceptor model and a receptor kinase model. However, due to the high dynamic range of the ammonium response, multiple feedback loops in ammonium signaling network were discussed (Lanquar et al. 2009). Indeed, results from this study support the hypothesis that the regulation of ammonium transporters activity is complex.

Foremost, data from this study does not correlate with the receptor kinase model. Free CIPK23 kinase in plant cells is localized in the cytosol and nucleus (Cheong et al. 2007) and therefore cannot be involved in the extracellular ammonium perception. Importantly, apoplastic ammonium itself rather than intracellular ammonium or ammonium assimilation products (Gln or Glu) act as the primary signal for AMT phosphorylation (Lanquar et al. 2009). Extracellular ammonium sensing and further signal transduction requires the activity of a cell-surface receptor. To date, a specific ammonium receptor is unknown, but alternatively, AMT1s might have a dual function: ammonium transport and signaling, aligning to the transceptor model. Indeed, bacterial AmtB (Tremblay and Hallenbeck 2009) and yeast MEP2 (Thevelein et al. 2005) ammonium transporters are transporters with receptor activity. Additionally, the nitrate transporter NRT1.1 probably functions as both a sensor and a transporter in plants (Ho et al. 2009). Based on these I hypothesize, that high, potentially toxic levels of external ammonium are perceived by AMT1 transporters with subsequent activation of the calcium signalling pathway. However, the existence of a plasma membrane ammonium sensor for ammonium-induced signalling cannot be excluded. Overall, elevated ammonium concentrations cause perturbations in cytosolic calcium levels. Increased cytosolic free calcium is bound by CBL1 proteins. The calcium activated CBL1 connects to the CIPK23 kinase and removes the auto-inhibition of the kinase domain, additionally, it recruits CIPK23 to the plasma membrane. CIPK23 phosphorylates ammonium transporters and thereby inhibits further ammonium uptake via allosteric inactivation of the AMT1 trimers (Fig. 56).

However, the absence of CIPK23 did not completely abolish phosphorylation of AMT1;1 and AMT1;2 proteins in response to ammonium, suggesting another CIPK23-independent way to regulate AMT1 activity by phosphorylation.
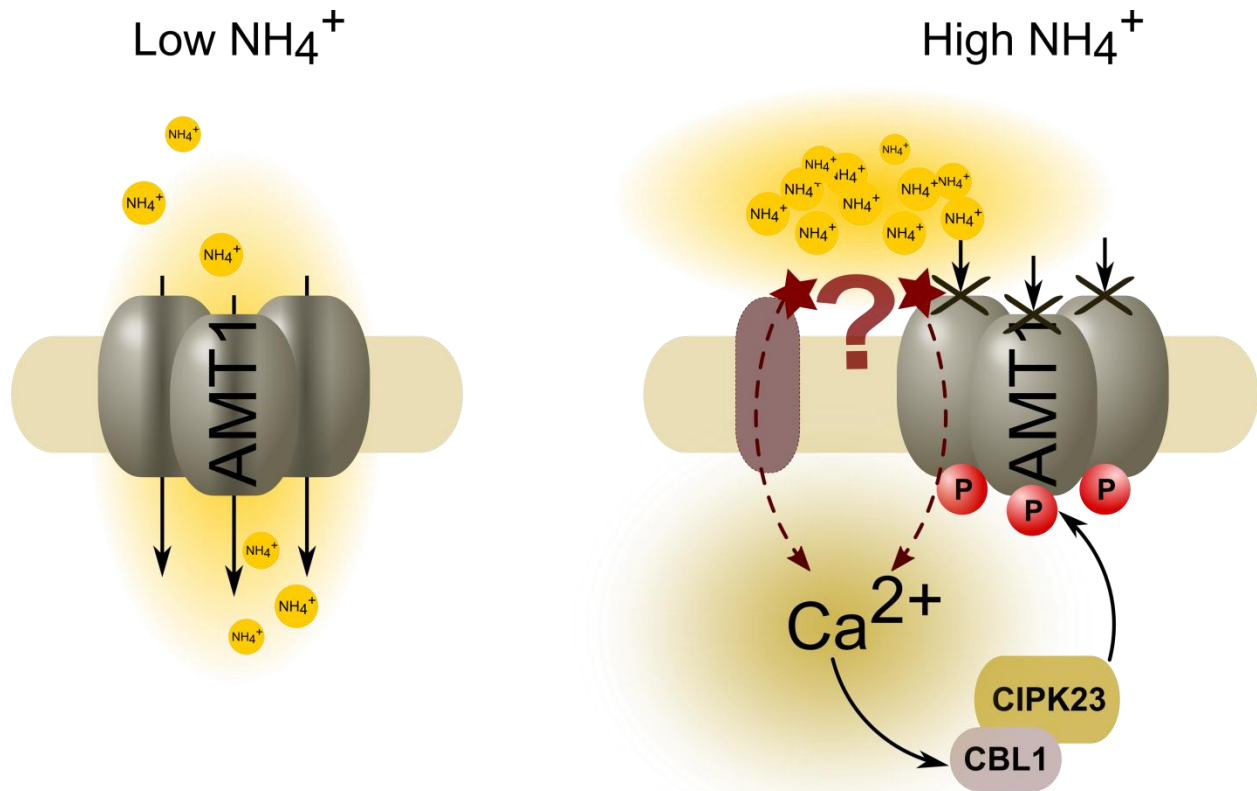
Figure 56: Model of AMT1 activity regulation.
Left: At low external ammonium concentrations, AMTs are not phosphorylated and conduct NH_4^+ into root cells. Right: Elevated external NH_4^+ concentrations trigger calcium signaling pathway. CBL1 activates CIPK23 kinase and CBL1-CIPK23 complex is relocated to the plasma membrane, where CIPK23 kinase phosphorylates AMT1 transporters. Phosphorylation inactivates ammonium transporters via the allosteric trans-regulatory mechanism and prevents ammonium accumulation to toxic levels.

8 Acknowledgements

9 Literature

Albrecht, Verónica, Olga Ritz, Sabine Linder, Klaus Harter, and Jörg Kudla. 2001. "The NAF Domain Defines a Novel Protein–protein Interaction Module Conserved in Ca2+-regulated Kinases." *The EMBO Journal* 20 (5): 1051–63. doi:10.1093/emboj/20.5.1051.

Alemán, Fernando, Manuel Nieves-Cordones, Vicente Martínez, and Francisco Rubio. 2011. "Root K(+) Acquisition in Plants: The Arabidopsis Thaliana Model." *Plant & Cell Physiology* 52 (9): 1603–12. doi:10.1093/pcp/pcr096.

Batistic, Oliver, and Jörg Kudla. 2009. "Plant Calcineurin B-like Proteins and Their Interacting Protein Kinases." *Biochimica Et Biophysica Acta* 1793 (6): 985–92. doi:10.1016/j.bbamcr.2008.10.006.

Batistic, Oliver, Rainer Waadt, Leonie Steinhorst, Katrin Held, and Jörg Kudla. 2010. "CBL-Mediated Targeting of CIPKs Facilitates the Decoding of Calcium Signals Emanating from Distinct Cellular Stores." *The Plant Journal: For Cell and Molecular Biology* 61 (2): 211–22. doi:10.1111/j.1365-313X.2009.04045.x.

Bertl, Adam, John D. Reid, Hervé Sentenac, and Clifford L. Slayman. 1997. "Functional Comparison of Plant Inward-Rectifier Channels Expressed in Yeast." *Journal of Experimental Botany* 48 (Special Issue): 405–13. doi:10.1093/jxb/48.Special_Issue.405.

Blakey, Dan, Andrew Leech, Gavin H. Thomas, Graham Coutts, Kim Findlay, and Mike Merrick. 2002. "Purification of the Escherichia Coli Ammonium Transporter AmtB Reveals a Trimeric Stoichiometry." *The Biochemical Journal* 364 (Pt 2): 527–35. doi:10.1042/BJ20011761.

Blanksby, Stephen J., and G. Barney Ellison. 2003. "Bond Dissociation Energies of Organic Molecules." *Accounts of Chemical Research* 36 (4): 255–63. doi:10.1021/ar020230d.

Boeckstaens, Mélanie, Bruno André, and Anna Maria Marini. 2007. "The Yeast Ammonium Transport Protein Mep2 and Its Positive Regulator, the Npr1 Kinase, Play an Important Role in Normal and Pseudohyphal Growth on Various Nitrogen Media through Retrieval of Excreted Ammonium." *Molecular Microbiology* 64 (2): 534–46. doi:10.1111/j.1365-2958.2007.05681.x.

Boeckstaens, Mélanie, Elisa Llinares, Pascale Van Vooren, and Anna Maria Marini. 2014. "The TORC1 Effector Kinase Npr1 Fine Tunes the Inherent Activity of the Mep2 Ammonium Transport Protein." *Nature Communications* 5: 3101. doi:10.1038/ncomms4101.

Britto, D. T., M. Y. Siddiqi, A. D. Glass, and H. J. Kronzucker. 2001. "Futile Transmembrane NH4(+) Cycling: A Cellular Hypothesis to Explain Ammonium Toxicity in Plants." *Proceedings of the National Academy of Sciences of the United States of America* 98 (7): 4255–58. doi:10.1073/pnas.061034698.

Canales, Javier, Tomás C. Moyano, Eva Villarroel, and Rodrigo A. Gutiérrez. 2014. "Systems Analysis of Transcriptome Data Provides New Hypotheses about Arabidopsis Root Response to Nitrate Treatments." *Frontiers in Plant Science* 5 (February). doi:10.3389/fpls.2014.00022.

Chen, Gui, Shiwei Guo, Herbert J. Kronzucker, and Weiming Shi. 2013. "Nitrogen Use Efficiency (NUE) in Rice Links to NH4 + Toxicity and Futile NH4 + Cycling in Roots." *Plant and Soil* 369 (1-2): 351–63. doi:10.1007/s11104-012-1575-y.

Cheong, Yong Hwa, Girdhar K. Pandey, John J. Grant, Oliver Batistic, Legong Li, Beom-Gi Kim, Sung-Chul Lee, Jörg Kudla, and Sheng Luan. 2007. "Two Calcineurin B-like Calcium Sensors, Interacting with Protein Kinase CIPK23, Regulate Leaf Transpiration and Root Potassium Uptake in Arabidopsis." *The Plant Journal: For Cell and Molecular Biology* 52 (2): 223–39. doi:10.1111/j.1365-313X.2007.03236.x.

Clarkson, D. T., L. H. P. Jones, and J. V. Purves. 1992. "Absorption of Nitrate and Ammonium Ions by Lolium Perenne from Flowing Solution Cultures at Low Root Temperatures." *Plant, Cell & Environment* 15 (1): 99–106. doi:10.1111/j.1365-3040.1992.tb01462.x.

Claussen, W., and F. Lenz. 1999. "Effect of Ammonium or Nitrate Nutrition on Net Photosynthesis, Growth, and Activity of the Enzymes Nitrate Reductase and Glutamine Synthetase in Blueberry, Raspberry and Strawberry." *Plant and Soil* 208 (1): 95–102. doi:10.1023/A:1004543128899.

Clough, S. J., and A. F. Bent. 1998. "Floral Dip: A Simplified Method for Agrobacterium-Mediated Transformation of Arabidopsis Thaliana." *The Plant Journal: For Cell and Molecular Biology* 16 (6): 735–43.

Conroy, Matthew J., Anne Durand, Domenico Lupo, Xiao-Dan Li, Per A. Bullough, Fritz K. Winkler, and Mike Merrick. 2007. "The Crystal Structure of the Escherichia Coli AmtB-GlnK Complex Reveals How GlnK Regulates the Ammonia Channel." *Proceedings of the National Academy of Sciences of the United States of America* 104 (4): 1213–18. doi:10.1073/pnas.0610348104.

Conroy, Matthew J., Stuart J. Jamieson, Daniel Blakey, Thomas Kaufmann, Andreas Engel, Dimitrios Fotiadis, Mike Merrick, and Per A. Bullough. 2004. "Electron and Atomic Force Microscopy of the Trimeric Ammonium Transporter AmtB." *EMBO Reports* 5 (12): 1153–58. doi:10.1038/sj.embor.7400296.

Cranenburgh, R. M. 2004. "An Equation for Calculating the Volumetric Ratios Required in a Ligation Reaction." *Applied Microbiology and Biotechnology* 65 (2): 200–202. doi:10.1007/s00253-004-1577-7.

Demidchik, Vadim, Romola Jane Davenport, and Mark Tester. 2002. "Nonselective Cation Channels in Plants." *Annual Review of Plant Biology* 53 (1): 67–107. doi:10.1146/annurev.arplant.53.091901.161540.

Dixon, Ray, and Daniel Kahn. 2004. "Genetic Regulation of Biological Nitrogen Fixation." *Nature Reviews. Microbiology* 2 (8): 621–31. doi:10.1038/nrmicro954.

Du, Wenming, Huixin Lin, She Chen, Yisheng Wu, Jun Zhang, Anja T. Fuglsang, Michael G. Palmgren, Weihua Wu, and Yan Guo. 2011. "Phosphorylation of SOS3-like Calcium-Binding Proteins by Their Interacting SOS2-like Protein Kinases Is a Common Regulatory Mechanism in Arabidopsis." *Plant Physiology* 156 (4): 2235–43. doi:10.1104/pp.111.173377.

Engelsberger, Wolfgang R, and Waltraud X Schulze. 2012. "Nitrate and Ammonium Lead to Distinct Global Dynamic Phosphorylation Patterns When Resupplied to Nitrogen-Starved Arabidopsis Seedlings." *The Plant Journal* 69 (6): 978–95. doi:10.1111/j.1365-313X.2011.04848.x.

Gage, Daniel J. 2004. "Infection and Invasion of Roots by Symbiotic, Nitrogen-Fixing Rhizobia during Nodulation of Temperate Legumes." *Microbiology and Molecular Biology Reviews: MMBR* 68 (2): 280–300. doi:10.1128/MMBR.68.2.280-300.2004.

Gallagher, Sean, Scott E. Winston, Steven A. Fuller, and John G. R. Hurrell. 2008. "Immunoblotting and Immunodetection." *Current Protocols in Molecular Biology / Edited by Frederick M. Ausubel ... [et Al.]* Chapter 10 (July): Unit 10.8. doi:10.1002/0471142727.mb1008s83.

Gazzarrini, S., L. Lejay, A. Gojon, O. Ninnemann, W. B. Frommer, and N. von Wirén. 1999. "Three Functional Transporters for Constitutive, Diurnally Regulated, and Starvation-Induced Uptake of Ammonium into Arabidopsis Roots." *The Plant Cell* 11 (5): 937–48.

Gong, Deming, Yan Guo, Andre T. Jagendorf, and Jian-Kang Zhu. 2002. "Biochemical Characterization of the Arabidopsis Protein Kinase SOS2 That Functions in Salt Tolerance." *Plant Physiology* 130 (1): 256–64. doi:10.1104/pp.004507.

Gong, Deming, Yan Guo, Karen S. Schumaker, and Jian-Kang Zhu. 2004. "The SOS3 Family of Calcium Sensors and SOS2 Family of Protein Kinases in Arabidopsis." *Plant Physiology* 134 (3): 919–26. doi:10.1104/pp.103.037440.

Good, Allen G., Susan J. Johnson, Mary De Pauw, Rebecka T. Carroll, Nic Savidov, John Vidmar, Zhongjin Lu, Gregory Taylor, and Virginia Stroeher. 2007. "Engineering Nitrogen Use Efficiency with Alanine Aminotransferase." *Canadian Journal of Botany* 85 (3): 252–62. doi:10.1139/B07-019.

Graff, Lucile, Petr Obrdlik, Lixing Yuan, Dominique Loqué, Wolf B. Frommer, and Nicolaus von Wirén. 2011. "N-Terminal Cysteines Affect Oligomer Stability of the Allosterically Regulated Ammonium Transporter LeAMT1;1." *Journal of Experimental Botany* 62 (4): 1361–73. doi:10.1093/jxb/erq379.

Guo, Yan, Ursula Halfter, Manabu Ishitani, and Jian-Kang Zhu. 2001. "Molecular Characterization of Functional Domains in the Protein Kinase SOS2 That Is Required for Plant Salt Tolerance." *The Plant Cell* 13 (6): 1383–1400. doi:10.1105/TPC.010021.

Harper, J. E. 1994. "Nitrogen Metabolism." *Physiology and Determination of Crop Yield* acsesspublicati (physiologyandde): 285–302. doi:10.2134/1994.physiologyanddetermination.c19.

Hashimoto, Kenji, and Jörg Kudla. 2011. "Calcium Decoding Mechanisms in Plants." *Biochimie* 93 (12): 2054–59. doi:10.1016/j.biochi.2011.05.019.

Helali, Sabah M'rah, Heifa Nebli, Rym Kaddour, Hela Mahmoudi, Mokhtar Lachaâl, and Zeineb Ouerghi. 2010. "Influence of Nitrate—ammonium Ratio on Growth and Nutrition of Arabidopsis Thaliana." *Plant and Soil* 336 (1-2): 65–74. doi:10.1007/s11104-010-0445-8.

Hellemans, Jan, Geert Mortier, Anne De Paepe, Frank Speleman, and Jo Vandesompele. 2007. "qBase Relative Quantification Framework and Software for Management and Automated Analysis of Real-Time Quantitative PCR Data." *Genome Biology* 8 (2): R19. doi:10.1186/gb-2007-8-2-r19.

Hirsch, R. E., B. D. Lewis, E. P. Spalding, and M. R. Sussman. 1998. "A Role for the AKT1 Potassium Channel in Plant Nutrition." *Science (New York, N.Y.)* 280 (5365): 918–21.

Ho, Cheng-Hsun, Shan-Hua Lin, Heng-Cheng Hu, and Yi-Fang Tsay. 2009. "CHL1 Functions as a Nitrate Sensor in Plants." *Cell* 138 (6): 1184–94. doi:10.1016/j.cell.2009.07.004.

Hodge, Angela, and Kate Storer. 2014. "Arbuscular Mycorrhiza and Nitrogen: Implications for Individual Plants through to Ecosystems." *Plant and Soil* 386 (1-2): 1–19. doi:10.1007/s11104-014-2162-1.

Hrabak, Estelle M., Catherine W. M. Chan, Michael Gribskov, Jeffrey F. Harper, Jung H. Choi, Nigel Halford, Jörg Kudla, et al. 2003. "The Arabidopsis CDPK-SnRK Superfamily of Protein Kinases." *Plant Physiology* 132 (2): 666–80. doi:10.1104/pp.102.011999.

Hsieh, M. H., H. M. Lam, F. J. van de Loo, and G. Coruzzi. 1998. "A PII-like Protein in Arabidopsis: Putative Role in Nitrogen Sensing." *Proceedings of the National Academy of Sciences of the United States of America* 95 (23): 13965–70.

Jahn, Thomas P., Anders L. B. Møller, Thomas Zeuthen, Lars M. Holm, Dan A. Klærke, Brigitte Mohsin, Werner Kühlbrandt, and Jan K. Schjoerring. 2004. "Aquaporin Homologues in Plants and Mammals Transport Ammonia." *FEBS Letters* 574 (1–3): 31–36. doi:10.1016/j.febslet.2004.08.004.

Javelle, Arnaud, Domenico Lupo, Pierre Ripoche, Tim Fulford, Mike Merrick, and Fritz K. Winkler. 2008. "Substrate Binding, Deprotonation, and Selectivity at the Periplasmic Entrance of the Escherichia Coli Ammonia Channel AmtB." *Proceedings of the National Academy of Sciences of the United States of America* 105 (13): 5040–45. doi:10.1073/pnas.0711742105.

Kaldenhoff, Ralf, Adam Bertl, Beate Otto, Menachem Moshelion, and Norbert Uehlein. 2007. "Characterization of Plant Aquaporins." *Methods in Enzymology* 428: 505–31. doi:10.1016/S0076-6879(07)28028-0.

Khademi, Shahram, Joseph O'Connell, Jonathan Remis, Yaneth Robles-Colmenares, Larry J. W. Miercke, and Robert M. Stroud. 2004. "Mechanism of Ammonia Transport by Amt/MEP/Rh: Structure of AmtB at 1.35 A." *Science (New York, N.Y.)* 305 (5690): 1587–94. doi:10.1126/science.1101952.

Kim, Kyung-Nam, Yong Hwa Cheong, Rajeev Gupta, and Sheng Luan. 2000. "Interaction Specificity of Arabidopsis Calcineurin B-Like Calcium Sensors and Their Target Kinases." *Plant Physiology* 124 (4): 1844–53. doi:10.1104/pp.124.4.1844.

Kolukisaoglu, Uner, Stefan Weinl, Dragica Blazevic, Oliver Batistic, and Jörg Kudla. 2004. "Calcium Sensors and Their Interacting Protein Kinases: Genomics of the Arabidopsis and Rice CBL-CIPK Signaling Networks." *Plant Physiology* 134 (1): 43–58. doi:10.1104/pp.103.033068.

Kronzucker, Herbert J., Anthony D.M. Glass, and M. Yaeesh Siddiqi. 1999. "Inhibition of Nitrate Uptake by Ammonium in Barley. Analysis of Component Fluxes." *Plant Physiology* 120 (1): 283–92.

Kronzucker, Herbert J., M. Yaeesh Siddiqi, and Anthony D. M. Glass. 1997. "Conifer Root Discrimination against Soil Nitrate and the Ecology of Forest Succession." *Nature* 385 (6611): 59–61. doi:10.1038/385059a0.

Kronzucker, Herbert J., Mark W. Szczerba, and Dev T. Britto. 2003. "Cytosolic Potassium Homeostasis Revisited: 42K-Tracer Analysis in Hordeum Vulgare L. Reveals Set-Point Variations in [K+]." *Planta* 217 (4): 540–46. doi:10.1007/s00425-003-1032-5.

Kronzucker, H. J., M. Y. Siddiqi, and Adm Glass. 1996. "Kinetics of NH4+ Influx in Spruce." *Plant Physiology* 110 (3): 773–79. doi:10.1104/pp.110.3.773.

Kudla, Jörg, Oliver Batistič, and Kenji Hashimoto. 2010. "Calcium Signals: The Lead Currency of Plant Information Processing." *The Plant Cell* 22 (3): 541–63. doi:10.1105/tpc.109.072686.

Lagarde, D., M. Basset, M. Lepetit, G. Conejero, F. Gaymard, S. Astruc, and C. Grignon. 1996. "Tissue-Specific Expression of Arabidopsis AKT1 Gene Is Consistent with a Role in K+ Nutrition." *The Plant Journal: For Cell and Molecular Biology* 9 (2): 195–203.

Lanquar, Viviane, Dominique Loqué, Friederike Hörmann, Lixing Yuan, Anne Bohner, Wolfgang R. Engelsberger, Sylvie Lalonde, Waltraud X. Schulze, Nicolaus von Wirén, and Wolf B. Frommer. 2009. "Feedback Inhibition of Ammonium Uptake by a Phospho-Dependent Allosteric Mechanism in Arabidopsis." *The Plant Cell* 21 (11): 3610–22. doi:10.1105/tpc.109.068593.

Larsen, Martin R., Tine E. Thingholm, Ole N. Jensen, Peter Roepstorff, and Thomas J. D. Jørgensen. 2005. "Highly Selective Enrichment of Phosphorylated Peptides from Peptide Mixtures Using Titanium Dioxide Microcolumns." *Molecular & Cellular Proteomics: MCP* 4 (7): 873–86. doi:10.1074/mcp.T500007-MCP200.

Lea, Peter J., and Ben J. Miflin. 2003. "Glutamate Synthase and the Synthesis of Glutamate in Plants." *Plant Physiology and Biochemistry* 41 (6–7): 555–64. doi:10.1016/S0981-9428(03)00060-3.

"Learn How to Analyze Emission Fingerprinting with Lambda Stacks." 2016. Accessed March 9. http://www.zeiss.com/microscopy/en_de/solutions/reference/all-tutorials/spectral-imaging/emission-fingerprinting-with-lambda-stacks.html.

Lee, R. B., and M. C. Drew. 1989. "Rapid, Reversible Inhibition of Nitrate Influx in Barley by Ammonium." *Journal of Experimental Botany* 40 (7): 741–52. doi:10.1093/jxb/40.7.741.

Lee, Sung Chul, Wen-Zhi Lan, Beom-Gi Kim, Legong Li, Yong Hwa Cheong, Girdhar K. Pandey, Guihua Lu, Bob B. Buchanan, and Sheng Luan. 2007. "A Protein Phosphorylation/dephosphorylation Network Regulates a Plant Potassium Channel." *Proceedings of the National Academy of Sciences* 104 (40): 15959–64. doi:10.1073/pnas.0707912104.

Lejay, Laurence, Xavier Gansel, Miguel Cerezo, Pascal Tillard, Cathrin Müller, Anne Krapp, Nicolaus von Wirén, Françoise Daniel-Vedele, and Alain Gojon. 2003. "Regulation of Root Ion Transporters by Photosynthesis: Functional Importance and Relation with Hexokinase." *The Plant Cell* 15 (9): 2218–32.

Li, Baohai, Weiming Shi, and Yanhua Su. 2010. "The Differing Responses of Two Arabidopsis Ecotypes to Ammonium Are Modulated by the Photoperiod Regime." *Acta Physiologiae Plantarum* 33 (2): 325–34. doi:10.1007/s11738-010-0551-5.

Li, Guangjie, Gangqiang Dong, Baohai Li, Qing Li, Herbert J. Kronzucker, and Weiming Shi. 2011. "Isolation and Characterization of a Novel Ammonium Overly Sensitive Mutant, amos2, in Arabidopsis Thaliana." *Planta* 235 (2): 239–52. doi:10.1007/s00425-011-1504-y.

Lin, Huixin, Yongqing Yang, Ruidang Quan, Imelda Mendoza, Yisheng Wu, Wenming Du, Shuangshuang Zhao, Karen S. Schumaker, José M. Pardo, and Yan Guo. 2009. "Phosphorylation of SOS3-LIKE CALCIUM BINDING PROTEIN8 by SOS2 Protein Kinase Stabilizes Their Protein Complex and Regulates Salt Tolerance in Arabidopsis." *The Plant Cell* 21 (5): 1607–19. doi:10.1105/tpc.109.066217.

LI, Su-Mei, Bao-Zhen LI, and Wei-Ming SHI. 2012. "Expression Patterns of Nine Ammonium Transporters in Rice in Response to N Status." *Pedosphere* 22 (6): 860–69. doi:10.1016/S1002-0160(12)60072-1.

Liu, Kun-Hsiang, C. Y. Huang, and Yi-Fang Tsay. 1999. "CHL1 Is a Dual-Affinity Nitrate Transporter of Arabidopsis Involved in Multiple Phases of Nitrate Uptake." *The Plant Cell* 11 (5): 865–74.

Liu, Kun-Hsiang, and Yi-Fang Tsay. 2003. "Switching between the Two Action Modes of the Dual-Affinity Nitrate Transporter CHL1 by Phosphorylation." *The EMBO Journal* 22 (5): 1005–13. doi:10.1093/emboj/cdg118.

Loqué, Dominique, and Nicolaus von Wirén. 2004. "Regulatory Levels for the Transport of Ammonium in Plant Roots." *Journal of Experimental Botany* 55 (401): 1293–1305. doi:10.1093/jxb/erh147.

Luan, Sheng. 2009. "The CBL-CIPK Network in Plant Calcium Signaling." *Trends in Plant Science* 14 (1): 37–42. doi:10.1016/j.tplants.2008.10.005.

Luan, Sheng, Jörg Kudla, Manuel Rodriguez-Concepcion, Shaul Yalovsky, and Wilhelm Gruissem. 2002. "Calmodulins and Calcineurin B-like Proteins: Calcium Sensors for Specific Signal Response Coupling in Plants." *The Plant Cell* 14 Suppl: S389–400.

Ludewig, Uwe, Nico von Wirén, Doris Rentsch, and Wolf B Frommer. 2001. "Rhesus Factors and Ammonium: A Function in Efflux?" *Genome Biology* 2 (3): reviews1010.1–reviews1010.5.

Ludewig, Uwe, Stephanie Wilken, Binghua Wu, Wolfgang Jost, Petr Obrdlik, Mohamed El Bakkoury, Anne-Marie Marini, et al. 2003. "Homo- and Hetero-Oligomerization of Ammonium Transporter-1 NH4 Uniporters." *The Journal of Biological Chemistry* 278 (46): 45603–10. doi:10.1074/jbc.M307424200.

MacDonald, Lee H., Alan W. Smart, R. C. Wissmar, and United States Forest Service. 1994. *Evaluating the Effectiveness of Forestry Best Management Practices in Meeting Water Quality Goals or Standards*. United States Dept. of Agriculture, Forest Service.

Mäck, Gisela, and Rudolf Tischner. 1994. "Constitutive and Inducible Net NH+4 Uptake of Barley (Hordeum Vulgare L.) Seedlings." *Journal of Plant Physiology* 144 (3): 351–57. doi:10.1016/S0176-1617(11)81198-3.

Marini, A. M., J. Y. Springael, W. B. Frommer, and B. André. 2000. "Cross-Talk between Ammonium Transporters in Yeast and Interference by the Soybean SAT1 Protein." *Molecular Microbiology* 35 (2): 378–85.

Marini, A. M., A. Urrestarazu, R. Beauwens, and B. André. 1997. "The Rh (rhesus) Blood Group Polypeptides Are Related to NH4+ Transporters." *Trends in Biochemical Sciences* 22 (12): 460–61.

Marini, A M, S Vissers, A Urrestarazu, and B Andre. 1994. "Cloning and Expression of the MEP1 Gene Encoding an Ammonium Transporter in Saccharomyces Cerevisiae." *The EMBO Journal* 13 (15): 3456–63.

"Market Outlooks Reports." 2015. Accessed September 14. http://www.fertilizer.org/MarketOutlooks.

Mayer, M., and U. Ludewig. 2006. "Role of AMT1;1 in NH4+ Acquisition in Arabidopsis Thaliana." *Plant Biology (Stuttgart, Germany)* 8 (4): 522–28.

McDonald, Tami R., Fred S. Dietrich, and François Lutzoni. 2012. "Multiple Horizontal Gene Transfers of Ammonium Transporters/Ammonia Permeases from Prokaryotes to Eukaryotes: Toward a New Functional and Evolutionary Classification." *Molecular Biology and Evolution* 29 (1): 51–60. doi:10.1093/molbev/msr123.

"Measure Nucleic Acids with NanoDrop Products." 2016. Accessed February 12. http://www.nanodrop.com/nucleicacid.aspx.

Mehrer, Ingrid, and Hans Mohr. 1989. "Ammonium Toxicity: Description of the Syndrome in Sinapis Alba and the Search for Its Causation." *Physiologia Plantarum* 77 (4): 545–54. doi:10.1111/j.1399-3054.1989.tb05390.x.

Meletzus, D., P. Rudnick, N. Doetsch, A. Green, and C. Kennedy. 1998. "Characterization of the glnK-amtB Operon of Azotobacter Vinelandii." *Journal of Bacteriology* 180 (12): 3260–64.

Monahan, Brendon J., James A. Fraser, Michael J. Hynes, and Meryl A. Davis. 2002. "Isolation and Characterization of Two Ammonium Permease Genes, meaA and mepA, from Aspergillus Nidulans." *Eukaryotic Cell* 1 (1): 85–94. doi:10.1128/EC.1.1.85-94.2002.

Monahan, Brendon J., Shiela E. Unkles, Tchuc Tsing I, James R. Kinghorn, Michael J. Hynes, and Meryl A. Davis. 2002. "Mutation and Functional Analysis of the Aspergillus Nidulans Ammonium Permease MeaA and Evidence for Interaction with Itself and MepA." *Fungal Genetics and Biology: FG & B* 36 (1): 35–46. doi:10.1016/S1087-1845(02)00004-X.

Montesinos, M. L., A. M. Muro-Pastor, A. Herrero, and E. Flores. 1998. "Ammonium/methylammonium Permeases of a Cyanobacterium. Identification and Analysis of Three Nitrogen-Regulated Amt Genes in Synechocystis Sp. PCC 6803." *The Journal of Biological Chemistry* 273 (47): 31463–70.

Moroni, A., L. Bardella, and G. Thiel. 1998. "The Impermeant Ion Methylammonium Blocks K+ and NH+ 4 Currents through KAT1 Channel Differently: Evidence for Ion Interaction in Channel Permeation." *The Journal of Membrane Biology* 163 (1): 25–35. doi:10.1007/s002329900367.

Neuhäuser, Benjamin, Nico Dunkel, Somisetty V. Satheesh, and Joachim Morschhäuser. 2011. "Role of the Npr1 Kinase in Ammonium Transport and Signaling by the Ammonium Permease Mep2 in Candida Albicans." *Eukaryotic Cell* 10 (3): 332–42. doi:10.1128/EC.00293-10.

Neuhäuser, Benjamin, Marek Dynowski, and Uwe Ludewig. 2009. "Channel-like NH3 Flux by Ammonium Transporter AtAMT2." *FEBS Letters* 583 (17): 2833–38. doi:10.1016/j.febslet.2009.07.039.

Neuhäuser, Benjamin, Marek Dynowski, Maria Mayer, and Uwe Ludewig. 2007. "Regulation of NH4+ Transport by Essential Cross Talk between AMT Monomers through the Carboxyl Tails." *Plant Physiology* 143 (4): 1651–59. doi:10.1104/pp.106.094243.

Niemietz, C. M., and S. D. Tyerman. 2000. "Aquaporin Homologues in Plants and Mammals Transport Ammonia." *FEBS Letters* 574 (1–3): 31–36.

Ninnemann, O., J. C. Jauniaux, and W. B. Frommer. 1994. "Identification of a High Affinity NH4+ Transporter from Plants." *The EMBO Journal* 13 (15): 3464–71.

Nühse, Thomas S., Allan Stensballe, Ole N. Jensen, and Scott C. Peck. 2004. "Phosphoproteomics of the Arabidopsis Plasma Membrane and a New Phosphorylation Site Database." *The Plant Cell* 16 (9): 2394–2405. doi:10.1105/tpc.104.023150.

Nygaard, Thomas P., Carme Rovira, Günther H. Peters, and Morten Ø Jensen. 2006. "Ammonium Recruitment and Ammonia Transport by E. Coli Ammonia Channel AmtB." *Biophysical Journal* 91 (12): 4401–12. doi:10.1529/biophysj.106.089714.

Ohad, Nir, Keren Shichrur, and Shaul Yalovsky. 2007. "The Analysis of Protein-Protein Interactions in Plants by Bimolecular Fluorescence Complementation." *Plant Physiology* 145 (4): 1090–99. doi:10.1104/pp.107.107284.

Ohta, Masaru, Yan Guo, Ursula Halfter, and Jian-Kang Zhu. 2003. "A Novel Domain in the Protein Kinase SOS2 Mediates Interaction with the Protein Phosphatase 2C ABI2." *Proceedings of the National Academy of Sciences* 100 (20): 11771–76. doi:10.1073/pnas.2034853100.

Osakabe, Yuriko, Naoko Arinaga, Taishi Umezawa, Shogo Katsura, Keita Nagamachi, Hidenori Tanaka, Haruka Ohiraki, et al. 2013. "Osmotic Stress Responses and Plant Growth Controlled by Potassium Transporters in Arabidopsis." *The Plant Cell* 25 (2): 609–24. doi:10.1105/tpc.112.105700.

Ossowski, Stephan, Rebecca Schwab, and Detlef Weigel. 2008. "Gene Silencing in Plants Using Artificial microRNAs and Other Small RNAs." *The Plant Journal: For Cell and Molecular Biology* 53 (4): 674–90. doi:10.1111/j.1365-313X.2007.03328.x.

Ourry, Alain, James H. Macduff, Marie-Pascale Prudhomme, and Jean Boucaud. 1996. "Diurnal Variation in the Simultaneous Uptake and 'sink' Allocation of NH4+ and NO3- by Lolium Perenne in Flowing Solution Culture." *Journal of Experimental Botany* 47 (12): 1853–63. doi:10.1093/jxb/47.12.1853.

Patterson, Kurt, Turgay Cakmak, Andrew Cooper, Ida Lager, Allan G. Rasmusson, and Matthew A. Escobar. 2010. "Distinct Signaling Pathways and Transcriptome Response Signatures Differentiate Ammonium- and Nitrate-Supplied Plants." *Plant, Cell & Environment* 33 (9): 1486–1501. doi:10.1111/j.1365-3040.2010.02158.x.

Pertl, H., M. Himly, R. Gehwolf, R. Kriechbaumer, D. Strasser, W. Michalke, K. Richter, F. Ferreira, and G. Obermeyer. 2001. "Molecular and Physiological Characterisation of a 14-3-3 Protein from Lily Pollen Grains Regulating the Activity of the Plasma Membrane H+ ATPase during Pollen Grain Germination and Tube Growth." *Planta* 213 (1): 132–41. doi:10.1007/s004250000483.

"Plant Analysis." 2015. Accessed December 14. http://www.cropnutrition.com/efu-plant-analysis#diagnosis-of-nutrient-status.

Pyo, Young Jae, Markus Gierth, Julian I. Schroeder, and Myeon Haeng Cho. 2010. "High-Affinity K+ Transport in Arabidopsis: AtHAK5 and AKT1 Are Vital for Seedling Establishment and Postgermination Growth under Low-Potassium Conditions1[C][W][OA]." *Plant Physiology* 153 (2): 863–75. doi:10.1104/pp.110.154369.

Raab, T. K., and N. Terry. 1994. "Nitrogen Source Regulation of Growth and Photosynthesis in Beta Vulgaris L." *Plant Physiology* 105 (4): 1159–66.

Ragel, Paula, Reyes Ródenas, Elena García-Martín, Zaida Andrés, Irene Villalta, Manuel Nieves-Cordones, Rosa M. Rivero, et al. 2015. "CIPK23 Regulates HAK5-Mediated High-Affinity K+ Uptake in Arabidopsis Roots." *Plant Physiology*, October. doi:10.1104/pp.15.01401.

Rappsilber, Juri, Yasushi Ishihama, and Matthias Mann. 2003. "Stop and Go Extraction Tips for Matrix-Assisted Laser Desorption/ionization, Nanoelectrospray, and LC/MS Sample Pretreatment in Proteomics." *Analytical Chemistry* 75 (3): 663–70.

Rawat, Suman R., Salim N. Silim, Herbert J. Kronzucker, M. Yaeesh Siddiqi, and Anthony D. M. Glass. 1999. "AtAMT1 Gene Expression and NH4+ Uptake in Roots of Arabidopsis

Thaliana: Evidence for Regulation by Root Glutamine Levels." *The Plant Journal* 19 (2): 143–52. doi:10.1046/j.1365-313X.1999.00505.x.

Rubio, Francisco, Mario Fon, Reyes Ródenas, Manuel Nieves-Cordones, Fernando Alemán, Rosa M. Rivero, and Vicente Martínez. 2014. "A Low K+ Signal Is Required for Functional High-Affinity K+ Uptake through HAK5 Transporters." *Physiologia Plantarum* 152 (3): 558–70. doi:10.1111/ppl.12205.

Sánchez-Barrena, María José, Hiroaki Fujii, Ivan Angulo, Martín Martínez-Ripoll, Jian-Kang Zhu, and Armando Albert. 2007. "The Structure of the C-Terminal Domain of the Protein Kinase AtSOS2 Bound to the Calcium Sensor AtSOS3." *Molecular Cell* 26 (3): 427–35. doi:10.1016/j.molcel.2007.04.013.

Santa-María, G. E., F. Rubio, J. Dubcovsky, and A. Rodríguez-Navarro. 1997. "The HAK1 Gene of Barley Is a Member of a Large Gene Family and Encodes a High-Affinity Potassium Transporter." *The Plant Cell* 9 (12): 2281–89. doi:10.1105/tpc.9.12.2281.

Sanyal, Sibaji K., Amita Pandey, and Girdhar K. Pandey. 2015. "The CBL-CIPK Signaling Module in Plants: A Mechanistic Perspective." *Physiologia Plantarum*, May. doi:10.1111/ppl.12344.

Saparov, Sapar M., Kun Liu, Peter Agre, and Peter Pohl. 2007. "Fast and Selective Ammonia Transport by Aquaporin-8." *The Journal of Biological Chemistry* 282 (8): 5296–5301. doi:10.1074/jbc.M609343200.

Schachtman, D. P., J. I. Schroeder, W. J. Lucas, J. A. Anderson, and R. F. Gaber. 1992. "Expression of an Inward-Rectifying Potassium Channel by the Arabidopsis KAT1 cDNA." *Science (New York, N.Y.)* 258 (5088): 1654–58.

Schjoerring, J. K., S. Husted, G. Mäck, and M. Mattsson. 2002. "The Regulation of Ammonium Translocation in Plants." *Journal of Experimental Botany* 53 (370): 883–90.

Schneider, Caroline A., Wayne S. Rasband, and Kevin W. Eliceiri. 2012. "NIH Image to ImageJ: 25 Years of Image Analysis." *Nature Methods* 9 (7): 671–75.

Schortemeyer, Marcus, Peter Stamp, and Boy Feil. 1997. "Ammonium Tolerance and Carbohydrate Status in Maize Cultivars." *Annals of Botany* 79 (1): 25–30. doi:10.1006/anbo.1996.0298.

Schwab, Rebecca, Stephan Ossowski, Markus Riester, Norman Warthmann, and Detlef Weigel. 2006. "Highly Specific Gene Silencing by Artificial microRNAs in Arabidopsis." *The Plant Cell* 18 (5): 1121–33. doi:10.1105/tpc.105.039834.

Severi, Emmanuele, Arnaud Javelle, and Mike Merrick. 2007. "The Conserved Carboxy-Terminal Region of the Ammonia Channel AmtB Plays a Critical Role in Channel Function." *Molecular Membrane Biology* 24 (2): 161–71. doi:10.1080/09687860601129420.

Siewe, R. M., B. Weil, A. Burkovski, B. J. Eikmanns, M. Eikmanns, and R. Krämer. 1996. "Functional and Genetic Characterization of the (methyl)ammonium Uptake Carrier of Corynebacterium Glutamicum." *The Journal of Biological Chemistry* 271 (10): 5398–5403.

Smil, Vaclav. 1999. "Detonator of the Population Explosion." *Nature* 400 (6743): 415–415. doi:10.1038/22672.

Smith, F. A., and S. E. Smith. 1997. "Structural Diversity in (vesicular)–arbuscular Mycorrhizal Symbioses." *New Phytologist* 137 (3): 373–88. doi:10.1046/j.1469-8137.1997.00848.x.

Smith, Sally E., and David J. Read. 2010. *Mycorrhizal Symbiosis*. Academic Press.

Sohlenkamp, Christian, Craig C. Wood, Gerhard W. Roeb, and Michael K. Udvardi. 2002. "Characterization of Arabidopsis AtAMT2, a High-Affinity Ammonium Transporter of the Plasma Membrane." *Plant Physiology* 130 (4): 1788–96. doi:10.1104/pp.008599.

Spalding, Edgar P., Rebecca E. Hirsch, Daniel R. Lewis, Zhi Qi, Michael R. Sussman, and Bryan D. Lewis. 1999. "Potassium Uptake Supporting Plant Growth in the Absence of AKT1 Channel Activity Inhibition by Ammonium and Stimulation by Sodium." *The Journal of General Physiology* 113 (6): 909–18. doi:10.1085/jgp.113.6.909.

Straub, Daniel, Uwe Ludewig, and Benjamin Neuhäuser. 2014. "A Nitrogen-Dependent Switch in the High Affinity Ammonium Transport in Medicago Truncatula." *Plant Molecular Biology* 86 (4-5): 485–94. doi:10.1007/s11103-014-0243-4.

Sugiyama, Kenjiro, Toshihiko Hayakawa, Toru Kudo, Takashi Ito, and Tomoyuki Yamaya. 2004. "Interaction of N-Acetylglutamate Kinase with a PII-Like Protein in Rice." *Plant and Cell Physiology* 45 (12): 1768–78. doi:10.1093/pcp/pch199.

Sumner, Malcolm E. 1999. *Handbook of Soil Science*. CRC Press.

Sun, Ji, John R. Bankston, Jian Payandeh, Thomas R. Hinds, William N. Zagotta, and Ning Zheng. 2014. "Crystal Structure of the Plant Dual-Affinity Nitrate Transporter NRT1.1." *Nature* 507 (7490): 73–77. doi:10.1038/nature13074.

"T-DNA Primer Design." 2015. Accessed October 6. http://signal.salk.edu/tdnaprimers.2.html.

ten Hoopen, Floor, Tracey Ann Cuin, Pai Pedas, Josefine N. Hegelund, Sergey Shabala, Jan K. Schjoerring, and Thomas P. Jahn. 2010. "Competition between Uptake of Ammonium and Potassium in Barley and Arabidopsis Roots: Molecular Mechanisms and Physiological Consequences." *Journal of Experimental Botany* 61 (9): 2303–15. doi:10.1093/jxb/erq057.

Thevelein, J. M., R. Geladé, I. Holsbeeks, O. Lagatie, Y. Popova, F. Rolland, F. Stolz, et al. 2005. "Nutrient Sensing Systems for Rapid Activation of the Protein Kinase A Pathway in Yeast." *Biochemical Society Transactions* 33 (Pt 1): 253–56. doi:10.1042/BST0330253.

Thomas, G. H., J. G. Mullins, and M. Merrick. 2000. "Membrane Topology of the Mep/Amt Family of Ammonium Transporters." *Molecular Microbiology* 37 (2): 331–44.

"Tools >> The Sequence Manipulation Suite." 2015. Accessed September 14. http://imed.med.ucm.es/Tools/SMS/ref.html.

Tremblay, Pier-Luc, and Patrick C. Hallenbeck. 2009. "Of Blood, Brains and Bacteria, the Amt/Rh Transporter Family: Emerging Role of Amt as a Unique Microbial Sensor." *Molecular Microbiology* 71 (1): 12–22. doi:10.1111/j.1365-2958.2008.06514.x.

Untergasser, Andreas, Harm Nijveen, Xiangyu Rao, Ton Bisseling, René Geurts, and Jack A.M. Leunissen. 2007. "Primer3Plus, an Enhanced Web Interface to Primer3." *Nucleic Acids Research* 35 (Web Server issue): W71–74. doi:10.1093/nar/gkm306.

von Wirén, N., and M. Merrick. 2004. "Regulation and Function of Ammonium Carriers in Bacteria, Fungi and Plants." *Trends Curr. Genet.* 9: 95–120.

Walburg, G., M. E. Bauer, and C.S.T. Daughtry. 1982. "Effects of Nitrogen Nutrition on the Growth, Yield and Reflectance Characteristics of Corn Canopies." *Agronomy Journal* 74: 677–83.

Walch-Liu, P., G. Neumann, F. Bangerth, and C. Engels. 2000. "Rapid Effects of Nitrogen Form on Leaf Morphogenesis in Tobacco." *Journal of Experimental Botany* 51 (343): 227–37.

Wang, M. Y., M. Y. Siddiqi, T. J. Ruth, and A. D. M. Glass. 1993. "Ammonium Uptake by Rice Roots (II. Kinetics of 13NH4+ Influx across the Plasmalemma)." *Plant Physiology* 103 (4): 1259–67.

Wang, Yi-Hong, David F. Garvin, and Leon V. Kochian. 2001. "Nitrate-Induced Genes in Tomato Roots. Array Analysis Reveals Novel Genes That May Play a Role in Nitrogen Nutrition." *Plant Physiology* 127 (1): 345–59. doi:10.1104/pp.127.1.345.

Weinl, Stefan, and Jörg Kudla. 2009. "The CBL–CIPK Ca2+-Decoding Signaling Network: Function and Perspectives." *New Phytologist* 184 (3): 517–28. doi:10.1111/j.1469-8137.2009.02938.x.

Xu, Jiang, Hao-Dong Li, Li-Qing Chen, Yi Wang, Li-Li Liu, Liu He, and Wei-Hua Wu. 2006. "A Protein Kinase, Interacting with Two Calcineurin B-like Proteins, Regulates K+ Transporter AKT1 in Arabidopsis." *Cell* 125 (7): 1347–60. doi:10.1016/j.cell.2006.06.011.

Yuan, Lixing, Lucile Graff, Dominique Loqué, Soichi Kojima, Yumiko N. Tsuchiya, Hideki Takahashi, and Nicolaus von Wirén. 2009. "AtAMT1;4, a Pollen-Specific High-Affinity Ammonium Transporter of the Plasma Membrane in Arabidopsis." *Plant & Cell Physiology* 50 (1): 13–25. doi:10.1093/pcp/pcn186.

Yuan, Lixing, Riliang Gu, Yuanhu Xuan, Erika Smith-Valle, Dominique Loqué, Wolf B. Frommer, and Nicolaus von Wiren. 2013. "Allosteric Regulation of Transport Activity by Heterotrimerization of Arabidopsis Ammonium Transporter Complexes in Vivo." *The Plant Cell* 25 (3): 974–84. doi:10.1105/tpc.112.108027.

Yuan, Lixing, Dominique Loqué, Soichi Kojima, Sabine Rauch, Keiki Ishiyama, Eri Inoue, Hideki Takahashi, and Nicolaus von Wirén. 2007. "The Organization of High-Affinity Ammonium Uptake in Arabidopsis Roots Depends on the Spatial Arrangement and Biochemical Properties of AMT1-Type Transporters." *The Plant Cell* 19 (8): 2636–52. doi:10.1105/tpc.107.052134.

Zheng, Lei, Dirk Kostrewa, Simon Berneche, Fritz K. Winkler, and Xiao-Dan Li. 2004. "The Mechanism of Ammonia Transport Based on the Crystal Structure of AmtB of Escherichia Coli." *Proceedings of the National Academy of Sciences of the United States of America* 101 (49): 17090–95. doi:10.1073/pnas.0406475101.

10 Zusammenfassung

Ammonium ist ein ubiquitäres Schlüsselelement in landwirtschaftlichen Böden und ist die bevorzugte Stickstoffquelle von Pflanzen. Exzessive Stickstoffakkumulation hemmt allerdings Pflanzenwachstum und -entwicklung. Pflanzen nehmen Ammonium mittels hoch-affiner Ammonium Transporter (AMTs) auf. In *Arabidopsis* wurden sechs *AMT* Gene identifiziert, die in zwei verschiedene Gruppen eingeteilt wurden, fünf *AMT1* und ein *AMT2*. AMT-Proteine formen Homo- und Heterotrimere in der Plasmamembran mit extracytoplasmatischen N-termini und cytoplasmatischen C-termini. Zusätzlich zu transkriptioneller und post-translationaler Kontrolle der AMTs durch Ammonium, dient eine Phosphorylierung am C-terminus als ein schneller allosterischer Schalter der AMT-Aktivität und verhindert eine weitere interne Ammoniumakkumulation.

In einem physiologischen Test wurde eine Kinase (CIPK23) identifiziert, welche die Aktivität der AMTs bei hohen externen Ammoniumkonzentrationen direkt reguliert. Interessanterweise ist schon bekannt, dass CIPK23 auch die Aufnahme von Nitrat und Kalium reguliert. Ein defektes *CIPK23* Gen erhöhte den Transport von Ammonium signifikant, aber die Pflanzen waren in ihrem Wachstum gehemmt. Wie erwartet waren *cipk23* Mutanten auch in ihrer Kaliumaufnahme limitiert, aber ein hohes Kaliumangebot konnte diesen Phänotyp nicht vollständig komplementieren. Weiterhin waren *cipk23* Pflanzen sensitiver für Methylammonium (MeA), ein toxisches Ammoniumanalog. Wenn die Expression der *AMT1* Gene unterdrückt wurde, reagierten die *cipk23* Mutanten weniger empfindlich auf MeA.

Die Daten deuten darauf hin, dass CIPK23 in einem Komplex mit CBL1 (Calcineurin B-like protein) die AMT1 Proteine direkt phosphoryliert und dadurch ihre Transportaktivität reguliert. Die Expression der *CIPK23* und *CBL1* Gene war abhängig vom Ammoniumangebot und steigerte sich, wenn Stickstoff limitierte Pflanzen mit Ammonium wiederversorgt wurden. Weiterhin hatten *cbl1* Pflanzen eine erhöhte Ammoniumakkumulation und ahmten damit den Effekt eines *cipk23* Funktionsverlusts nach.

In vivo Experimente demonstrierten eine bimolekulare Interaktion zwischen CIPK23, AMT1;1 und AMT1;2, aber nicht mit AMT2;1, was auf eine direkte Phosphorylierung der AMT1s durch CIPK23 hinweist.

Allerdings verhinderte der Verlust der Kinase nicht komplett die Phosphorylierung von AMT1;1 und AMT1;2, was mehrere unabhängige Wege zur Regulation der Aktivität der AMT-Trimere nahelegt. Die Daten legen eine vielschichtige post-transkriptionelle Regulation der Ammoniumtransporter via dem CBL1-CIPK23-Komplex nahe, die sicherstellt, dass die Aktivität der AMT1s reduziert und die Ammoniumaufnahme bei hohen externen Ammoniumkonzentrationen verhindert wird.

11 Curriculum vitae

Name, first name	Straub (born Tsap), Tatsiana
Date of birth	07.10.1982
Address	Teglholm Alle 9C, 4mf, Copenhagen, 2450, Denmark
Phone	+4591110347
Nationality	Belarus
Email	tatsianastraub@gmail.com

Research

November 2011 – September 2015

Doctorate in Agriculture.

University of Hohenheim, Nutritional Crop Physiology (340h), Stuttgart, Germany.

PhD thesis title: Plant ammonium transporter (AMT) integration in regulatory networks.

PhD supervisor – Prof. Dr. U. Ludewig.

August 2010 – September 2011

DAAD fellowship: "Research grant for doctoral candidates and young academics and scientists".

University of Hohenheim, Nutritional Crop Physiology (340h), Stuttgart, Germany.

Project title: Functional characterisation of AMT-type NH_4^+/NH_3 transporters in *Arabidopsis thaliana*.

November 2005 – October 2008

Postgraduate research.

Byelorussian State University, Faculty of Biology, Department of plant physiology and biochemistry, Minsk, Belarus.

Project title: Some aspects of ammonium transport regulation in plants.

Employment

November 2008 – July 2010	**Assistant lecturer.**
	Mogilev State University of Food Technology, Mogilev, Belarus.
	Subjects teached: Fundamentals of Ecological Sciences, Radiation Safety.

Education

August 2010 – September 2010	**German language course.**
	DID Deutsch-Institut, Frankfurt/Main, Germany.
September 2000 – June 2005	**Diploma in Biology-Biotechnology**. Additional qualification of biology teacher.
	Byelorussian State University, Minsk, Belarus
	Diploma thesis title: "Estimation of biological activity of various herbal extracts using algae bioelectrosensor".
September 1997 – June 2000	**High school certificate.**
	Mogilev Regional Technological Lyceum, Mogilev, Belarus.
	Specialization: biology and chemistry.

Languages

Russian: native.

English: advanced.

German: basic.

Copenhagen, 09.03.2016